A Spatial Ecosystem Model for Atlantic Coast Multispecies Fisheries Assessments of Menhaden and Bluefish

Jiangang Luo and Jerald S. Ault

Donald B. Olson, Ashley McCrea, Kyle J. Hartman[1], L. Kline[2], G. White[2] and Patrick Kilduff[2]

University of Miami
Rosenstiel School of Marine and Atmospheric Science
Miami, Florida 33149

[1]West Virginia University
Morgantown, West Virginia

[2]Atlantic States Marine Fisheries Commission
Washington, DC

NOAA/CMER Award #NA17FE2747

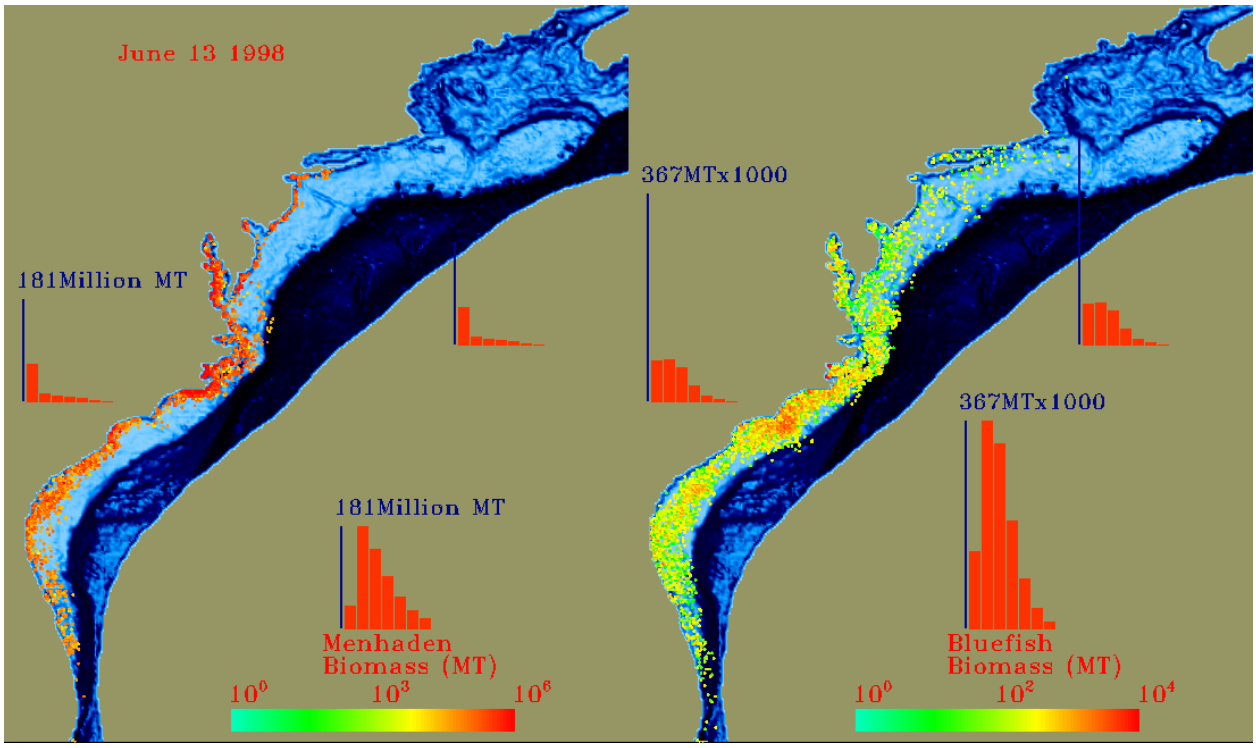

Discussion Draft of 15-16 June 2005

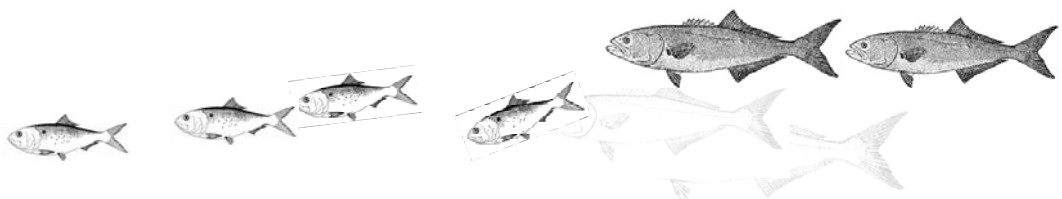

Spatial Multispecies Model Review Workshop

June 15-16, 2005

Sheraton Waterside Hotel, Norfolk VA

Agenda

GOAL: *To review the second year of work on model development and to discuss future research directions and management applications.*

Wednesday, June 15, 2005 1:00 PM – 5:00 PM

1:00 PM Welcome and introduction of workshop participants

1:10 PM Overview of workshop goals and agenda

1:30 PM Presentation of model type, scope, and purpose

2:15 PM Discussion of spatial ecosystem model structure

2:45 PM Review of model inputs and parameters – What has changed since last year?

3:15 PM Break

3:30PM Review of preliminary results:

- Plume model dynamics.
- Biophysical model dynamics including all menhaden age classes.
- Effects of introduction of predators and spatial fishing intensity.

5:00 PM End for day.

Thursday, June 16, 2005 8:30 AM – 12:00 PM

8:30 AM Summary of Day 1 Activities and Workshop Goals for Day 2.

9:00 AM Continue with review of preliminary results:

- Pros and cons of the model as configured.
- Next steps in spatial multispecies ecosystem model development.
- Long-term directions and opportunities for model applications.

12:00 - 12:30 PM Workshop wrap-up

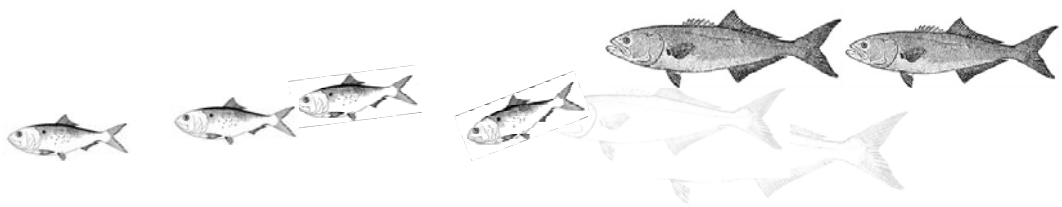

A Spatial Ecosystem Model for Atlantic Coast Multispecies Fisheries Assessments of Menhaden and Bluefish

Executive Summary

This report summarizes accomplishments from a two-year project to develop a spatial ecosystem-based management model focused on the dynamic interactions in the Atlantic States (Nova Scotia to southeastern Florida) coastal ocean among and between the core multispecies fisheries complex of menhaden, bluefish, striped bass and weakfish. The spatial fishery ecosystem model was designed to allow evaluation of how fishery management actions may impact fishery yields and stock productivity goals for a particular target species when the species complex is directly coupled to spatial patterns of fishing intensity, other predator and prey populations, ocean physics, and environmental changes. To date we have: (1) developed a prototype regional (Maine to Florida) spatial age-structured multispecies fishery ecosystem model; (2) assembled, assimilated and mapped a broad range of spatially-explicit databases on processes relevant to the model-building, i.e.,: physical-biological (e.g., ocean currents, water temperatures, bathymetry, chlorophyll, river flows, etc.), and population-dynamic (e.g., spatial abundance, biomass and fisheries catches by age/size for menhaden, bluefish, striped bass, and weakfish; diets; bioenergetics relationships, spatial fishing intensities by fleets, recruitment, etc.); (3) parameterized the prototype model for Atlantic menhaden and bluefish; (4) run some pilot scenarios to illustrate model dynamics and performance capabilities; and, (5) used advanced scientific visualization and GIS tools to facilitate presentation of results concerning policy alternatives and environmental impacts to assessment biologists, managers and decision-makers. As such, the model will assist establishment of quantitative ecological measures of fishery management success for the Atlantic States Marine Fisheries Commission and other regional US fishery management entities.

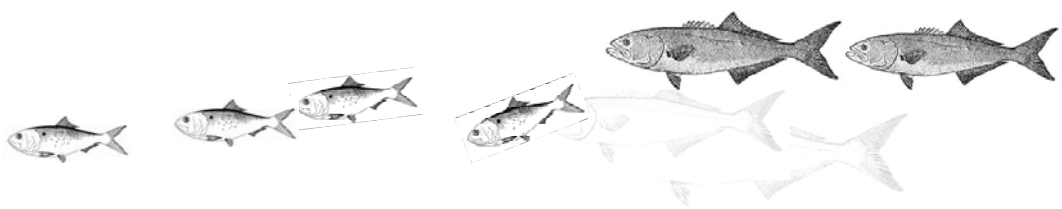

A Spatial Ecosystem Model for Atlantic Coast Multispecies Fisheries Assessments of Menhaden and Bluefish

Table of Contents

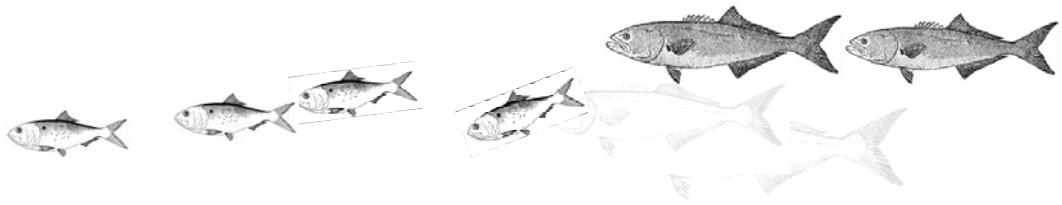

Model Parameterization and Calibration

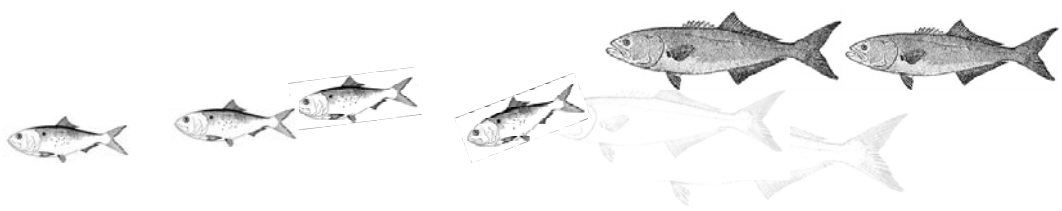

Introduction and Overview

1.1 Project Background and Justification

Marine fisheries management along the U.S. Atlantic coast is currently conducted through a single species approach by the Regional Fisheries Management Councils and the Atlantic States Marine Fisheries Commission ("Commission"). Scientists have been troubled for some time by strict reliance on age structured VPA assessments for individual stock assessments (Gibson and Lazar 1998), because these methods give little consideration to important linkages and dependencies among biological and physical components of ecosystems that affect community structure. Changes in the environment, fleet fishing effort, and species distribution are expected to affect many important inshore and coastal fish populations directly and indirectly through environmental changes and food web interactions. Concomitantly, the Atlantic coastal ocean ecosystem and its economically valuable fisheries are fully exploited, in many cases overfished, and waning from intense fishing, urbanization and human usages (Rothschild et al. 1994, Vaughn and Smith 2000, ASMFC 1999, SAW 2000). These impacts have reinforced public and scientific concern for protecting the environment and for the sustainable future of US Atlantic marine fisheries. Traditionally, water quality, critical habitats, and fish stocks have each been treated as separate management issues. However, pervasive declines in fishery production and widespread habitat degradation have emphasized the importance of taking a more holistic ecosystem approach to fisheries management (e.g., US Oceans Commission 2004, Pikitch et al. 2004, Ault et al. 2005). The new paradigm should refocus assessment and modeling efforts on linking the production dynamics of fish populations, fishing activities, biological community structure, physical environmental parameters, and essential fish habitats (Bohnsack and Ault 1996, Ault et al. 1999a,b, 2003, Humston et al. 2004, Walters and Martell 2004). Such an approach is clearly needed in the Atlantic coastal ocean ecosystem that supports an important multi-billion dollar fishing and tourism economy.

While substantial effort has been expended on the Atlantic coast to formulate the appropriate principles and policies required for multispecies management, few practical applications have been developed. During 2000 and 2001, the Commission investigated various multispecies models to evaluate fishery impacts of predator-prey interactions between several predator species (e.g., bluefish *Pomatomus saltatrix*; striped bass *Morone saxatilis*; and, weakfish *Cynoscion regalis*), and a key prey species (i.e., Atlantic menhaden (*Brevoortia tyrannus*). Initial development of a multispecies VPA (MSVPA) model focused on predation impacts on the Atlantic menhaden by the core predator species (Garrison et al. 2004). That model as currently configured is non-spatial and does not incorporate environmental or physical oceanographic processes, nor is it capable of evaluating interspecies interactions or other influences on the predator species. The current model is limited to evaluation of only management strategies on the menhaden fishery and not the key predator species. The MSVPA model has been presented in several public and Commission forums. Requests have been made to expand the scope and formulation of these concepts to a multipsecies model that explicitly includes spatial dynamics and important environmental processes to allow investigation of the impacts of localized fishing effort, predation, and recruitment events on management decision making and resource sustainability. To address that need, this project expanded on fundamental multispecies fishery modeling concepts to include coupling of the biophysical coastal ocean environment to the

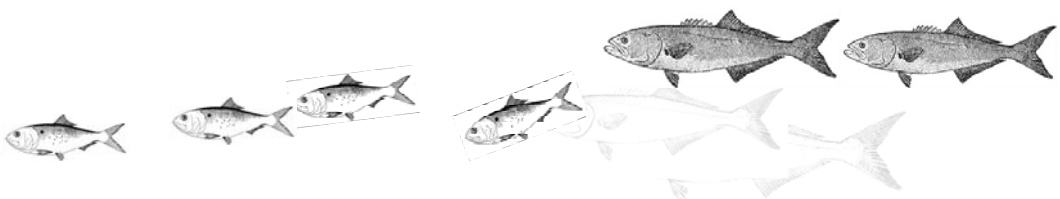

dynamics of key higher trophic-level populations and communities in response to exploitation and environmental changes. This multispecies ecosystem model will quantify linkages among predation, competition, directed fisheries and physical oceanographic processes for all species in a spatially explicit framework.

Current Commission stock assessments have concluded that striped bass and weakfish are recovered stocks and at high levels of abundance. Although bluefish stocks are defined as overfished, management is in the fifth year of a seven-year rebuilding schedule. A spatial multispecies model will provide the basis to further evaluate management options on these important species, and will begin to address several of the Commission's current research needs for bluefish and striped bass (ASMFC 2003). Examples of these priorities include research on species interactions (predator/prey and competition), development of alternative methods to assess bluefish, investigation of age-specific mortality rates, and determination of factors which may limit recruitment. The model should provide the analytical capabilities to explore a longstanding question of whether bluefish abundance has declined, or if the bulk of the population has simply moved offshore and out of range of the fishery. This project also addressed several priorities of the 2002 Bluefish-Striped Bass Dynamics Research Program:

Historical Information Synthesis – This project has compiled and quantitatively analyzed, through a multispecies modeling approach, the interactions between bluefish, menhaden, and potentially other key predator species (i.e., striped bass and weakfish). The model utilizes information on habitat requirements of these stocks can help to identify the influence of biotic and abiotic factors on stock structure and dynamics

Ecological Information Needs – This project provides a direct quantitative assessment of the effects of environmental variables on population dynamics of key predator species (e.g., bluefish), including both biotic and abiotic factors. Since this model is age-structured, information on recruitment mechanisms can also be provided.

Stock Assessment – This project expands on the current stock assessments for Atlantic menhaden and bluefish by incorporating environmental and physical information to more accurately evaluate stock status and potential management strategies.

1.1 Scientific Goals and Objectives

This project's goal was to develop a spatial multispecies fisheries model that extends traditional fish population dynamics theory using fundamental principles of bioenergetics, population ecology, and community trophodynamics for a key predator (bluefish) and prey (Atlantic menhaden) population. While the model's spatial coverage is relatively broad (Nova Scotia to central Florida), implications are strongest for the mid-Atlantic region as it is the core habitat for these migratory species. A specific hypothesis to be tested is whether a spatial coupled-biophysical fishery ecosystem model will provide more accurate assessments of multispecies stock dynamics by incorporating dynamic spatial interactions of exploitation and biotic-abiotic factors. This ecosystem-based approach to fisheries management provides a quantitative methodology to evaluate fisheries dynamics and ecological performance measures of management success.

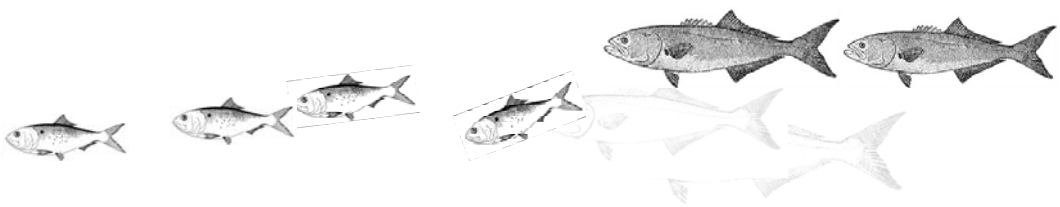

Atlantic Coast Spatial Dynamic Multispecies Model

2.1 Conceptual Model Description.- The prototype Atlantic coast spatial dynamic multispecies model uses both age-structured population dynamic and bioenergetic data layers for Atlantic menhaden, bluefish, striped bass, and weakfish. These data layers reflect linkages via species' ontogenetic usages of habitats, differing life histories and population-dynamic strategies including their critical placement in the trophodynamic structure of the ecosystem; and, responses to fishing, predator-prey relationships, ocean biophysics, and fishery management interventions and alternatives (**Figure 2.1**).

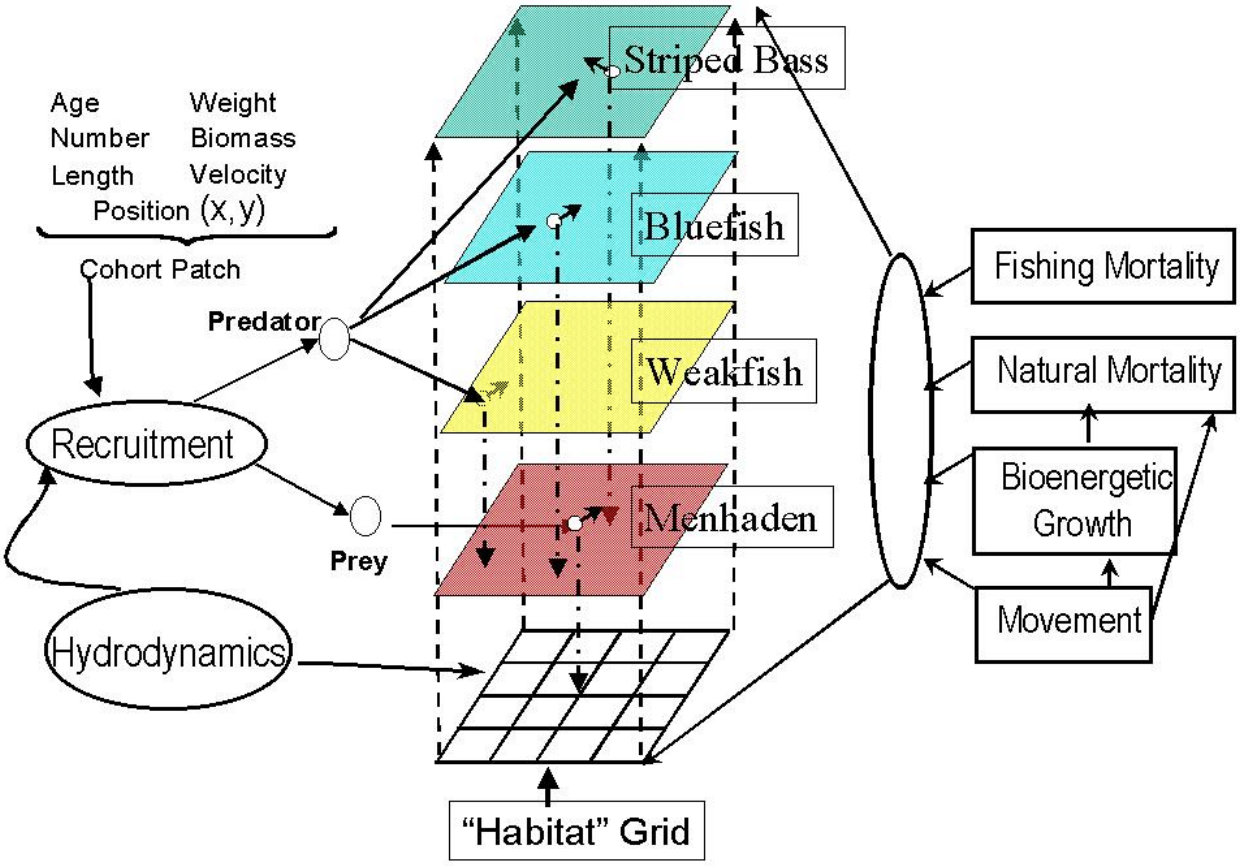

Figure 2.1.- Conceptual model of the Atlantic States multispecies fishery for the spatial dynamic coupled prey-predator and human-dominated biophysical environment of menhaden, bluefish, striped bass, and weakfish.

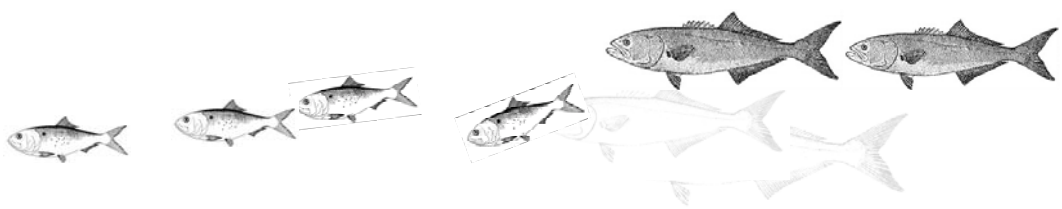

2.2 Defining the Model's Spatial Domain.- We reconfigured our published operational spatial dynamic age-structured multispecies biophysical prey-predator model from the south Florida coastal ocean ecosystem (Ault et al. 1999b, 2003; Wang et al. 2003) to study the fisheries ecosystem environment of west Atlantic coastal ocean from Nova Scotia, Canada to Miami, Florida (**Figure 2.2**). The Atlantic coast spatial dynamic multispecies model links inshore (coastal bays and estuaries) to offshore oceanic dynamics through the ontogenetic behaviors of the fishery resources as modulated by environmental variability (ocean fronts, eddies, etc.) and fishing.

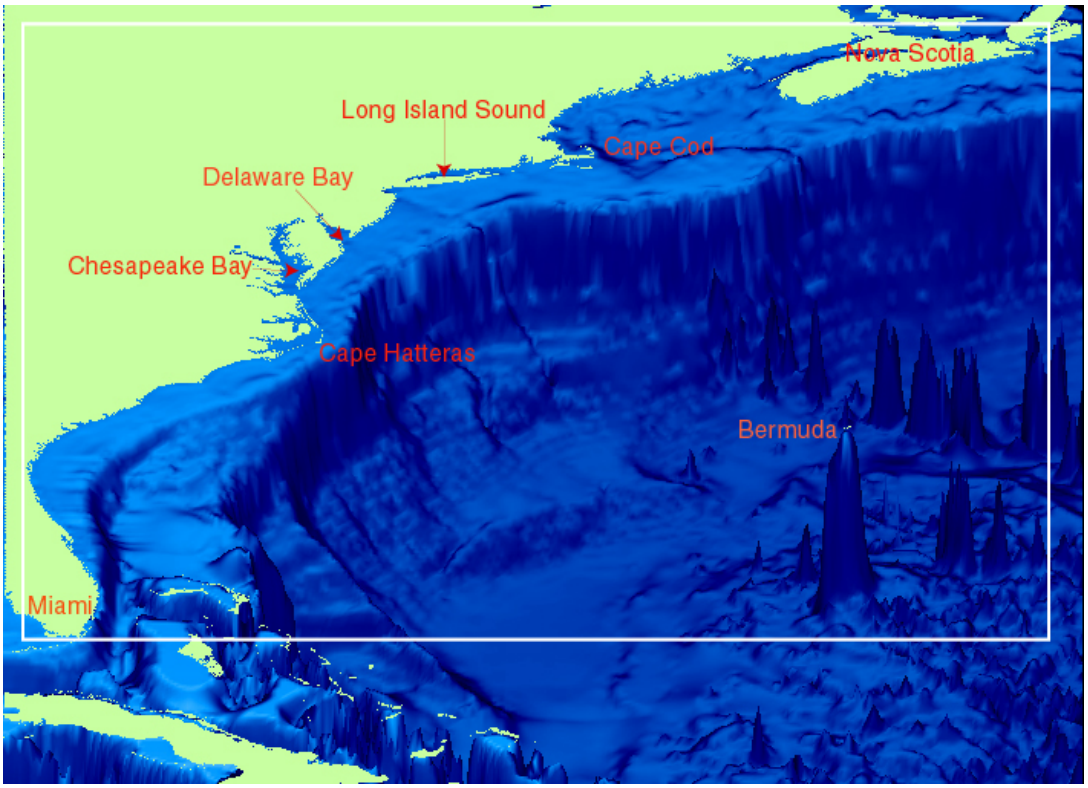

Figure 2.2.- Bathymetry of the Atlantic States coastal ocean ecosystem running from Nova Scotia in the north to Miami, Florida in the south. White box shows model spatial domain.

The model domain extends from 25^{o} N to 47^{o} N, and 82^{o} W to 60 ^{o} W. We have elected to use 3 minutes in latitude and longitude as the model spatial grid resolution, which gives the total grid dimension of 440 x 440 cells, with each cell size of 5.5 x 5.0 km in the south, and 5.5 x 3.8 km in the north. At this spatial resolution, model cells are small enough for sufficient detail to represent the dynamics of coastal bays and sounds, yet large enough to keep the total number of cells in the model domain to a computational minimum. What is desired is a minimum resolution for biological data at 60 x 60 mi (**Figure 2.3)**. In the current configuration there are 136,083 water cells in the domain. To further facilitate model computational efficiency, we reduced the number effective cells in the model by masking off pelagic waters where depths are greater than 3000 meters and those waters east of the Gulf Stream (**Figure 2.4**). This reduced the effective number of model cells by more than 3 fold to a 36,059 cells, equivalent to an average grid dimension of 190 x 190 km.

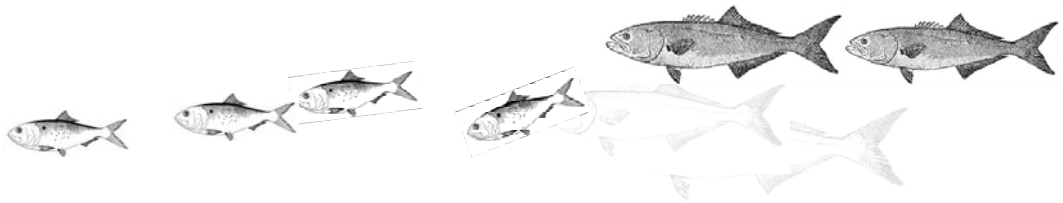

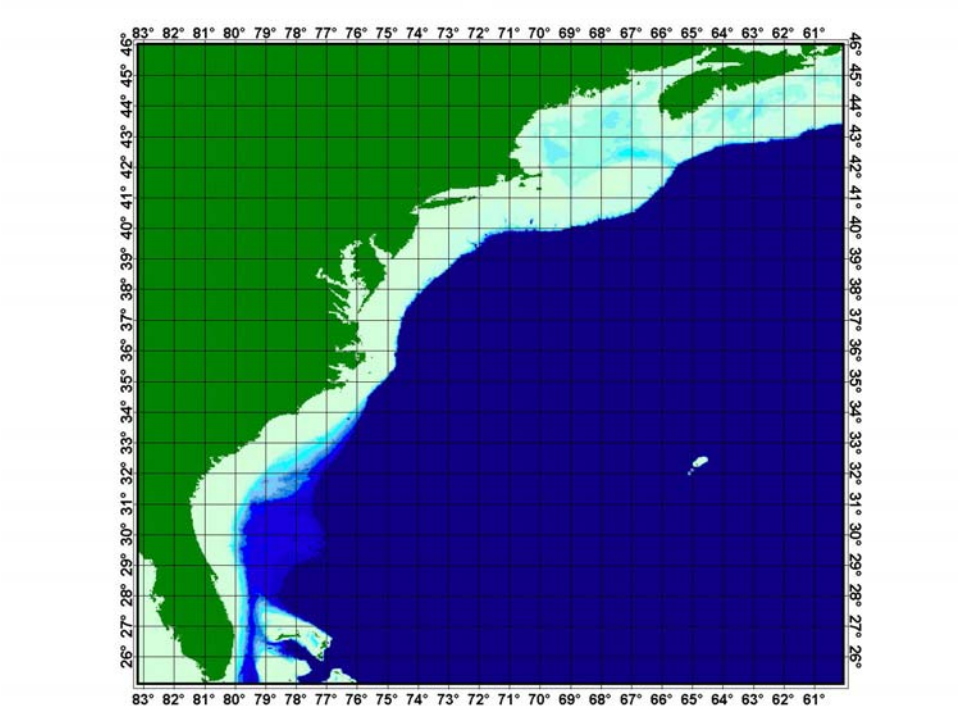

Figure 2.3.- Minimum desired grid resolution for biological and fisheries data defining the Atlantic States coastal ocean ecosystem running from Nova Scotia in the north to Miami, Florida in the south. Each cell is approximately 60 mi on a side.

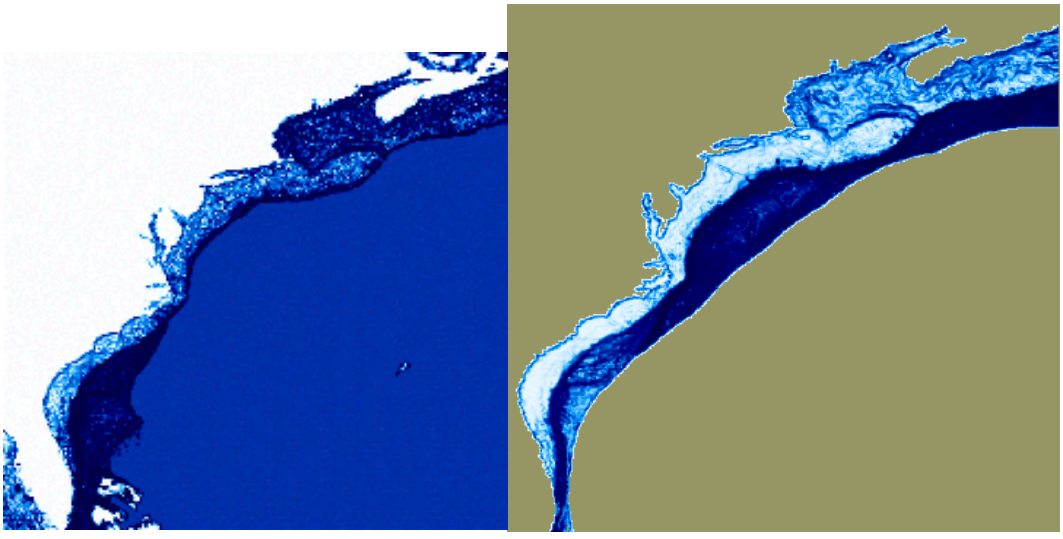

Figure 2.4.- Three-dimensional maps showing the effective spatial domain of the Atlantic coast multispecies fishery ecosystem model.

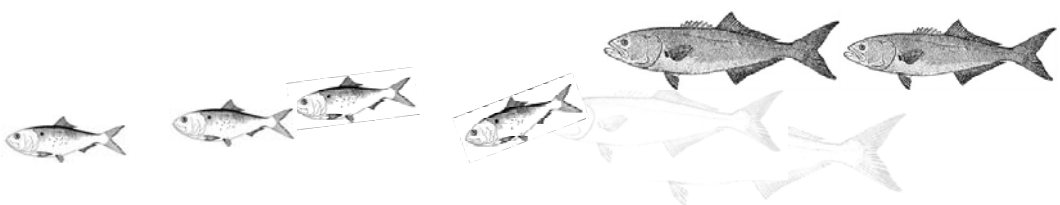

Regional Physical Oceanography

3.1 Fronts-Eddies and Biophysical Interactions.- The oceanographic setting inhabited by the target species is centered on the two major coastal indentations or bights that make up the eastern seaboard of the U.S. (see accompanying **Figures**). These are the Mid-Atlantic Bight extending from Cape Hatteras to Cape Cod and the South Atlantic Bight that between Hatteras and Cape Canaveral in Florida. The species also are found up into the Gulf of Maine to the north of the Mid-Atlantic Bight. All of this domain is characterized by wide continental shelves that are separated into three domains by the capes mentioned above. The northern two regions, Gulf of Maine and Mid-Atlantic Bight are dominated by a buoyancy driven southward flow that is created primarily by the flow of fresh water out of the Arctic (Chapman and Beardsley, 1989). This flow is intensified along the outer shelf edge in the shelf break front, and again at the inner edge of the shelf where freshwater input from riverine and estuarine outflows enhances the buoyancy flux. Both the shelfbreak and the coastal freshwater plumes strong fronts are found separating the fresh water on the landward side from the more saline offshore waters. Both of these fronts are retrograde in the sense that the density contours are roughly perpendicular to the bottom topography (Mooers et al., 1978; Olson, 2001). Flows in both fronts range from 0.20-0.50 m/s. The shelf flows between them are in the same sense in general but considerably slower (< 0.10 m/s). These flows terminate at Cape Hatteras where both fronts turn out to sea and are entrained into the edge of the Gulf Stream to form a low salinity band known as the Ford Water.

To the south of Cape Hatteras the inshore flow consists of a similar band of southward flowing freshwater feed by the coastal rivers of the Carolinas and Georgia. The shelf edge situation, however, is very different in the South Atlantic Bight where the prograde, isopycnals parallel to the topography, dominates the shelf/open ocean interactions. The intermediate shelf here is more variable and highly dependent on wind conditions (Lee et al., 1989). Again, the coastal flow is primarily swept offshore and into the Gulf Stream at Cape Canaveral where the shelf narrows considerably. To summarize the shelf domains that menhaden, bluefish, weakfish and striped bass inhabit consist of a buoyant anti-clockwise flow around the Gulf of Maine coupling into a southward shelf circulation that dominates the Mid-Atlantic Bight. The water masses that make up these flows are lost to the shelf by mixing into the offshore North American Slope Water and entrainment into the Gulf Stream as it separates from the coast at Cape Hatteras. The South Atlantic Bight circulation in contrast consists of a southward flow close to the coast and a northward flow at the shelf edge associated with the Gulf Stream.

3.2 Cross-Shelf Linkages.- As discussed in more detail below the menhaden are associated with the outer shelf off the Carolinas during their winter spawning activities. This puts them in proximity, but apparently not within the Gulf Stream front. The other higher tropic level animals also seem to be limited by the Gulf Stream as an outer boundary. An interesting question arises concerning the transfer of organisms between the Mid- and South Atlantic Bights. The Gulf Stream is essential on the shelf edge at its narrowest part of Cape Hatteras. The physical water mass data suggests little or no introduction of Mid-Atlantic Bight waters to the south of Hatteras. Some South Atlantic and Gulf Stream waters are mixed into the Slope Water and onto the Mid-Atlantic shelf. Otherwise the Gulf Stream seems to be an outer boundary and may serve as a barrier to these organisms.

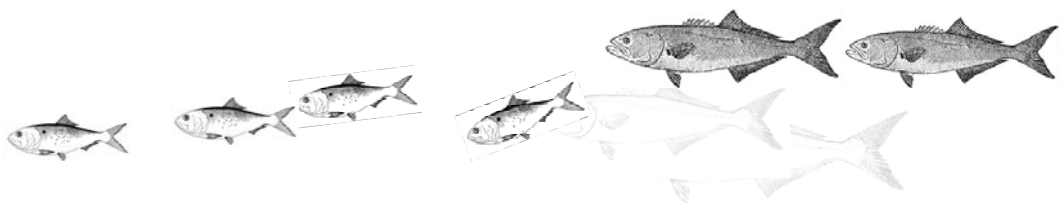

The most important flows for these species are then the coastal buoyancy fronts and their interaction with the estuaries that boarder the inner edge of the both shelves. The freshwaters coming out of the estuaries form a plume that is bound on its outer side by a series of retrograde fronts. The major plume in the Mid-Atlantic Bight is formed by the Hudson River outfall and forms a 5-20 km band of freshwater flowing southward down the New Jersey coast. This is augmented further by the flow out of Delaware Bay and then finally by the Chesapeake outflow (**Figures 3.1 & 3.2)**. The structures at the outfall of each estuary are complicated with the creation of new fronts as the freshwater from each system enters the more saline water on the shelf (**Figure 3.3**). Wind conditions can completely change the nature of the flows on the shelf by either augmenting the coastal plume through down-welling or disrupting the plume fronts under upwelling conditions (northward winds).

The target species also are dependent on the conditions within the estuaries themselves. Most of the estuaries in the Mid-Atlantic Bight are dominated by partially-mixed systems such that the flow is two layer in nature with saline water on the bottom. Transitions within broad estuaries such as Delaware Bay or the Chesapeake lead to inter-estuarine fronts separating the partially-mixed system and well-mixed regimes such as that found in the shallow bays along the eastern side of Chesapeake Bay. The cross channel changes from inflow to outflow provide habitat structure for organisms and shifts in both forage and behavioral clues that are expected to aggregate the target animals. Conditions are highly modulated by tidal effects both in terms of mixing, water level and tidal flows.

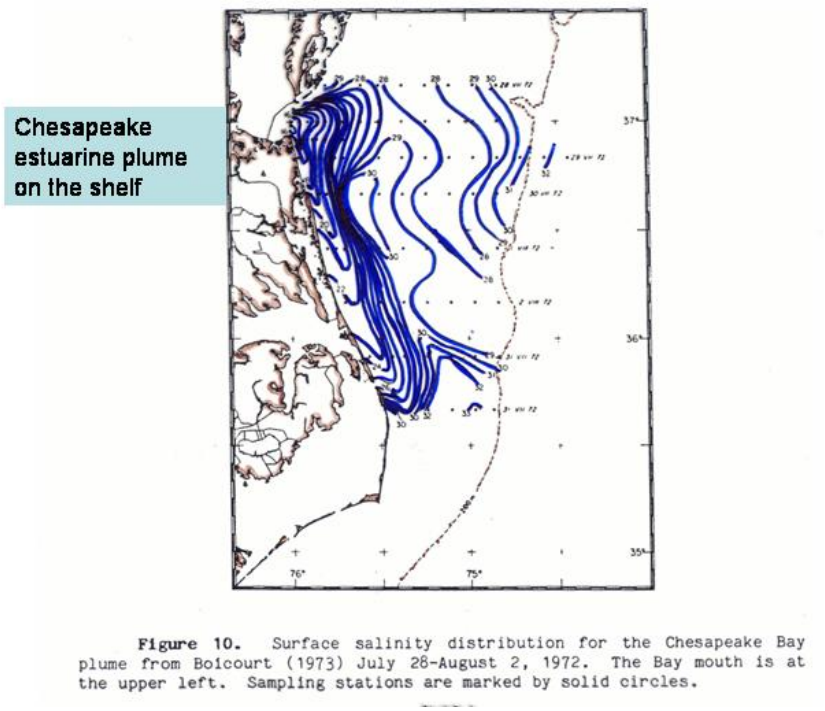

Figure 10. Surface salinity distribution for the Chesapeake Bay plume from Boicourt (1973) July 28-August 2, 1972. The Bay mouth is at the upper left. Sampling stations are marked by solid circles.

Figure 3.1- Surface salinity distribution for the Chesapeake Bay plume from Boicourt (1973) July 28-August 2, 1972. The Bay mouth is at the upper left. Sampling stations are marked by solid circles.

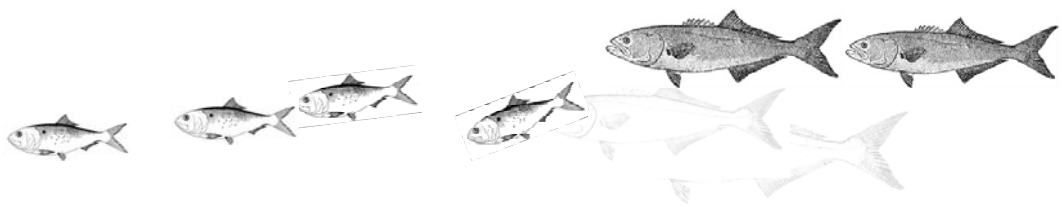

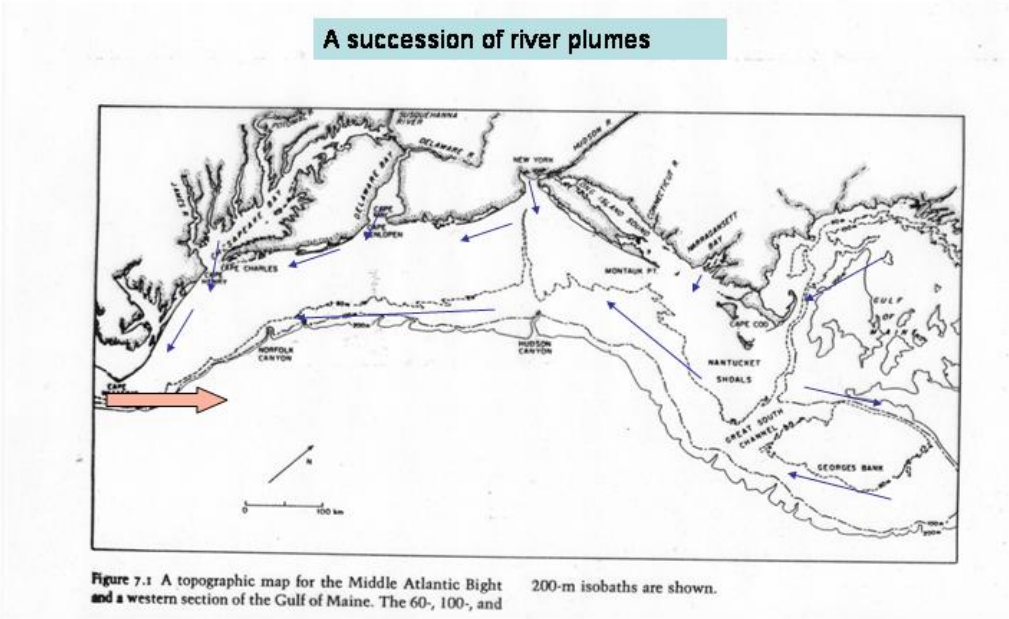

Figure 7.1 A topographic map for the Middle Atlantic Bight and a western section of the Gulf of Maine. The 60-, 100-, and 200-m isobaths are shown.

Figure 3.2.- A topographic map for the middle Atlantic Bight and a western section of the Gulf of Maine showing the succession of river plumes along the coastal margin. The 60-, 100- , and 200-m isobaths are shown.

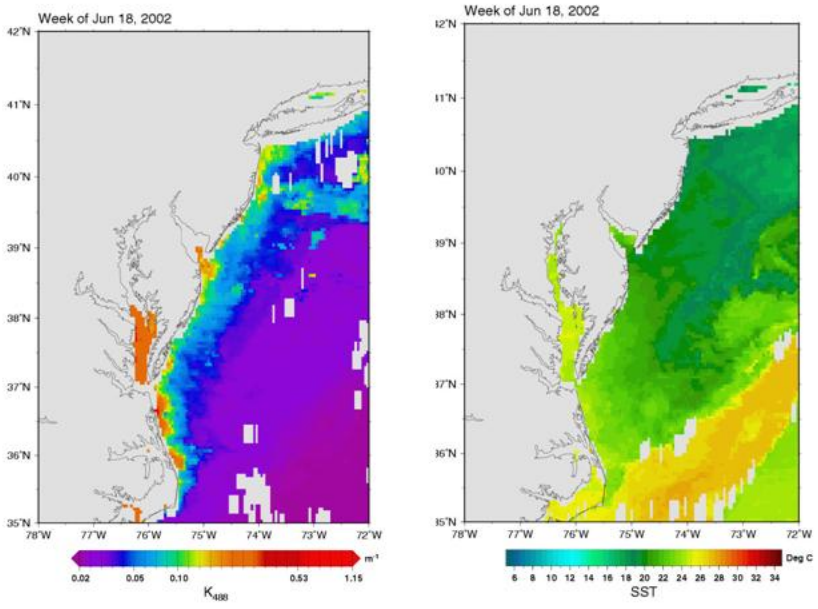

Figure 3.3.- Surface transparency (left panel) and sea surface temperature (right panel) for the Middle Atlantic Bight region.

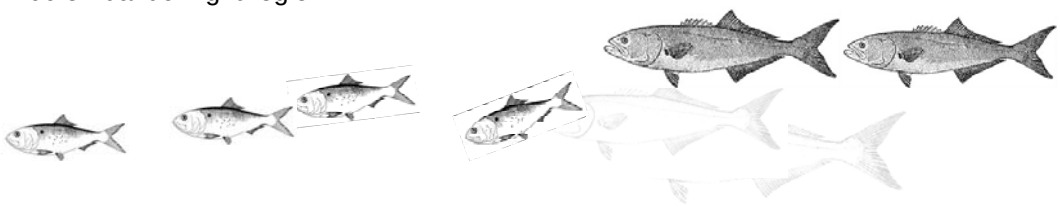

3.3 Development of a Feature-Based Estuary Plume Model.- In the previous version of our biophysical fishery ecosystem model, we used the average monthly salinity map as a proxy for physical ocean dynamics through-out the entire set of model simulations. There were no year to year variations. From the March 2004 workshop, all the participants agreed that the recruitments of juvenile fish to estuarine system were closely linked with the plume features at the entrance of a particular estuary. Therefore, during the last year it is a high priority to develop a feature-based estuary plume model to describe spatial salinity distribution patterns using empirical salinity and river flow gauge estimates, since a fully integrated hydrodynamic model is impossible given the time and financial constraints of this current project. To accomplish this task, we used a simple diagram (Figure 3.4) to illustrate the plume at the month of the estuary with freshwater at the top of density ρ_1 and oceanic water at bottom of density ρ_2.

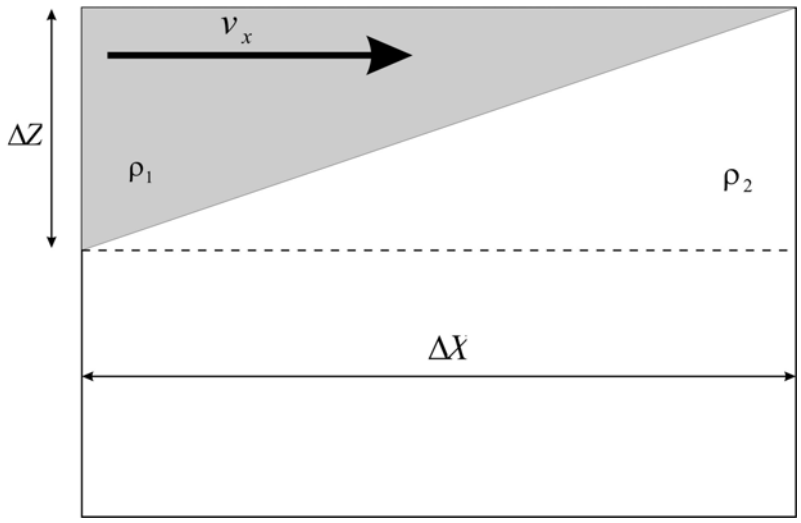

Figure 3.4.- Conceptual diagram of a hypothetical estuary along the Middle Atlantic Bight showing the depth of the freshwater layer (gray area) and extending a particular distance along the estuary.

The depth of freshwater layer at the month is ΔZ and the distance is ΔX. If we assume a particle of mass *m*, base on Newton's law, we have

$$F = am = \frac{v_x^{\,2}}{\Delta X} m$$

$$a = \frac{1}{\rho}\frac{\partial P}{\partial x} = g(\frac{\rho_2 - \rho_1}{\rho_2})\frac{\Delta Z}{\Delta X} = g'\frac{\Delta Z}{\Delta X}$$

where $g' = g(\rho_2 - \rho_1)/\rho_2 = g(\sigma_2 - \sigma_1)/(1000 + \sigma_2)$, g is gravity. Therefore,

$$\frac{v_x^{\,2}}{\Delta X} m = g'\frac{\Delta Z}{\Delta X} m$$

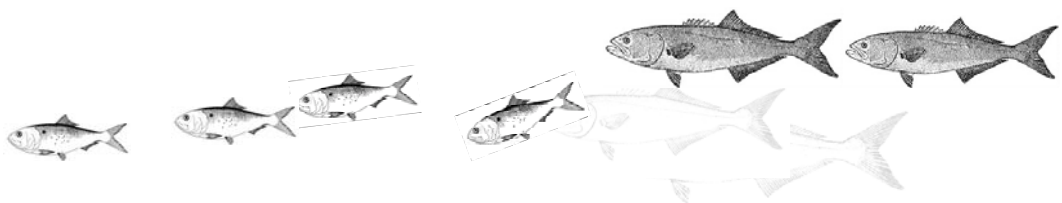

$$v_x = \sqrt{g' \Delta Z}$$

Similarly, we can get

$$v_y = \sqrt{g' \Delta Z}$$

With Coriolis force (f) added, we have

$$\frac{dv_x}{dt} = g' \frac{\Delta z}{\Delta X} + f v_x$$

$$\frac{dv_y}{dt} = f v_x$$

The solution of this is

$$X = \frac{g' \frac{\Delta Z}{\Delta X}}{f^2} (1 - \cos ft)$$

$$Y = \frac{g' \frac{\Delta Z}{\Delta X}}{f^2} (ft - \cos ft)$$

For long term average, it can be approximated with

$$\Delta X = \frac{g' \frac{\Delta Z}{\Delta X}}{f^2} = \frac{g' \Delta Z}{\Delta X f^2} = \frac{v_x^2}{\Delta X f^2}$$

$$\Delta X^2 = v_x^2 / f^2$$

$$\Delta X = v_x / f$$

$$\Delta Y = \frac{g' \frac{\Delta Z}{\Delta X}}{f^2} ft = \frac{g' \Delta Z}{f \frac{\Delta X}{t}} = \frac{v_x^2}{f v_x} = \frac{v_x}{f}$$

The above type of flow will only exist when the freshwater discharge is less then the critical flows (Q_c), which can be estimated as

$$Q_c = \frac{v_x \Delta Y \Delta Z}{2} = \frac{v_x \frac{v_y}{f} \Delta Z}{2} = \frac{v_x v_y \Delta Z}{2f} = \frac{\sqrt{g' \Delta Z} \sqrt{g' \Delta Z} \Delta Z}{2f} = g' \Delta Z^2 / 2f$$

If the freshwater discharge exceeds Q_c, the plume will breakup and form eddies and odd flows.

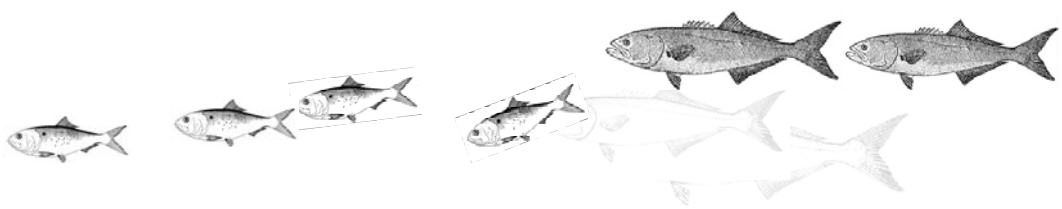

For our first attempt, we implemented the model at the mouth of Chesapeake Bay based on monthly salinity measurements collected by Old Dominion University. We first used the temperature and salinity at the mouth of Chesapeake Bay and offshore temperature and salinity to calculate the ΔX . Then we used the linear interpolation to estimate the salinity for the cells within the ΔX . The salinity within the Bay was scaled according the ratio of average month salinity and the current month salinity at the mouth of the Bay. An example of the results is shown (**Figure 3.5**). The left panel is the observed average salinity for January, and the right panel is the January 2004 salinity distribution estimated from the plume model.

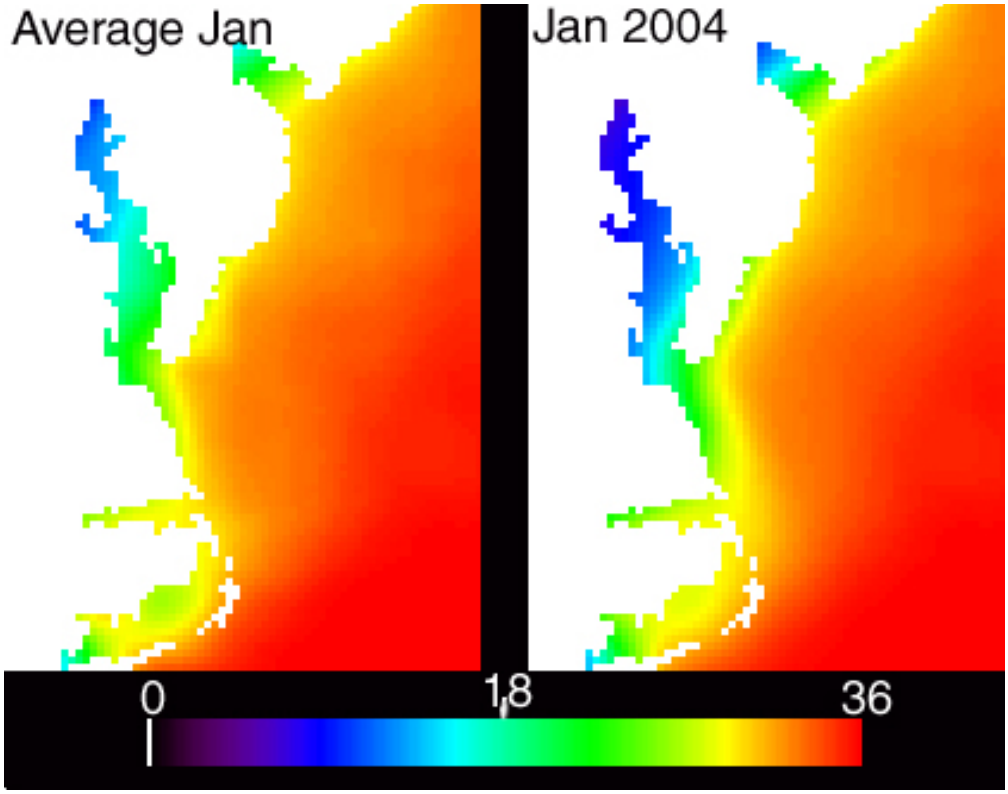

Figure 3.5.- Example output of surface salinities from feature-based estuary plume model for the Chesapeake Bay and Middle Atlantic Bight region. Scale of salinity is shown on bottom in units of parts per thousand.

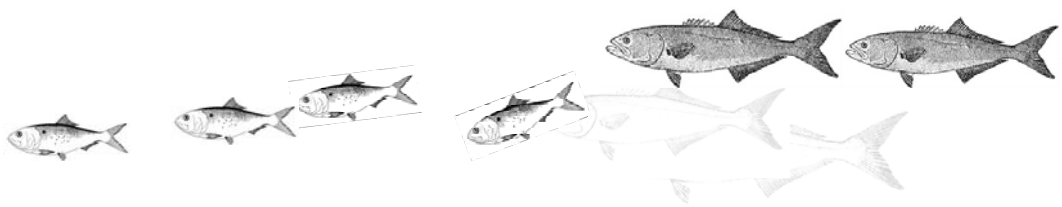

Spatial Biophysical Fishery Ecosystem Model Description

4.1 Population-Community Abundance and Biomass Dynamics.- We extended our operational spatial dynamic multispecies prey-predator coastal ocean production model of the Florida Keys ecosystem (Ault and Olson 1996; Cosner et al. 1999; Ault et al. 1999a, 2003; Meester et al. 2001; Wang et al. 2003, Humston et al. 2004) to the situation and environment of the Atlantic coast ocean ecosystem extending from Maine to Florida. The demonstration prototype model simultaneously tracks the abundance and spatial dynamics of cohorts of menhaden (prey, $N(a,t)$), striped bass, (predator, $P_1(a,t)$), bluefish (predator, $P_2(a,t)$), and weakfish (predator, $P_3(a,t)$) at age a and time t from spawning, through settlement and recruitment, and as they grow and age over their lifetime. The model mathematically links bioenergetic principles of fish physiology, population ecology, fish-habitat relationships, and community trophodynamics to regional hydrodynamic circulation models. The spatial simulation model is object-oriented with population-community dynamics considered in terms of the independent variables age and time, but also two-dimensional (x,y) space dependency. The spatial dynamic model divides each of n population cohorts into a number of patches and follows each of these patches over both space and time with fewer tactical assumptions about animal behavior than individual-based models. The model also explicitly links coastal ocean hydrodynamics and mass transport (i.e., Princeton Ocean Model(s), MICOM, etc.) and habitat dynamics through spatial maps of resources. Environmental variability and prey are dynamically linked to predator production through a "*spatial distribution of growth rate potential*" to explore the extent to which physics and biology couple to determine spatial and temporal effects on the growth and survival of each patch. In addition, by summing individual patches over space, we can obtain information on the survivorship and variability of cohort growth and recruitment. Summing the patches and cohorts projects the population, while comparison of prey and predator reflects community dynamics. The present numerical version of the spatial dynamic model tracks cohorts of a predator and prey at age a and time t in horizontal space from spawning, through settlement and recruitment, and as they grow through maturity to maximum size and age. The operational Atlantic coast fishery ecosystem model is conceptually organized around a simplified canonical population conservation equation

Population Abundance = Rate of change	[Reaction kinetics] *Prey-Predator Dynamics*	+	Advection + Diffusion + Taxis/Kinesis *Physical transport & Animal Behavior*

where, equations for species abundance and weight are functionally comprised of the reaction kinetics for the specified age-structured prey-predator dynamics and fishing, overlain in a biophysical environment where physical advection by currents plays a role in larval transport, diffusion deals with local environment carrying capacity in space, and taxis-kinesis behaviors are responsible for animal migrations. Thus, in formal mathematics fishery community dynamics are employ a spatial equation for the local rate of change of numbers (abundance) of individuals

$$\frac{\partial N}{\partial t} = -u_i \frac{\partial N}{\partial x_i} - \frac{\partial N}{\partial a} - Z(N)N + \frac{\partial}{\partial x_i}[K(N)\frac{\partial}{\partial x_i}N] - U_i \frac{\partial N}{\partial x_i} \qquad (4.1)$$

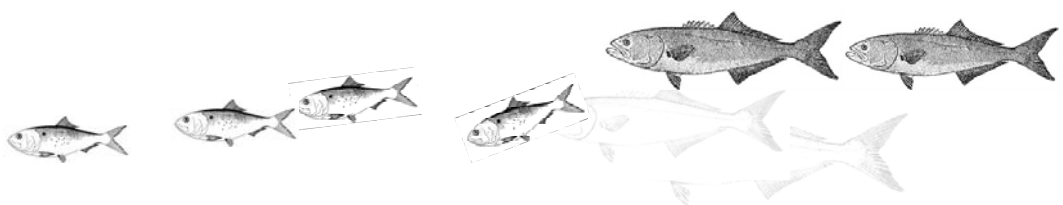

where the number of individuals $N = N(x_i, a, t)$, x_i = spatial coordinates, a = age, t = time, u_i = water velocity, $Z(N)$ = individual density-dependent mortality rate, $K(N)$ = number (and age) dependent diffusion coefficient, and U_i = active swimming velocity to preferred conditions. Normally birth would only contribute to the first (youngest) age group. The density-dependent total mortality (natural, fishing, etc.) expression $Z(N)N$ is linked to cohort recruitment and growth, and prey and predator are linked through a spatial functional response (Cosner et al. 1999). We will track cohorts of $N(a,t)$, and predators, $P_i(a,t)$ at age a and time t in space from spawning, through settlement and recruitment, and as they grow and age. Two types of spatial domains can be used in the model. A continuous spatial domain will be used for the recruitment phase of prey and predator, and the behavioral movement of adult predator. A discrete spatial domain, into order to reduce the simulation time, will be used for all environmental data (such as, depth grid and substrate grid) and adult prey movement. Hydrodynamic circulation models will ultimately drive both recruitment processes and habitat-population dynamics. This is accomplished by linking the environment and prey dynamics to fish (predator) production through the spatial distributions of growth rate potential to explore the extent to which physics and biology couple to determine spatial and temporal effects on the growth and survival of each patch. In addition, by summing individual patches over space, we can obtain information on the survivorship and variability of cohort growth and recruitment. To provide a background water column forage field for menhaden in the model, lower food chain dynamics can also be represented by remotely sensed primary production data. This could be made integrated by using a state-of-the-art nutrient (N), phytoplankton (P), zooplankton (Z), detritus (D) or $NPZD$ model (Lima et al. 2002, 2003) modified to run with dominant US Atlantic Coast species. The model includes either a single food chain depicting the dynamics of copepods as the Z component, or a two chain microbial loop implementation consisting of picoplankton and ciliate herbivores. The lower food chain model has already been incorporated into a Caribbean Sea POM circulation model (Lima et al. 2003).

A bioenergetic framework will be used to explicitly couple the population-dynamic responses of prey and predator to the vagaries of the Atlantic coast physical and biophysical environments. The basic population-dynamic bioenergetic model was fashioned after that of Ault et al. (1999a, 2003). This analytical approach recognizes that traditional models describe the growth of fish with respect to time as the difference between rates of tissue synthesis (anabolism) and degeneration (catabolism) (von Bertalanffy 1949), where both anabolic and catabolic rates are considered to be allometric functions of individual weight (Jobling 1994). Thus, age-structured growth can be written as a general conservation equation following Ault and Olson (1996)

$$dW(a,t) = (anabolism - catabolism)\,dt = (\alpha W^m - \beta W^n)dt \tag{4.2}$$

where $W(a,t)$ is weight at age a and time t. Anabolism relates to the proportionality between gut surface area of digestion and body volume, whereas catabolism is assumed to be proportional to body volume. Eq. 4.2 provides equivalency between the Chapman-Richards equation, and can be rewritten in a bioenergetic modeling framework (e.g., Adams and Breck 1990)

$$\frac{dW(a,t)}{W(a,t)dt} = (C - C * p_E - C * p_U) - R = C * (1 - p_E - p_u) - R = C * A - R \tag{4.3}$$

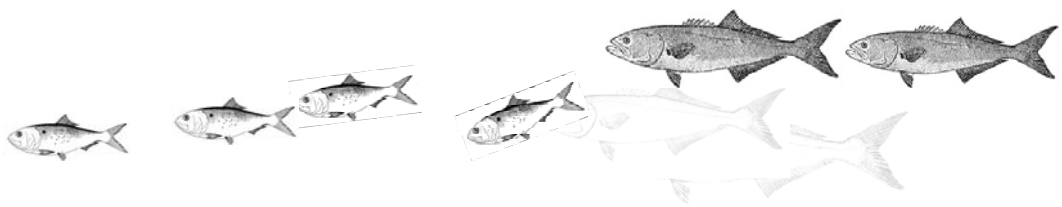

where, the parameters *C* is consumption and *R* is respiration or total metabolic costs. Rate functions for egestion and excretion are modeled as relative proportions of *C* , i.e., *Egestion* $\equiv C * p_E$ and *Excretion* $\equiv C * p_U$, each function ranging between 0 and 1. Finally, $A = 1 - p_E - p_U$ is food assimilation efficiency, a quantity that reflects what is consumed minus what the body cannot process or does not use. Predator consumption rate *C* can be modeled as a function of fish size in weight *W(a,t)*, water temperature *T(t)*, salinity *S(t)*, and prey abundance *N(a,t)*. This leads to the relative growth rate potential of fish

$$\frac{dW(a,t)}{W(a,t)dt} = \alpha_C [f_C(T) * f_C(S) * f_C(N)] W(a,t)^{\beta_C} - \alpha_R [f_R(T) * f_R(S) * f_R(V)] W(a,t)^{\beta_R} \qquad (4.4)$$

The water temperature dependence function $f_C(T)$ is a function describing the ascending and descending portions of a parabolic curve. The term $f_C(S)$ is a salinity-dependent consumption function derived from field and laboratory experiments. The predator 'functional response' $f_C(N)$ relates the average spatial arrangement of predator to prey (Cosner et al. 1999). Respiration rate *R* can be modeled as an allometric function of body weight, water temperature *T(t)*, salinity *S(t)*, and average swimming speed $V_p(a)$, $f_R(T)$ and $f_R(S)$ are temperature- and salinity-dependent proportional adjustment factors of the respiratory rate; and $f_R(V)$ is an activity-dependent proportional adjustment to specify respiration rate above the standard reference level. Thus, eq. (4.4) captures fundamental bioenergetic growth principles into the ensemble weight equation.

Cohort abundance at age over time *P(a,t)* for predator and prey can be represented by the McKendrick-von Forester (Ault and Olson 1996) population conservation equation

$$\frac{dP(a,t)}{dt} = -\left[M \left\langle 1 - \gamma \left(\frac{W(a,t) - W_{opt}(a)}{W_{opt}} \right) \right\rangle + F(a,t) \right] P(a,t) \qquad (4.5)$$

where *F(a,t)* is fishing mortalities. The base natural mortality rate *M* (i.e., the rate for average environmental conditions) for both species can be estimated using maximum average lifespan methods. The realized natural mortality rate can be determined as the base rate modulated as a function of the physical (e.g., "habitat quality") and biological (predator and prey densities) features of the environment. In our model, we can link predator *P(a,t)* natural mortality to growth by making the magnitude of realized *M* proportional to optimum size of a fish at age *W(a,t)* relative to a current size where $W_{opt}(a)$ is the optimum weight-at-age of a fish growing in an environment with no competitive effects (i.e., unlimited food resources), and γ is a mortality scale factor to weight the factor response. Predator stock biomass at age is the product of numbers-at-age times weight-at-age. Since weight-at-age is an 'environment-dependent' function, this arrangement explicitly makes predator stock biomass a function of predator density, prey density, age, time, location, bottom type, salinity, temperature, and swimming velocity.

In the model, prey natural mortality rate M is separated into two components: environmental M_H, and predation (and/or fishing) M_P mortalities. We will compute

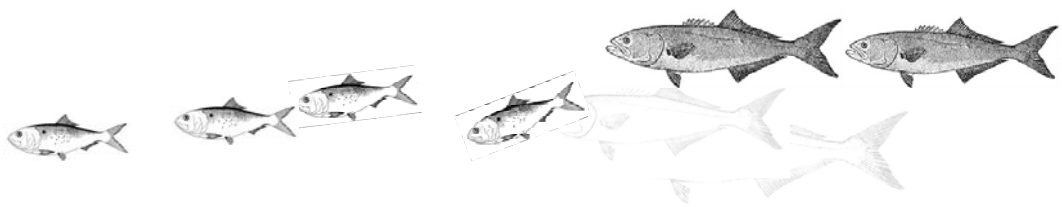

environmental mortality of prey as $M_H = M^* f(D,S.B)$. The term $f(D,B,S)$ relates mortality rates to features of the environment: depth $D(x,y,t)$, salinity $S(x,y,t)$, and bottom substrate $B(x,y,t)$ at location (x,y) at time t. Using a conservation principle, predation mortality M_P can be computed as $M_P = M^* \Psi^* f_c(N)$, where this mortality is proportional to the consumption rate calculated in the predator energetic submodel (eq. 4.4), $f_C(N)$ is the functional response of predator P to prey density N, and Ψ is a mortality effect weighting factor. This arrangement makes prey mortality a function of the redistribution of predators due to changing environmental fields. In essence, the mortality rates of predator and prey are higher while searching to reflect the basic foraging-movement risk notion that most juvenile mortality is likely to occur while feeding or dispersing. This creates an explicit link between feeding and mortality rates.

An important feature of the coupled biophysical model is its capability to estimate "spatial growth rate potential", a quantity that defines the suitability of "habitats" to the production dynamics and sustainability of fishery resources. This quantity provides a formal definition of essential fish habitat (Bohnsack and Ault 1996, Rubec et al. 1999, 2001; Ault et al. 1999a, 2003), and is derived through explicit modeling of the fine-scale encounter dynamics and behaviors of foraging arena theory (Walters 2003). This arrangement makes prey mortality a function of the redistribution of predators due to changing environmental fields. In essence, the mortality rates of predator and prey are higher while searching to reflect the basic foraging-movement risk notion that most juvenile mortality is likely to occur while feeding or dispersing. This creates an explicit link between feeding and mortality rate.

Biomass $B_s(a,t)$ of a species s at age a and time t is the product of numbers-at-age $N_s(a,t)$ times weight-at-age $W_s(a,t)$. The population biomass $B_s(t)$ at time t is computed by integrating the biomass at age over all the age classes (a=0,..., λ):

$$B_s(t) = \int_{a_r}^{a_\lambda} N_s(a,t) W_s(a,t)\, da \qquad (4.6)$$

Fishing gear(s) are normally size, rather than age, selective. As written, weight-at-age is an 'environment-dependent' function that explicitly makes predator stock biomass at a particular space point a function of a complex "habitat" comprised of predator densities, prey density, age, time, bottom type, salinity, temperature, and swimming velocity. The yield (catch) in weight $Y_{ws}(F,L',t)$ from a given species s of size class L at time t is the product of numbers-at-age conditioned on size. $N_s(L|a,t)$, times weight-at-size $W_s(L|a,t)$. The total catch of species s in a given day is computed by integrating the catch at size L from the minimum size of first capture regulated by the fishery L' to the maximum size observed in the stock L_λ integrated over the time period

$$Y_w(F,L',t) = \int_{L'}^{L_\lambda} F(a,t) B(L \mid a,t) dL = \int_{L'}^{L_\lambda} F(a,t) N(L \mid a,t), W(L \mid a,t) dL \qquad (4.7)$$

Yields (or even yields per recruit) can be calculated from recruitment. Spawning stock biomass is a measure of the stock's reproductive potential or capacity to produce newborn, ultimately realized at the population level as successful cohorts or year classes. Spawning stock biomass is obtained by integrating over individuals between the minimum size of first maturity L_m, and maximum reproductive size (here assumed to be the maximum size L_λ) in the stock. These methods are easily adapted to look at contemporaneous fishery management benchmarks like SPR and limit control rules. In addition, fishing effort can be distributed over the model's spatial

domain in relation to observed patterns of nominal effort where the selectivity patterns of the various gear types are specifically accounted for in the scenario design.

4.2 Larval Transport and Recruitment Uncertainty.- Stock and recruitment is a complex series of biological- and physically-mediated processes and events that regulate the eventual recruitment of juveniles to the stock (Rothschild 1986, 2000). In our model, recruitment boundary conditions for each modeled species *N(0,t)* (either prey or predator) are simulated using physical transport of eggs and larvae from parent spawning locations to inshore recruitment areas. Each larval cohort will be divided into *n* number of manageable patches (realistic in population terms and computationally efficient) and distributed over spawning sites or over entrances of all possible pathways into the nursery grounds (such as mouth of Chesapeake Bay, Delaware Bay, New York Harbor, etc.).

Spatial movements of each patch are tracked during the pelagic larval transport period using a Lagrangian drift model (Ault et al. 1999a, Wang et al. 2003). To estimate Lagrangian drift for both 'passive' and biologically-active 'behavioral' particles, we will model horizontal particle movements in continuous two dimensional space as the distance change along the *x* and *y* coordinate axes during a time interval *dt* via the ordinary differential equation

$$\frac{dx}{dt} = X = X_c + (X_r + X_b) \qquad (4.8)$$
$$\frac{dy}{dt} = Y = Y_c + (Y_r + Y_b)$$

where *X* and *Y* are the *x* and *y* coordinate velocities for a patch, respectively. Subscripts *c*, *b*, and *r* respectively denote velocity components due to ocean currents X_c (i.e., passive movements), behavioral taxis X_b (i.e., directed movements towards optimal environmental-biological conditions by active swimming), and diffusion X_r (i.e., purely random movements). Terms X_r and Y_r are velocity components of density diffusion of the whole patch that were simulated as a two dimensional random walk (Berg 1993). The behavioral taxis (movement up a favorable gradient) component will be comprised of two parts: swimming velocity; and, a net resultant angular direction of movement (i.e., the angle of motion). This idea can be written in polar coordinate form as

$$X_b = \Lambda_b * \cos(\theta)$$

$$Y_b = \Lambda_b * \sin(\theta) \qquad (4.9)$$

$$\Lambda_b = V_N \left[\frac{E_{opt} - E(x,y,t)}{\max[E(\mathbf{X},\mathbf{Y},t)] - E_{opt}} \right]$$

$$\theta = \sin^{-1}\left(\frac{\phi_y}{\sqrt{\phi_x^2 - \phi_y^2}} \right) + \xi\pi$$

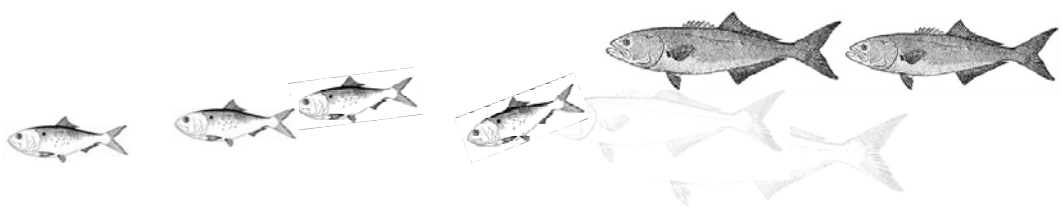

where, Λ_b is a function that modulates the maximum average swimming speed V_N , $E(x,y,t)$ is an environmental feature vector comprised of physical oceanographic variables such as salinity, temperature, chlorophyll concentrations, currents, etc., at location (x,y) at time t, E_{opt} is the optimal condition for growth, Max[$E(\boldsymbol{X},\boldsymbol{Y},t)$] is the maximum value for the entire grid, and ϕ_x and ϕ_y are gradients along x and y coordinate axes where, e.g., $\phi_x = \frac{\partial E(x,y,t)}{\partial x}$. The parameter ξ is a normally distributed random deviate that allows for behavioral error in directional movement.

4.3 Juvenile and Adult Ontogenetic Movements and Migrations.- Juvenile and adult movements and migrations were based on the idea that animals could detect gradients of "habitat" quality, which provide the stimuli for predator and prey movement behaviors. These spatially-explicit mosaics of habitat quality within model unit cells directly influenced population-dynamic rates of growth and mortality. Factors affecting menhaden "***spatial growth rate potential***" (Ω), measured as $\frac{dW}{Wdt}$, were components of an "essential habitat" vector that included such time-dependent physical variables salinity, prey density, chlorophyll, and temperature (Ault et al. 1999a, 2003; Luo et al. 2001). Mathematically, this complex dynamic feature vector can be resolved in a single variable (i.e., Ω the expected growth for an animal occupying that cell during a given time step) for each model cell. All point computations within the model domain produced a spatial map of Ω, which represents a quantitative spatial index of habitat quality over time and space. We modeled behavioral movements based on an optimization search by the fish at its present location relative to the spatial growth rate potential of adjacent habitat cells in the surrounding environment. Movement of fish patches on continuous two-dimensional coordinate space can be described by two velocity vector components that are dependent on Ω

$$X_b(\Omega) = \left(\tilde{V}(a,t) * \left[1 - e^{\phi\left(\frac{\Omega(t) - \Omega_{\max}}{\Omega_{\max}} \right)} \right] \right) * \cos\left(\theta_{\max} + \xi\pi\right)$$

$$Y_b(\Omega) = \left(\tilde{V}(a,t) * \left[1 - e^{\phi\left(\frac{\Omega(t) - \Omega_{\max}}{\Omega_{\max}} \right)} \right] \right) * \sin\left(\theta_{\max} + \xi\pi\right) \qquad (4.10)$$

where X_b, Y_b are coordinate velocity components due to behavior, ξ is a random normal variate, Ω_{max} is the maximum growth rate potential within the detection range of the fish, $\tilde{V}(a,t)$ is the net displacement velocity of the fish at age a, Φ is a scalar multiplier, and θ_{max} is the heading to the location of maximum growth rate potential within the detection range of the fish. The first term in parenthesis on the right hand side of the above equation represents the fish speed as a function of growth rate potential Ω, while the second term is the directional heading of fish as a function of the perceived proximal habitat quality. The net displacement speed is the actual distance moved between two points from the start and end of one time step, recognizing that substantial searching may occur during this time.

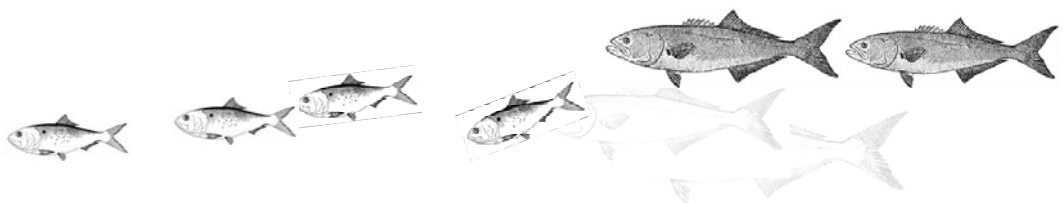

Assimilation of Physical and Biological Databases and Data-layers

All possible physical and biological data layers regarding the habitat and biological community and biophysical environments will be identified and compiled. This information set contains a relatively long time series of information comprised of a substantial database on predators and prey species, biophysical 'habitats', and quantitative characteristics of the fisheries. These data are somewhat 'spread out' and will require considerable synthesis and assimilation to ready them for model applications. All data sources will be strategically analyzed and processed to fill in gaps and produce a robust spatial description of the multispecies fisheries environment to be modeled.

5.1 Regional Bathymetry.- Two-minute global elevation data (ETOPO2) was obtained from National Geophysical Data Center. These data were from 3 major sources: (1) seafloor data between latitudes 64° North and 72° South were derived from satellite altimetry observations combined with carefully, quality-assured shipboard echo-sounding measurements, by Dr. Walter H.F. Smith, of the NOAA Laboratory for Satellite Altimetry, and Dr. David T. Sandwell of the Institute of Geophysics and Planetary Physics at the University of California, San Diego; (2) seafloor data southward of 72° South are from the US Naval Oceanographic Office's (NAVOCEANO) Digital Bathymetric Data Base Variable Resolution (DBDBV), version 4.1, gridded at 5 minute spacing; some data in this region are from the older DBDB5 (these data were also used in ETOPO5). Seafloor data northward from 64° North are from the new International Bathymetric Chart of the Arctic Ocean (IBCAO) Version 1; and, (3) land topography is from the GLOBE Project, an internationally designed, developed, and independently peer-reviewed global digital elevation model (DEM), at a latitude-longitude grid spacing of 30 arc-seconds (30"). The GLOBE Task Team was established by the Committee on Earth Observation Satellites (CEOS) and is part of Focus I of the International Geosphere-Biosphere Programme - Data and Information System. These three major data sources were assembled into the single ETOPO2 2-minute data base without formal edge matching or other methods that alter the data as initially posted. Higher-resolution data take precedence, for example: data derived from GLOBE mask all other data, Smith/Sandwell data come next, followed by IBCAO, with the 5-minute data filling any gaps. Five-minute data from DBDBV and ETOPO5 and 30-second data from GLOBE were regridded to 2 minute spacing by bicubic spline interpolation. IBCAO data were originally gridded in a polar stereographic projection; these data were interpolated along lines of constant latitude at 2 minute steps for every 2 minutes of latitude from 72° North to the pole.

5.2 Seawater Temperatures.- Daily sea surface temperature data were obtained from Naval Oceanographic Office Open Data Access Server (**Figure 5.1**). These temperature data were generated from real-time Global Area Coverage Advanced Very-High Resolution Radiometer (AVHRR) data from POES NOAA-14 and NOAA-15. Over 300,000 global Multi-Channel Sea Surface Temperature (MCSST) retrievals are generated and distributed daily in less than 5 hours from the time the satellites acquire the data. Global match-ups of satellite retrievals with drifting buoy measurements of sea surface temperature consistently maintain a global root-mean-square difference error of less than 0.7 ^{o}C. The spatial resolution of the MCSST is 6 minutes of latitude and longitude. Currently, we have obtained daily data from January 1, 2002 to September 20, 2003, weekly data from January 1, 1997, to January 1, 2001.

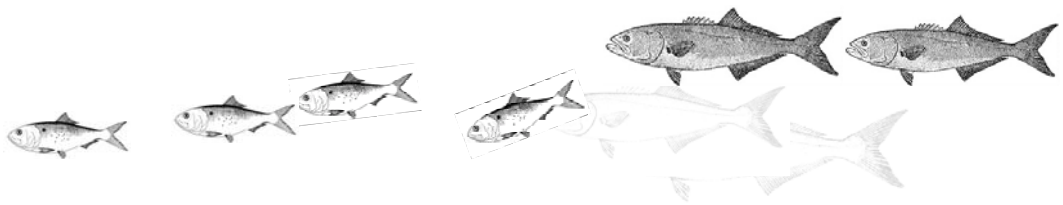

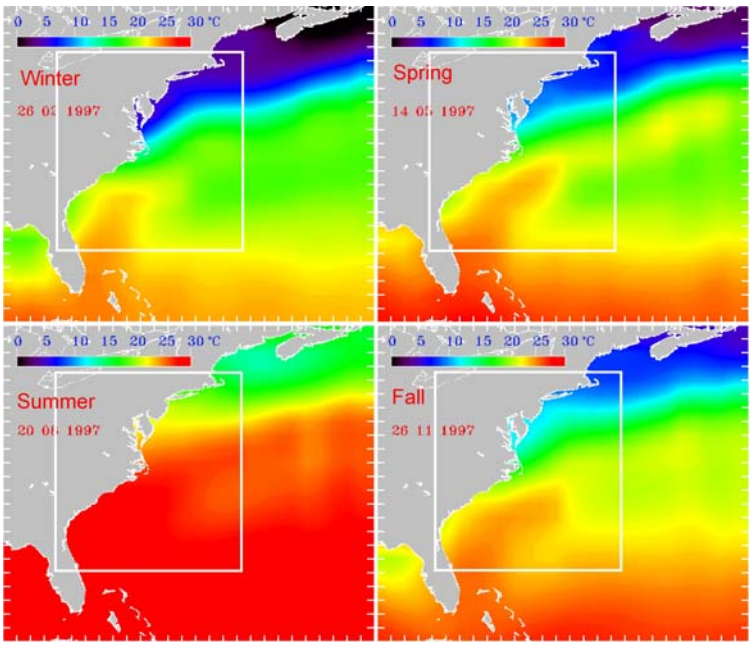

Figure 5.1- Seasonal sea surface temperatures for the model spatial domain. Source: U.S. Naval Oceanographic Office.

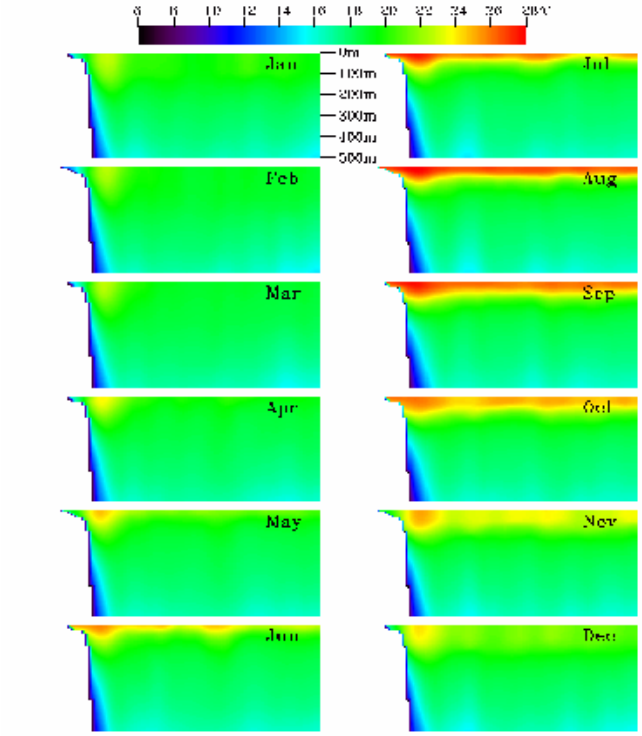

Figure 5.2. Monthly vertical temperature profiles for upper 500 meters. The transect is running from west to east at 34° N latitude. The Gulf Stream core is clearly visible at left end of each panel.

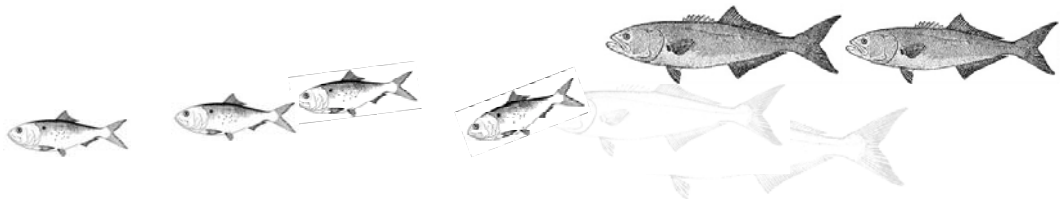

Average monthly vertical water temperature data were also obtained from Naval Oceanographic Office (**Figure 5.2**). The spatial resolution of the vertical temperature data is 15 minutes latitude and longitude. The monthly data have 88 vertical bins running from 0 to 6600 meters, where vertical spacing varied with depth. It has 2 meter bins for top 10 meters, 5 meter bins from10 to 100 meters, 10 meter bins from 100 to 200 meters, 20 meter bins from 200 to 300 meters, 50 meter bins from 300 to 400 meters, 100 meter bins from 400 to 1000 meters, and 200 meter bins from 1000 to 6600 meters.

5.3 Chlorophyll and Primary Production.- The purpose of the Sea-viewing Wide Field-of-view Sensor (SeaWiFS) Project is to provide quantitative data on global ocean bio-optical properties to the Earth science community. Subtle changes in ocean color signify various types and quantities of marine phytoplankton (microscopic marine plants), the knowledge of which has both scientific and practical applications. The SeaWiFS Project will develop and operate a research data system that will process, calibrate, validate, archive and distribute data received from an Earth-orbiting ocean color sensor. A detailed description of the objectives, organization and operations as well as the current status of the SeaWiFS Project is available at http://seawifs.gsfc.nasa.gov/SEAWIFS.html. Chlorophyll values are derived from multiple bands of SeaWiFS sensors by using field calibrated algorithms. The processes make atmospheric correction and validates the accuracy of chlorophyll concentration. The atmospheric correction is critical because only about 5% of the light seen at the satellite is reflected from within the ocean (water-leaving radiances). NASA and the SPO have placed the highest priority on assuring the accuracy of calculated water-leaving radiances, globally, over the life of the mission. Although meeting these requirements is an ongoing process, the accuracy and stability of the radiances has been well established, and development of global and regional bio-geochemical algorithms has proceeded on many fronts. Weekly composite SeaWiFS chlorophyll data from August 30, 1997 to Jul 31, 2003 have been down loaded (**Figure 5.3**). The spatial resolution of the SeaWiFS data is 5 minutes. To be consistent with the spatial resolution of the model, we re-grid the SeaWiFS data to 3 minutes using linear interpolation. Many missing data were also filled in using linear interpolation method.

We will seek out vertical chlorophyll profiles to enable estimation of chlorophyll concentrations from the upper 200 meters of the ocean along the Atlantic seaboard. Temporally, we need at least seasonal profile data, if not monthly. Spatially, we need coverage for four regions (Florida, South Atlantic Bight, Mid Atlantic Bight, Georges Bank), and within each region we need profile data for inshore, shelf, slope, and Gulf Stream environments (**Figure 5.4**). From these data we produced seasonal chlorophyll or monthly ratio profiles for each strata, such as that shown in the schematic plot (**Figure 5.5).** Chlorophyll concentrations at any depth can be estimated by multiplying the surface chlorophyll concentration by the ratio of the depths.

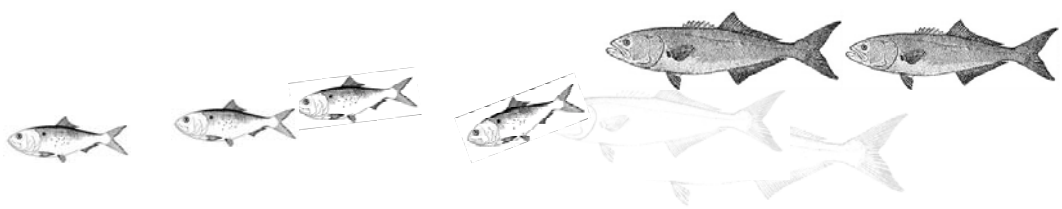

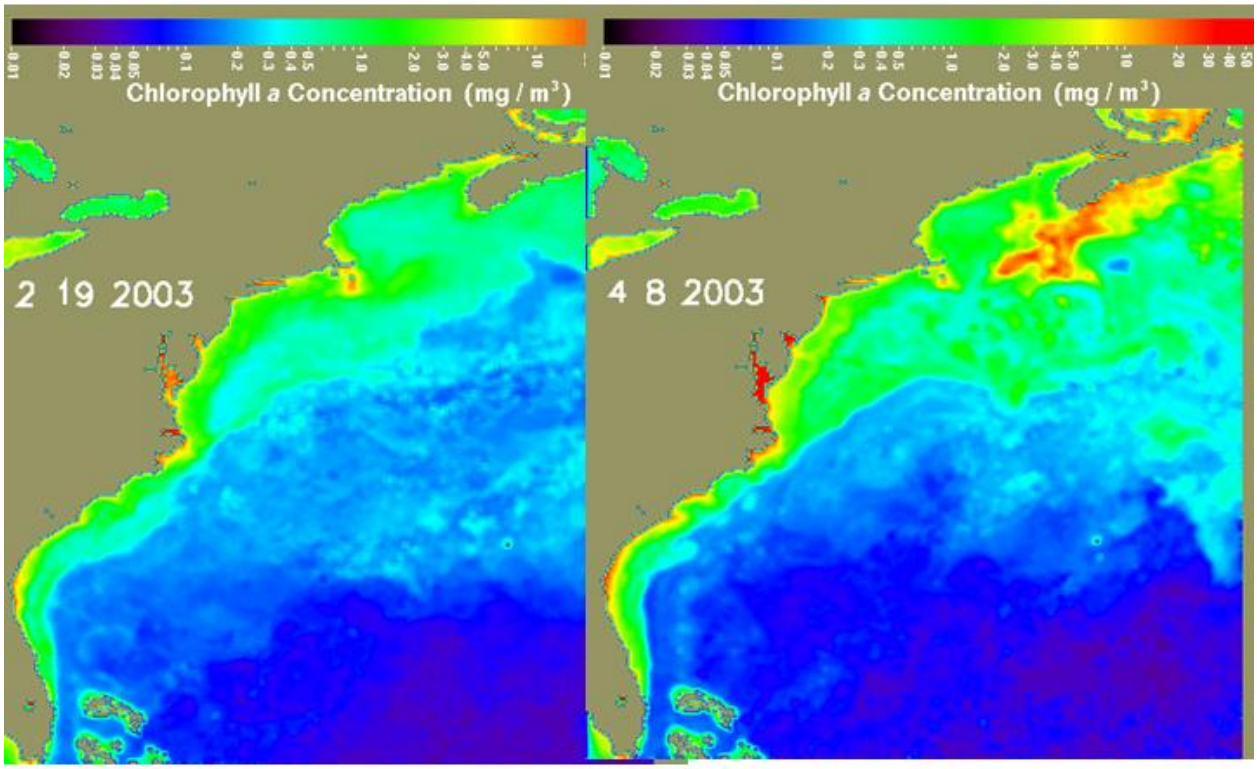

Figure 5.3.- SEAWIFS images of surface chlorophyll concentration for the Atlantic coast during February 19-27, and April 8-17, 2003.

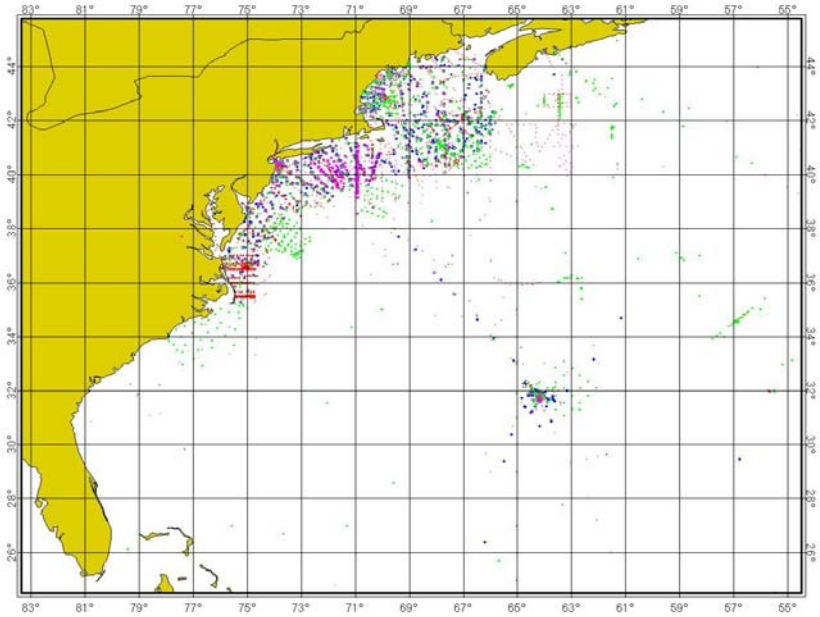

Figure 5.4.- Location of ship-board chlorophyll observations in the Atlantic coast region.

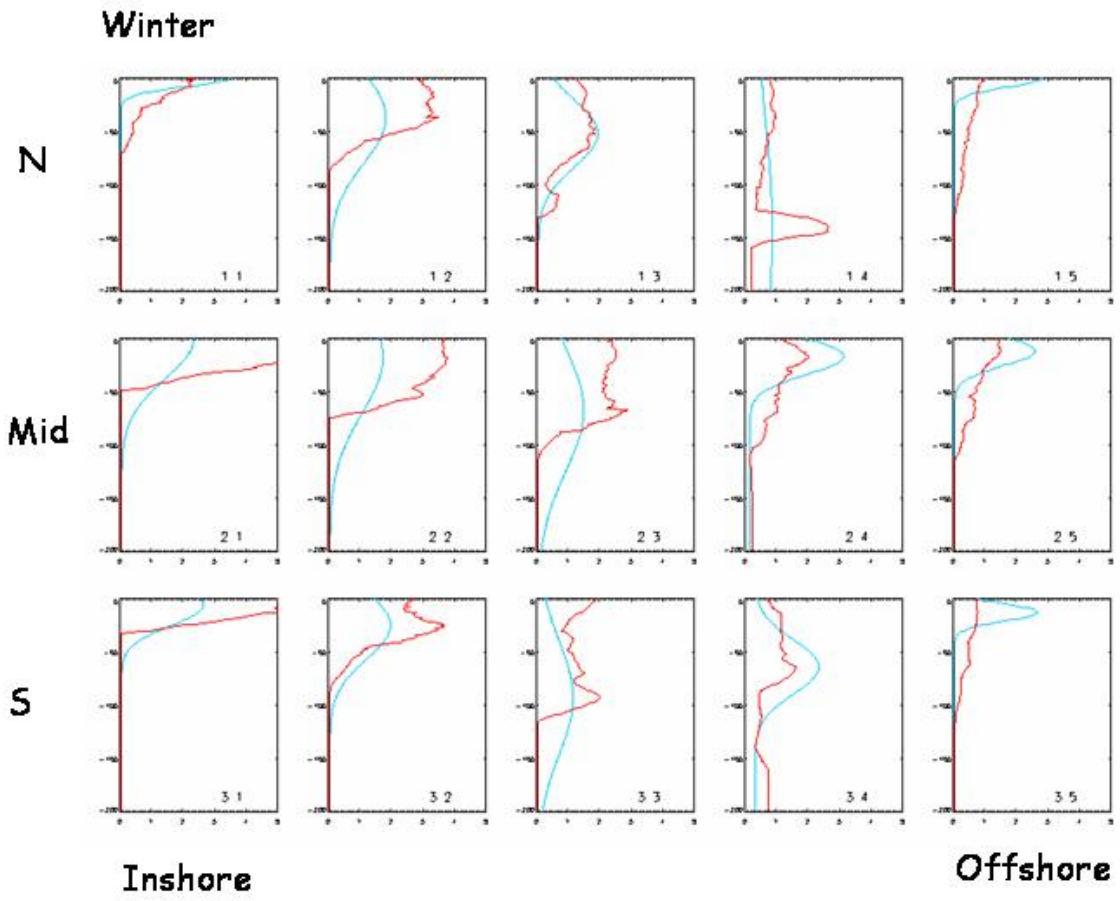

Figure 5.5.- Schematic profile of chlorophyll concentrations ratio to surface measurements.

Two other major sources of vertical chlorophyll profiles were:

South Atlantic Bight Recruitment Experiment (SABRE).- The goal of SABRE was to understand the relationship between variation in environmental factors and the variable recruitment of estuarine dependent fishes in the South Atlantic Bight. Information obtained through the SABRE project, principally focused on Atlantic menhaden, includes offshore spawning, onshore transport, estuarine development, and offshore migration and transport. Of particular interest to the modeling project are:

- Studies on temporal abundance and recruitment (W.F. Hettler, Stegmann et al.),
- Studies on larval distribution and transport (P.M. Stegmann and J.A. Yoder, Hare et al., Forward, Jr. et al., Blanton et al.),
- Modeling of inlet processes, alongshore transport, and physical oceanography (G.H. Wheless, Werner et al., Quinlan et al.),
- Spawning and nursery habitats (Checkley Jr., et al., Rice et al.)
- Spatial data from Larry Crowder (Duke U), D. Vaughan (NMFS), and Cisco Werner (UNC), Peter Ortner (NOAA), or others.

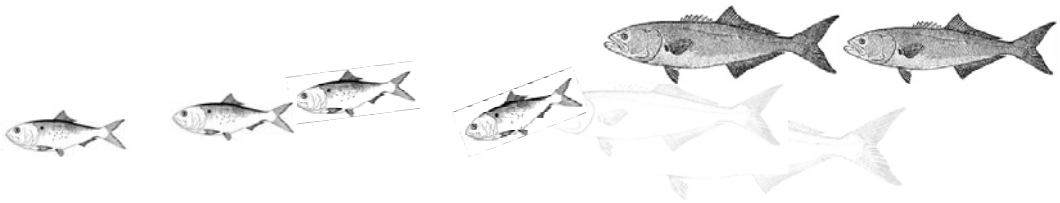

Global Oceans Ecosystems Dynamics (GLOBEC).- GLOBEC is a research program organized by oceanographers and fisheries scientists to address the question of how global climate change may affect the abundance and production of marine species. Of particular interest to the ASMFC proposed modeling project is the GLOBEC Georges Bank project which is studying the population dynamics of key Georges Bank species (cod, haddock and two species of zooplankton) in terms of their coupling to the physical environment and in terms of their predators and prey. That project also proposes to predict changes in distribution and abundance as a result of changes in physical and biotic environment, and to anticipate results of changes to climate changes. Other similar modeling projects are being conducted by GLOBEC in areas around the world, including studies focused on the Gulf Stream, western Pacific, and Southern Ocean. These studies will be reviewed for their applicability to the proposed project.

5.4 Benthic Habitats.- The Southeast Area Monitoring and Assessment Program (SEAMAP–South Atlantic) established a Bottom Mapping Work Group to develop a regional database that describes the location and characteristics of bottom habitats throughout the South Atlantic Bight. The primary focus of this effort was to identify the location and extent of hard-bottom reef habitats, since these areas represent essential fish habitat (EFH) for a wide variety of species that are commercially and recreationally harvested in the South Atlantic region. As part of the Work Group's overall effort to identify critical habitat areas, bottom areas where there was less definitive evidence of reef habitat, no evidence of reef habitat, and the locations of artificial reefs were also identified. To date, 65,727 data records have been compiled from databases obtained off North Carolina, South Carolina and Georgia, and Florida. Preliminary analysis of the SEAMAP database indicates that they may be of limited utility for this modeling project because the habitats were only broadly classified as hardbottoms, possible hardbottoms, or no hardbottom (**Figure 5.6**).

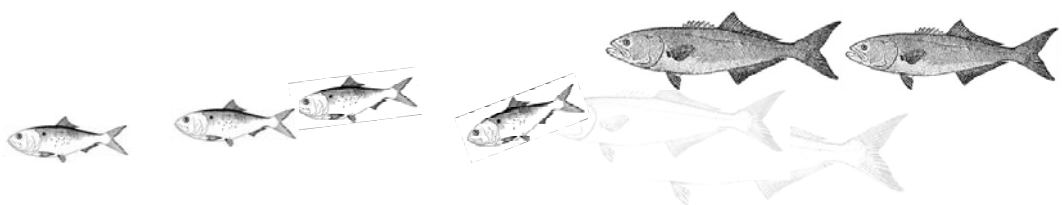

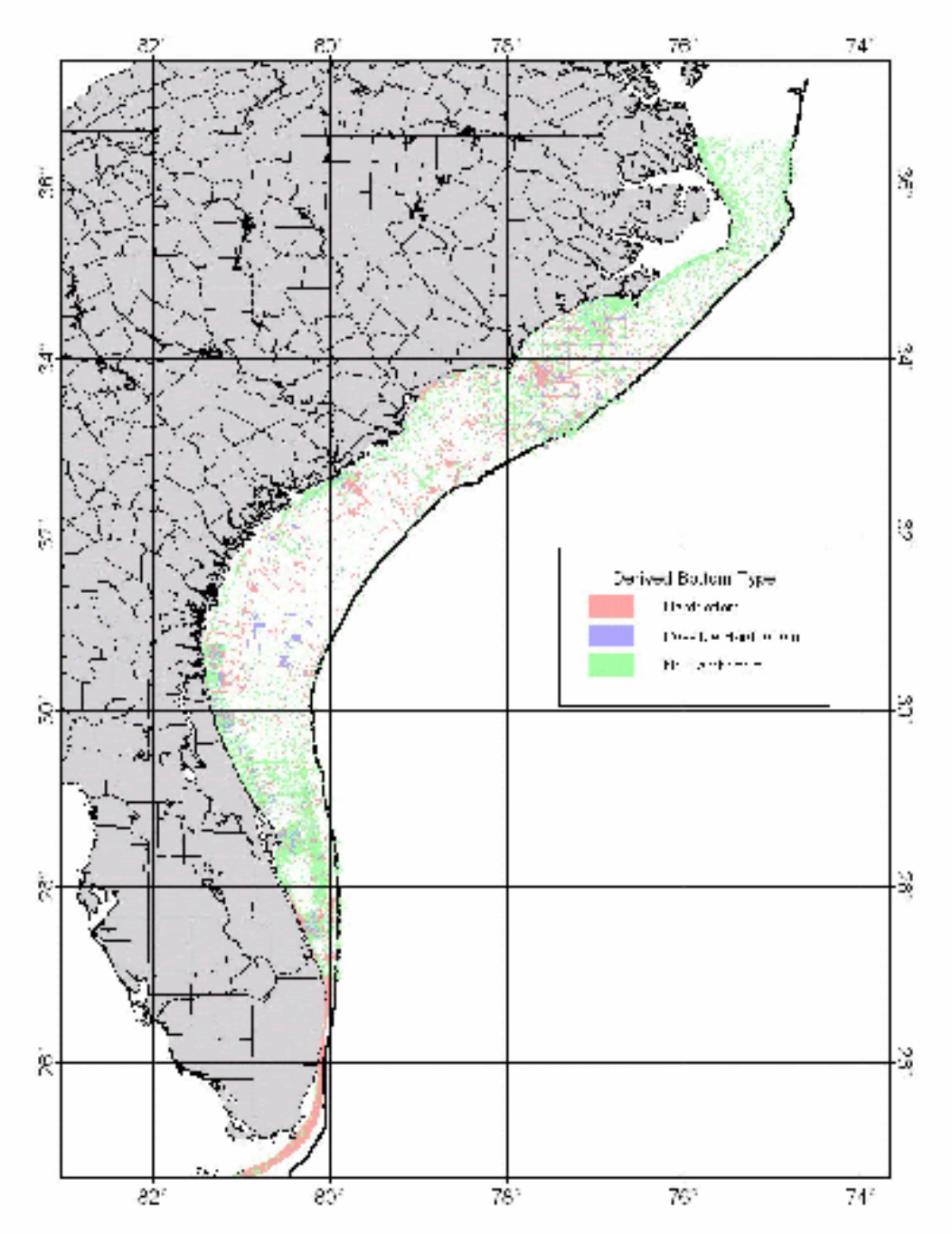

Figure 5.6.- Map of benthic habitats from the SEAMAP database.

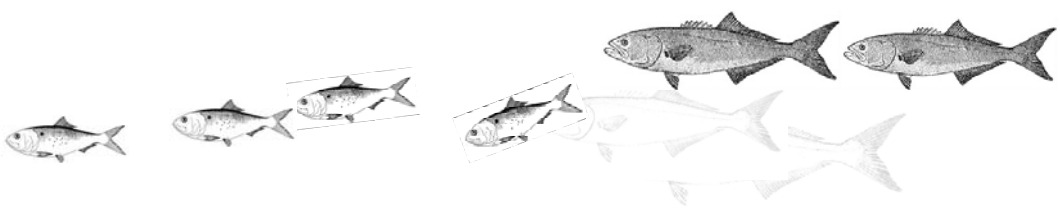

Fisheries and Population-Dynamic Components

A number of fisheries-dependent, fisheries-independent and population-dynamic databases were acquired, assimilated and mapped in GIS for the basis of creating model initial and boundary conditions, and to provide estimates of critical parameters or processes to calibrate the spatial ecosystem model performance. This section details those findings.

6.1 Fisheries-Dependent (Spatial Data).- Doug Vaughan and Joe Smith at NMFS-Beaufort, and Steve Murawski at the NEFSC served as contact persons and provided key regional fisheries data. These data for menhaden and bluefish have been organized along the following lines:

- Size composition of the catch, depth of the catches, etc., by state and federal waters.
- Abundance of stock by local or regional indices.
- Menhaden CDFR (captains daily fishing reports).
- Commercial logbooks and vessel trip reports.
- Spatial effective fishing effort data.

The following graphics highlight some of those results:

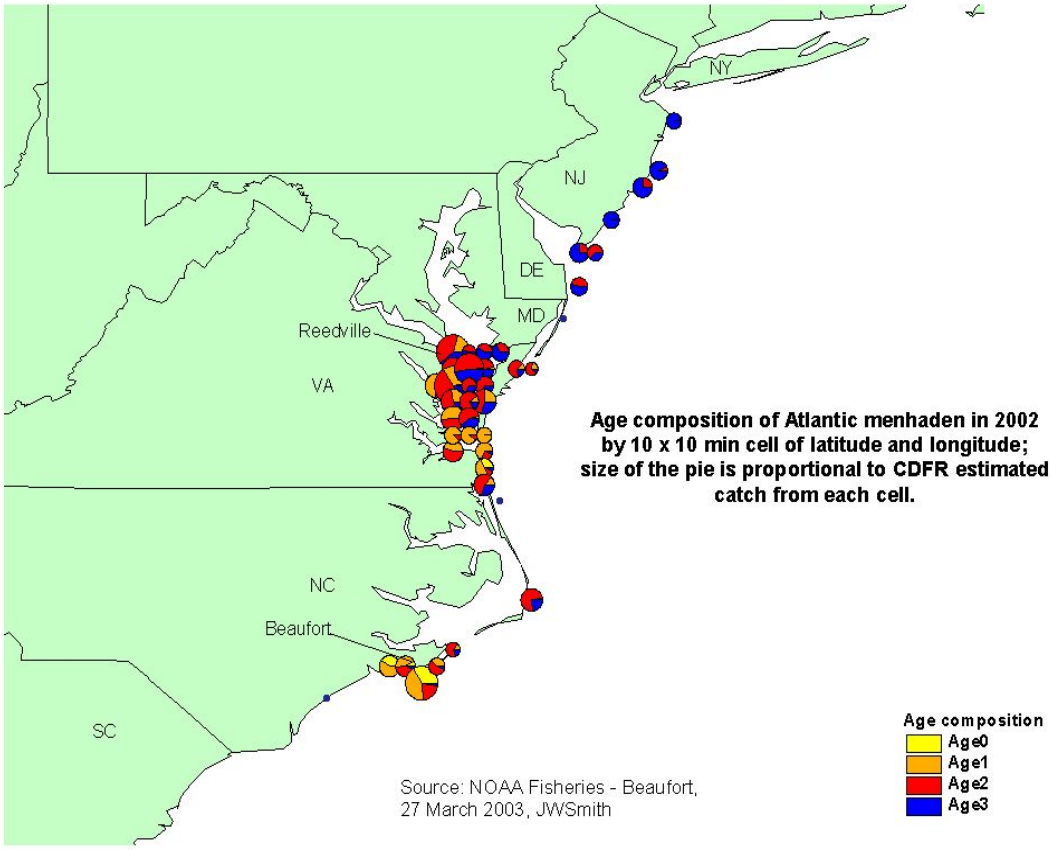

Figure 6.1.- Age composition of Atlantic menhaden in 2002 by 10 x 10 minute cells of latitude and longitude.

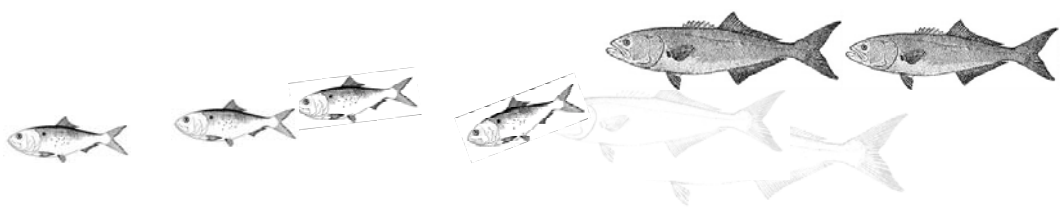

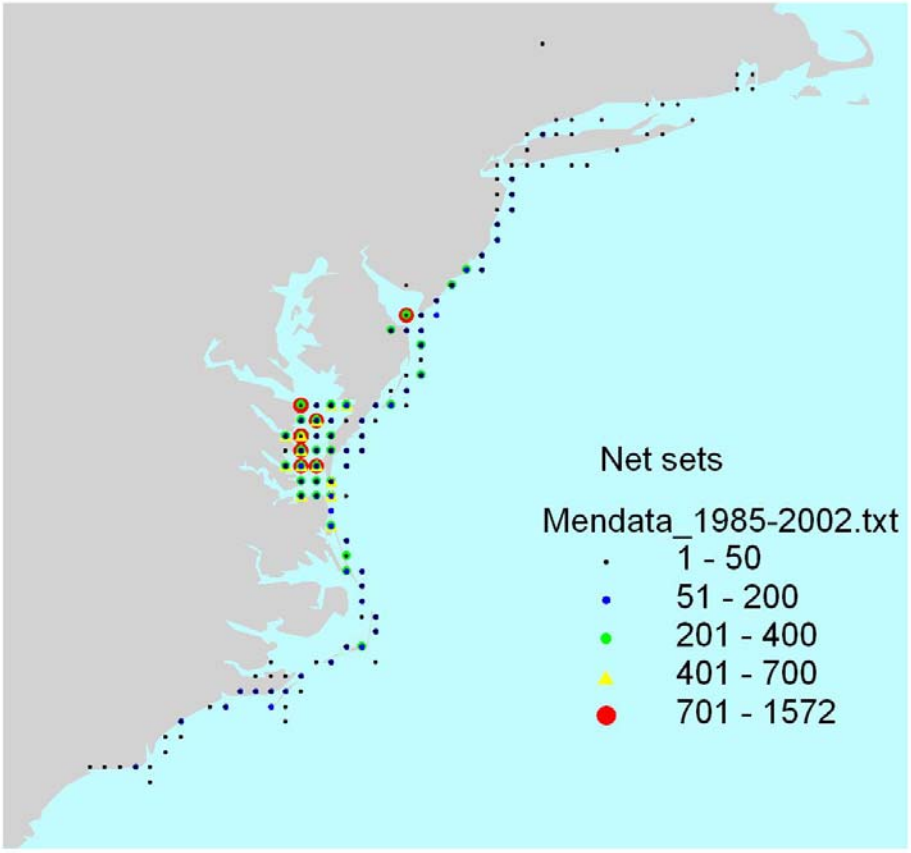

Figure 6.2.- Estimated spatial distribution of menhaden purse seine fleet fishing intensity compiled from menhaden nets sets conducted between 1985 and 2002

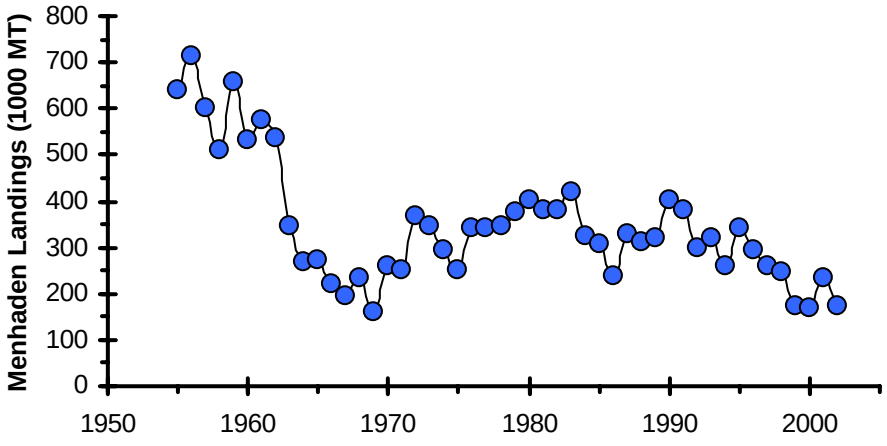

Figure 6.2a.- Atlantic menhaden fishery landings (metric tons) between 1955 and 2002.

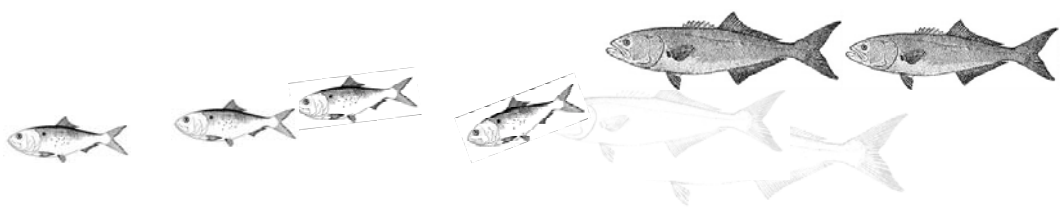

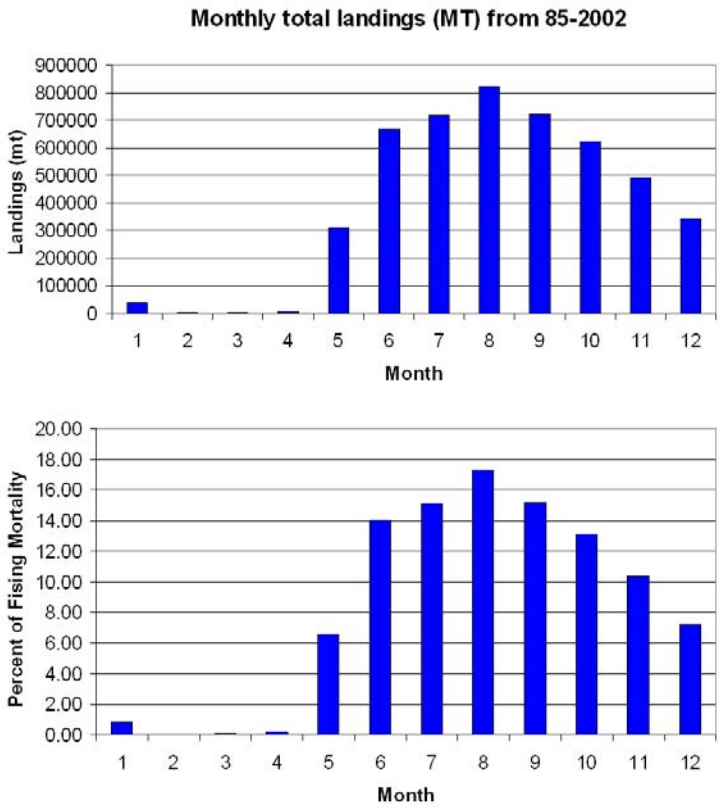

Figure 6.3.- Estimated monthly landing (metric tons) of menhaden from purse seine fleet fishing intensity compiled from menhaden nets sets conducted between 1985 and 2002.

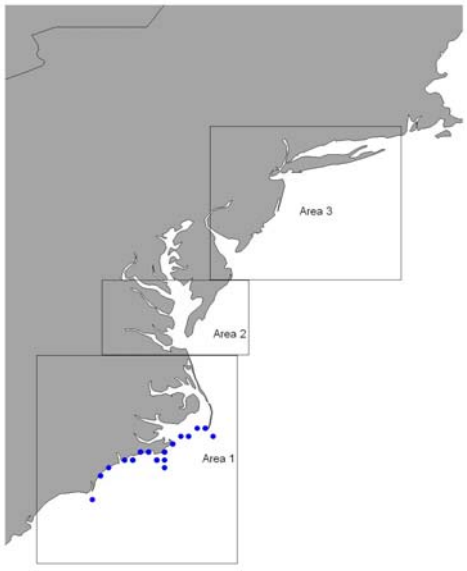

Figure 6.4.- Map showing regionalization of catch and effort data into 3 major zones along the US Atlantic coast: Area 1 (south); Area 2 (mid-Atlantic); and, Area 3 (northeast).

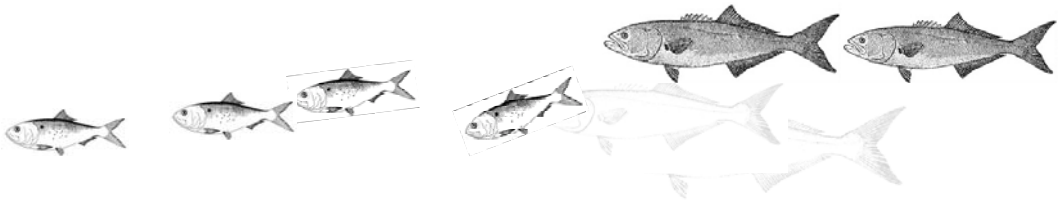

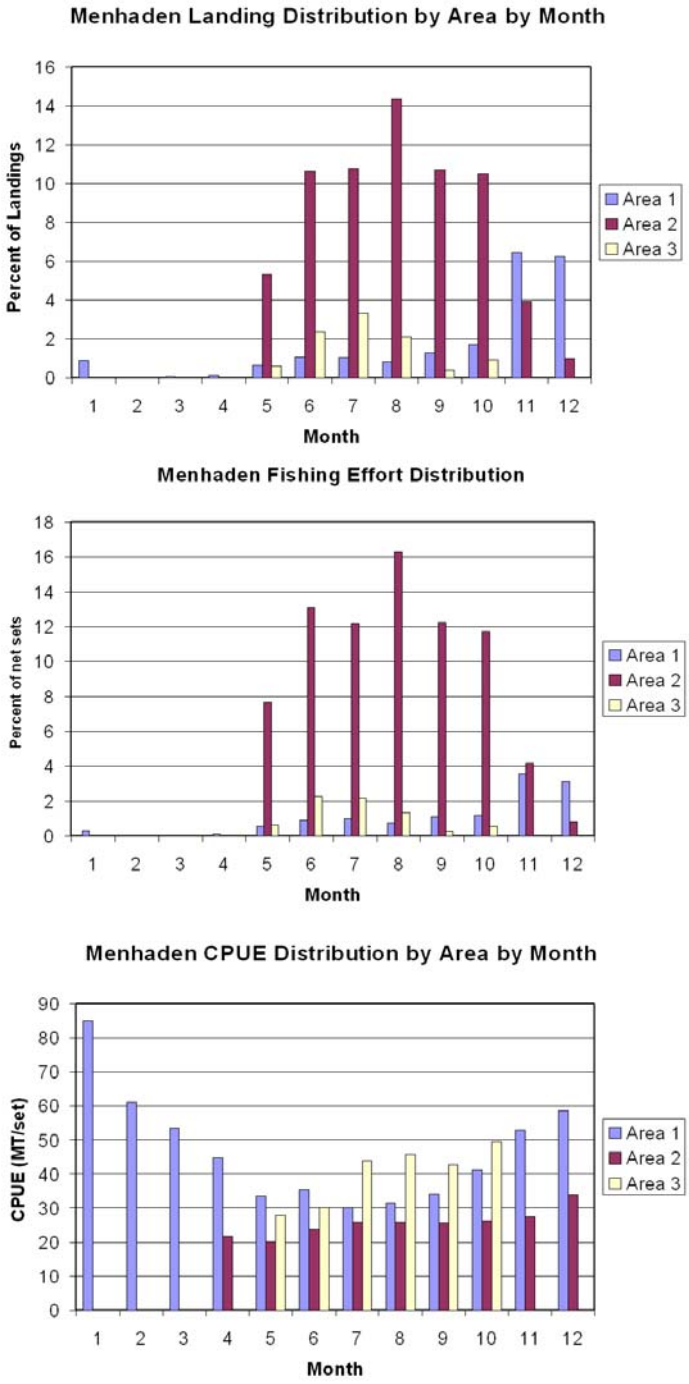

Figure 6.5.- Atlantic menhaden fishery landings and effort by 3 areas: (top) landings spatial distributions by month; (middle) fishing effort by month; and, (bottom) CPUE by month.

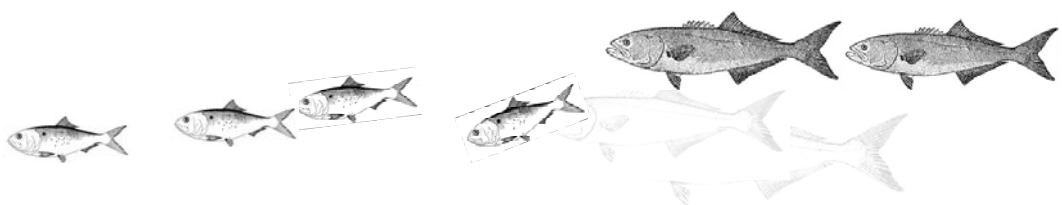

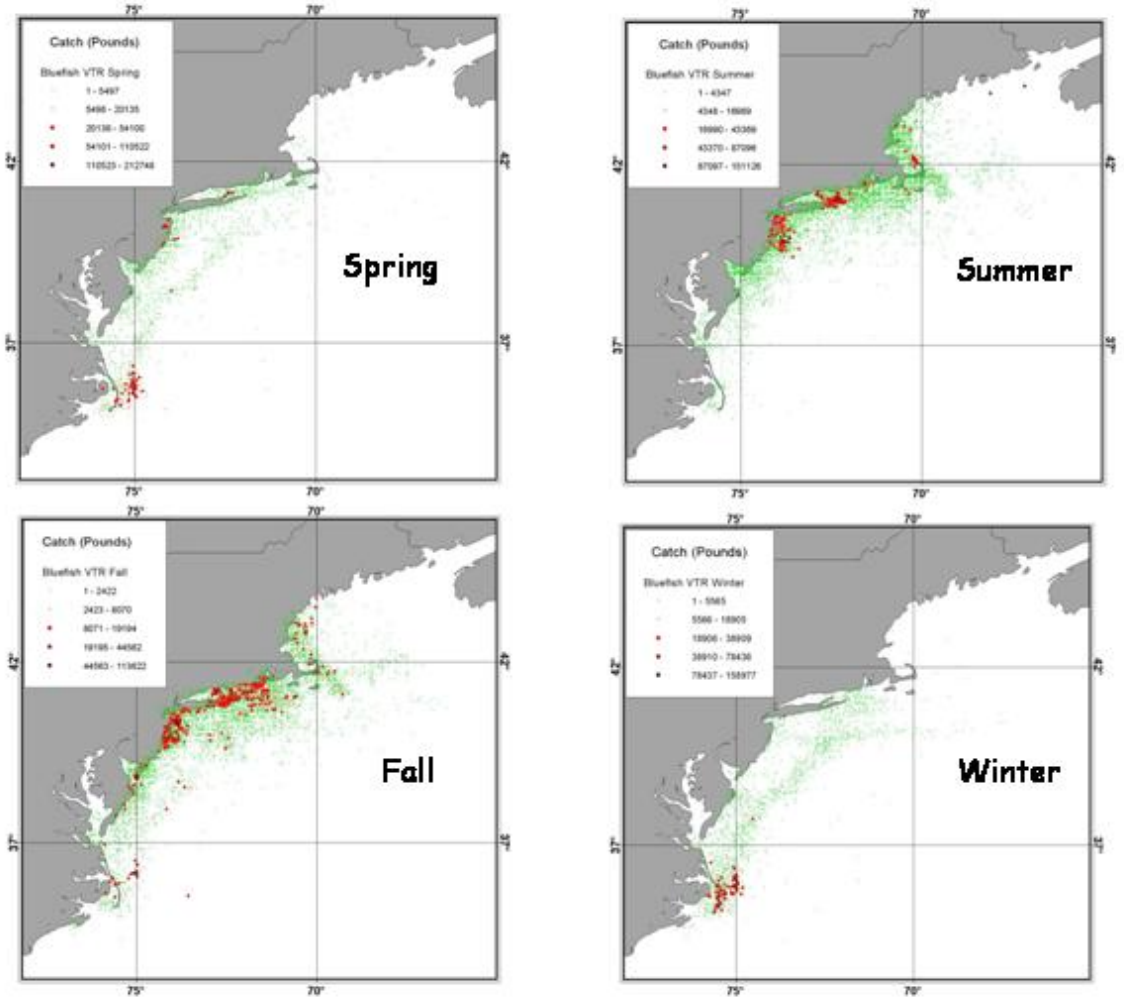

Figure 6.6.- The origin of bluefish landings by season as determined from the vessel trip reporting system for the period 1990-2002.

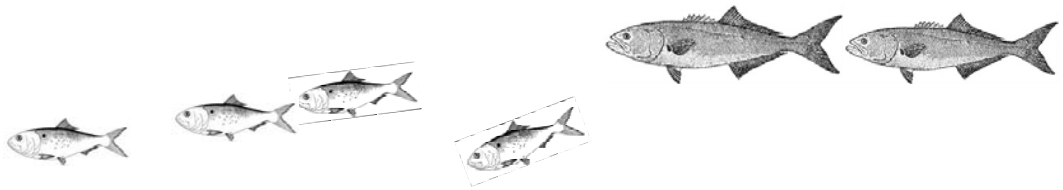

Bluefish Landings

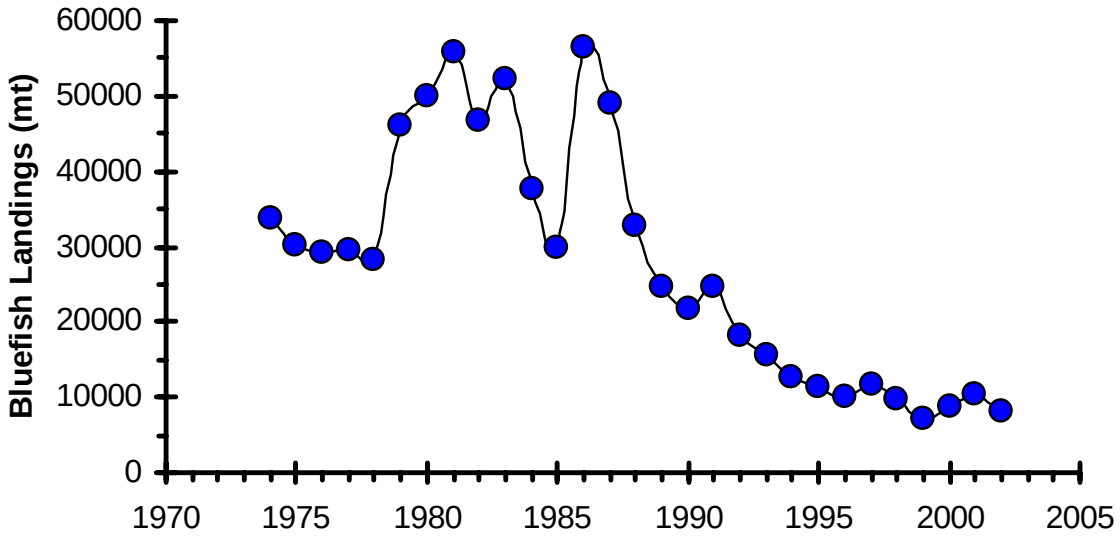

Figure 6.6a.- Landings (metric tons) of bluefish in the Atlantic coast region from 1973-2002.

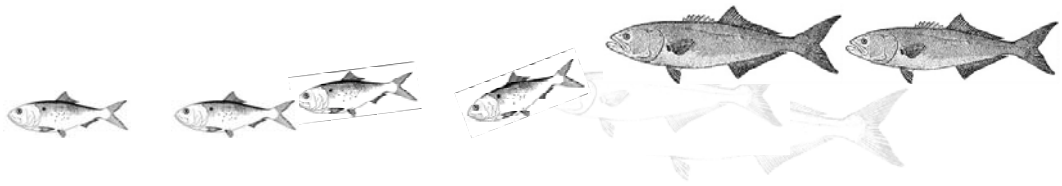

6.2 Fisheries-Independent Databases.- A number of sources of fisheries-independent data were identified to help determine the spatial and seasonal distributions of the target multispecies complex by species density and size-structure.

6.2.1 SEAMAP Trawl Survey Databases

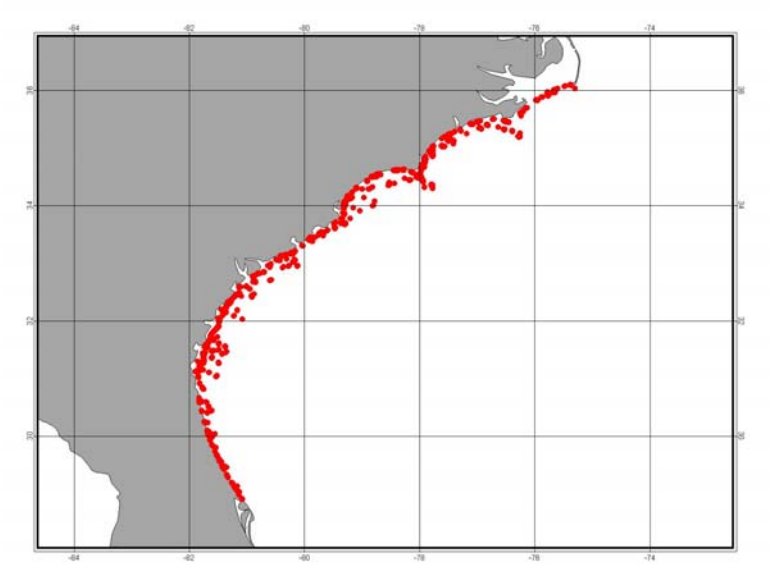

Figure 6.6.- Locations of SEAMAP trawl stations.

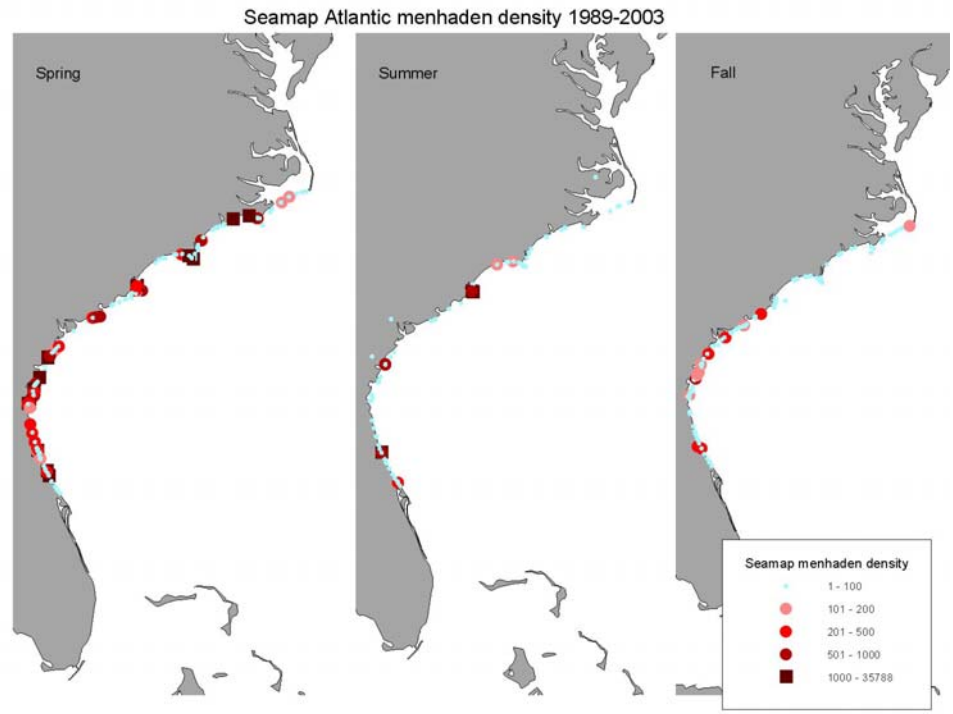

Figure 6.7.- Seasonal distribution of menhaden density in SEAMAP 1989-2003 trawl catches.

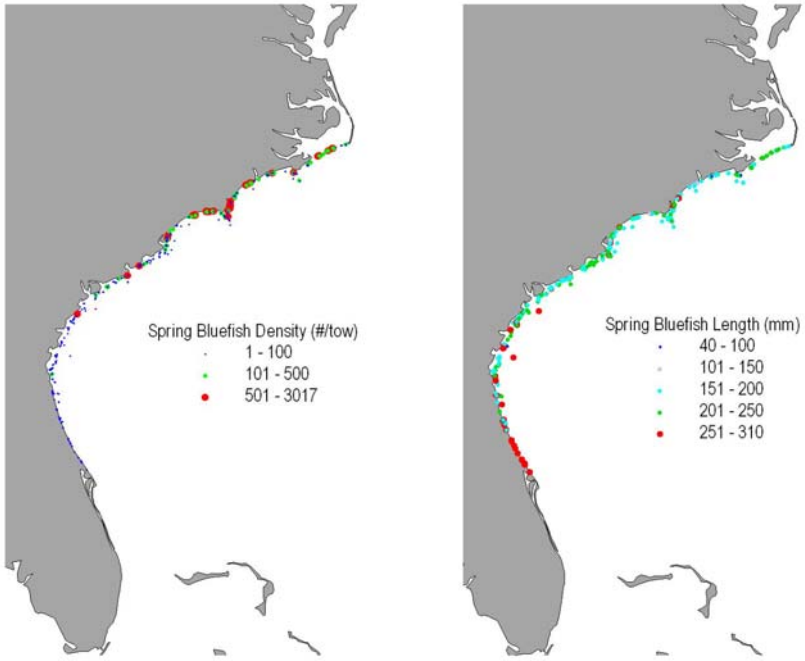

Figure 6.8.- Spring distribution of bluefish density and sizes in SEAMAP 1989-2003 trawl catches.

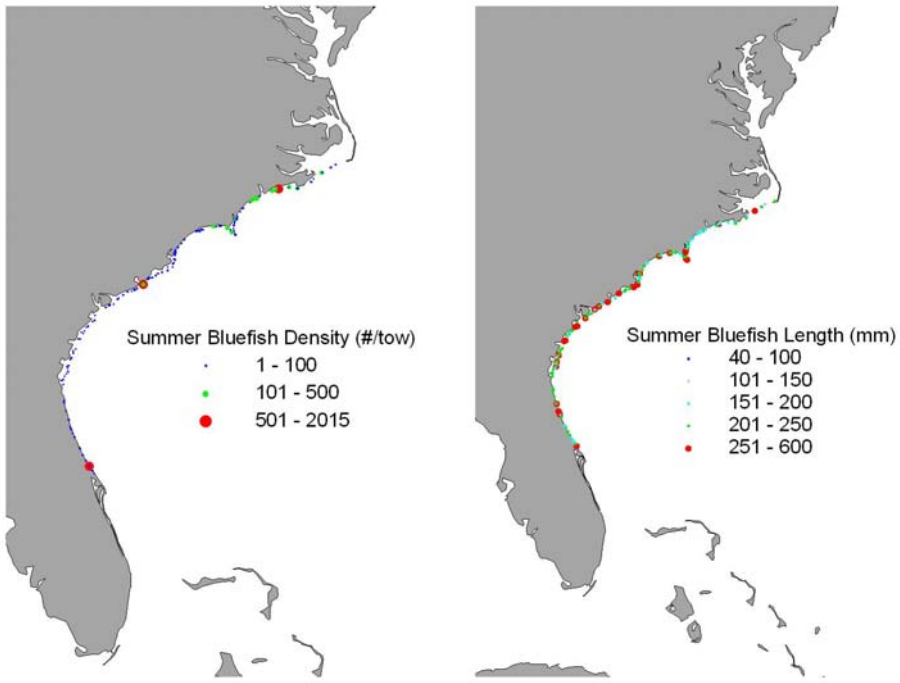

Figure 6.9.- Summer distribution of bluefish density and sizes in SEAMAP 1989-2003 trawl catches.

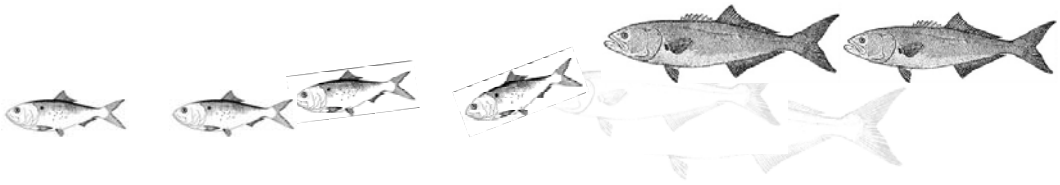

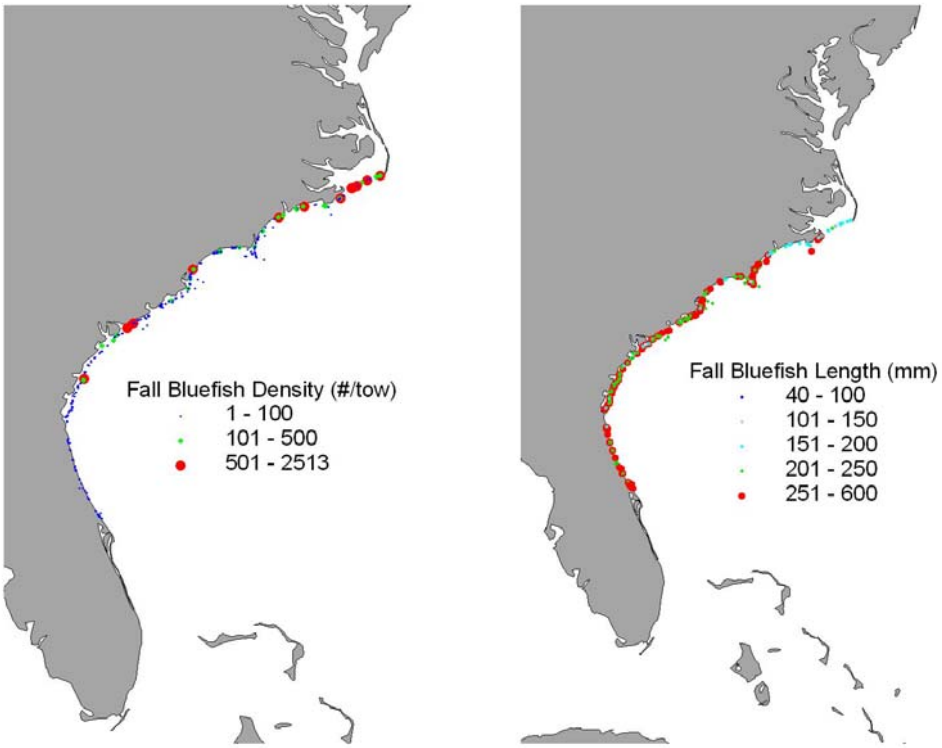

Figure 6.10.- Spring distribution of bluefish density and sizes in SEAMAP 1989-2003 trawl catches.

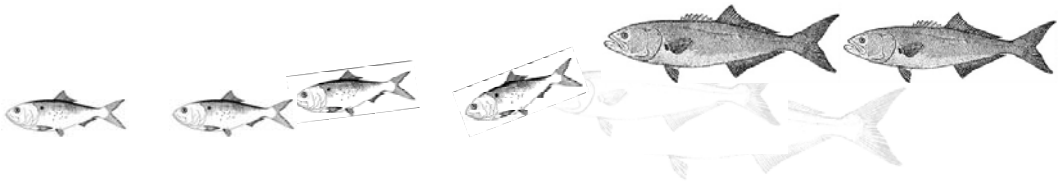

6.2.2. NMFS Northeast Fisheries Independent Trawl Survey.- The NEFSC trawl database provided a rich long-term source of spatial data on the target multispecies complex and a host of other potential prey resources.

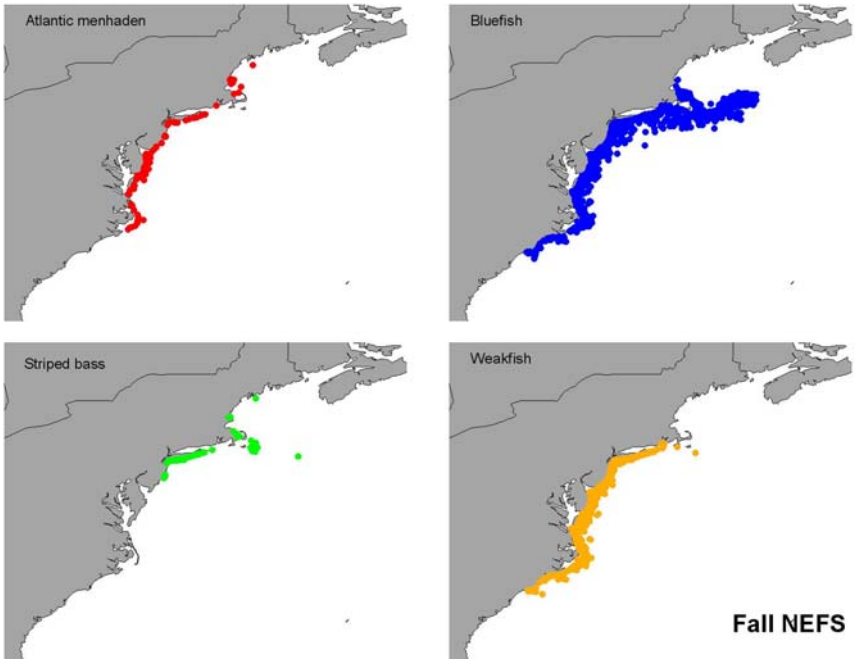

Figure 6.11.- NMFS northeast fisheries-independent Fall trawl survey sampling showing menhaden, striped bass, bluefish and weakfish distributions.

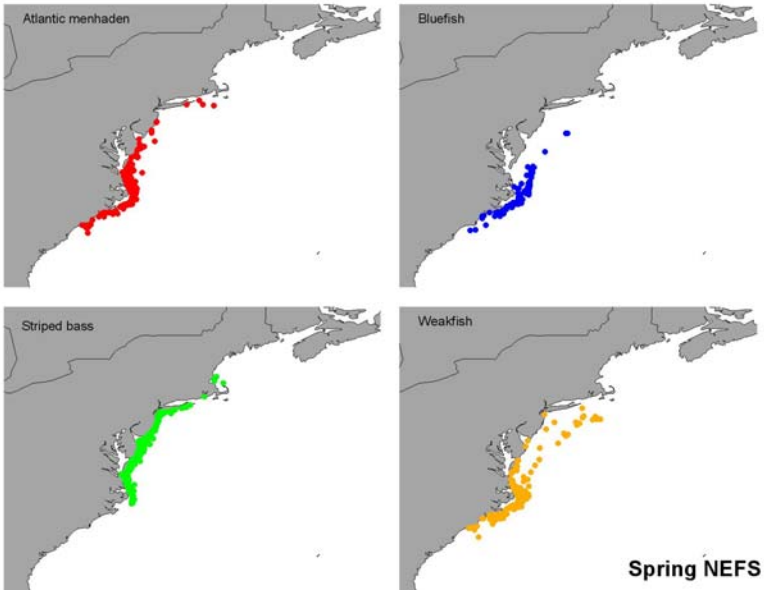

Figure 6.12.- NMFS northeast fisheries-independent Spring trawl survey sampling showing menhaden, striped bass, bluefish and weakfish distributions.

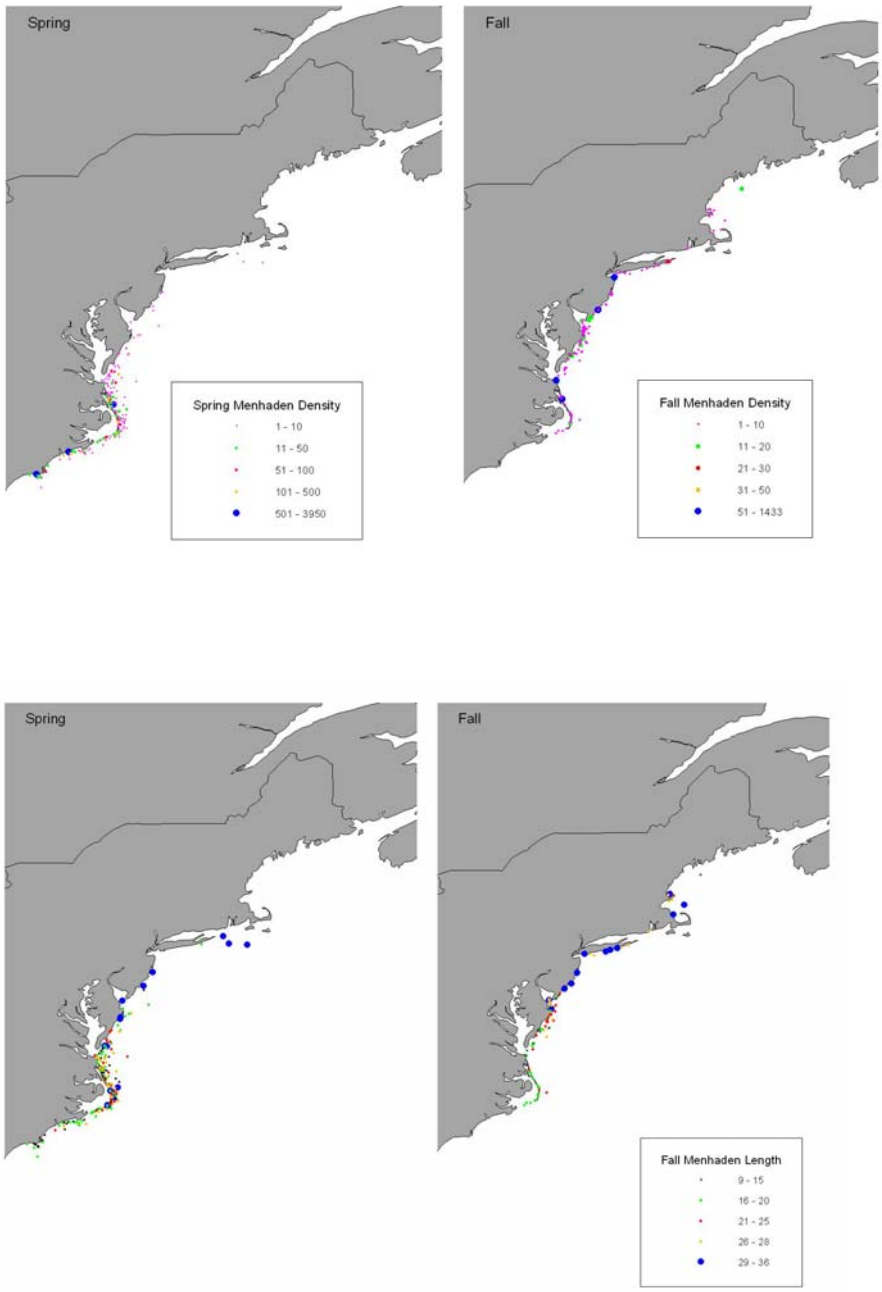

Figure 6.13.- Seasonal distribution patterns of menhaden (Spring and Fall) from the NMFS NEFS trawl survey for density (upper panels) and length (lower panels).

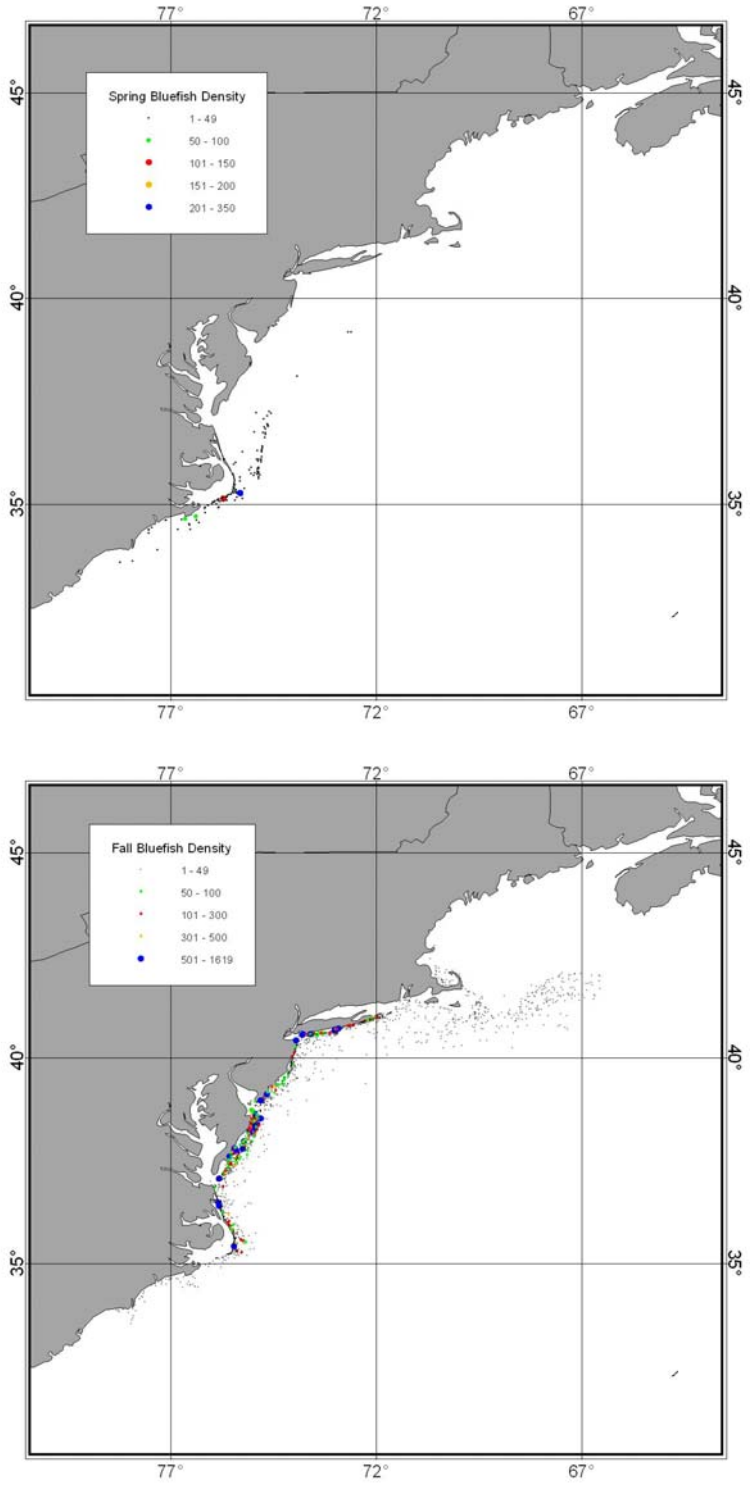

Figure 6.14.- Seasonal density distribution of bluefish (Spring and Fall) from the NMFS NEFS trawl survey for Spring (upper panels) and Fall (lower panels) sampling.

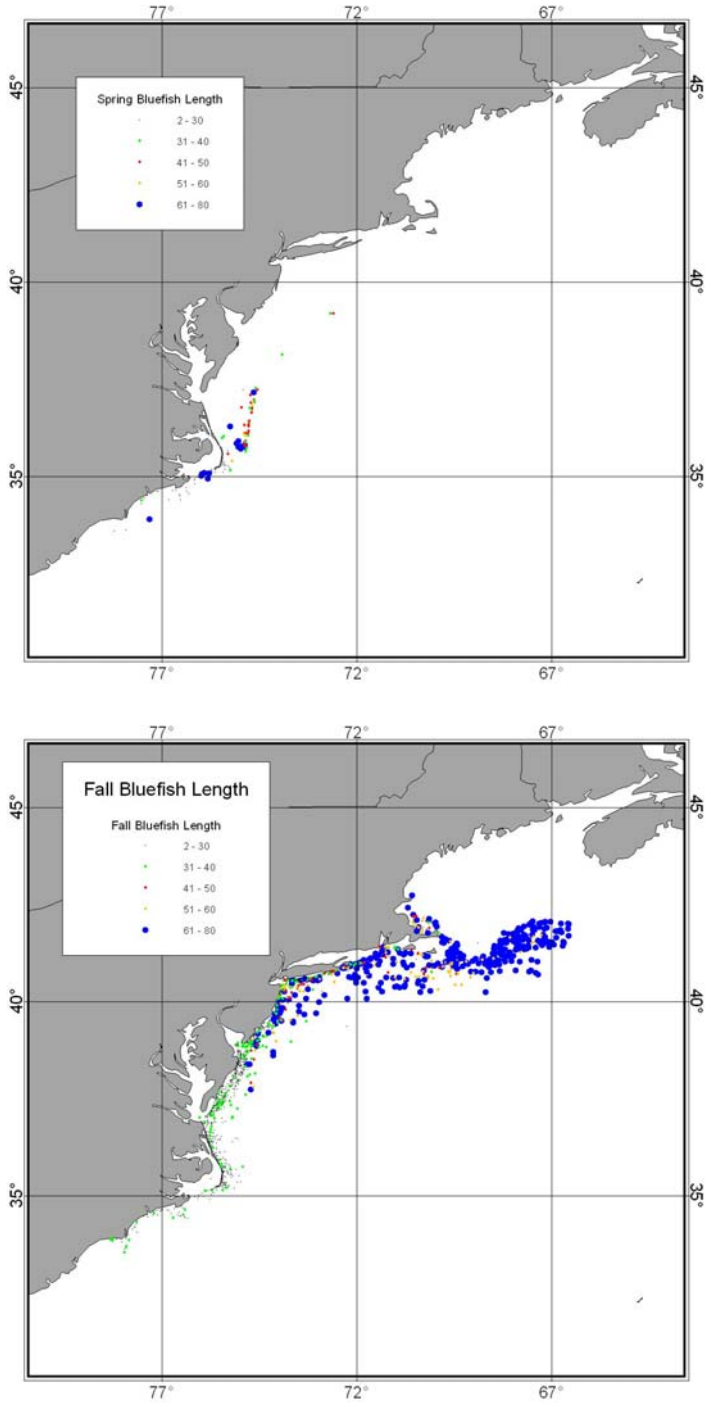

Figure 6.15.- Seasonal spatial size distribution of bluefish from the NMFS NEFS trawl survey during spring (upper panel -- March through April) and fall (lower panel -- September through November) sampling.

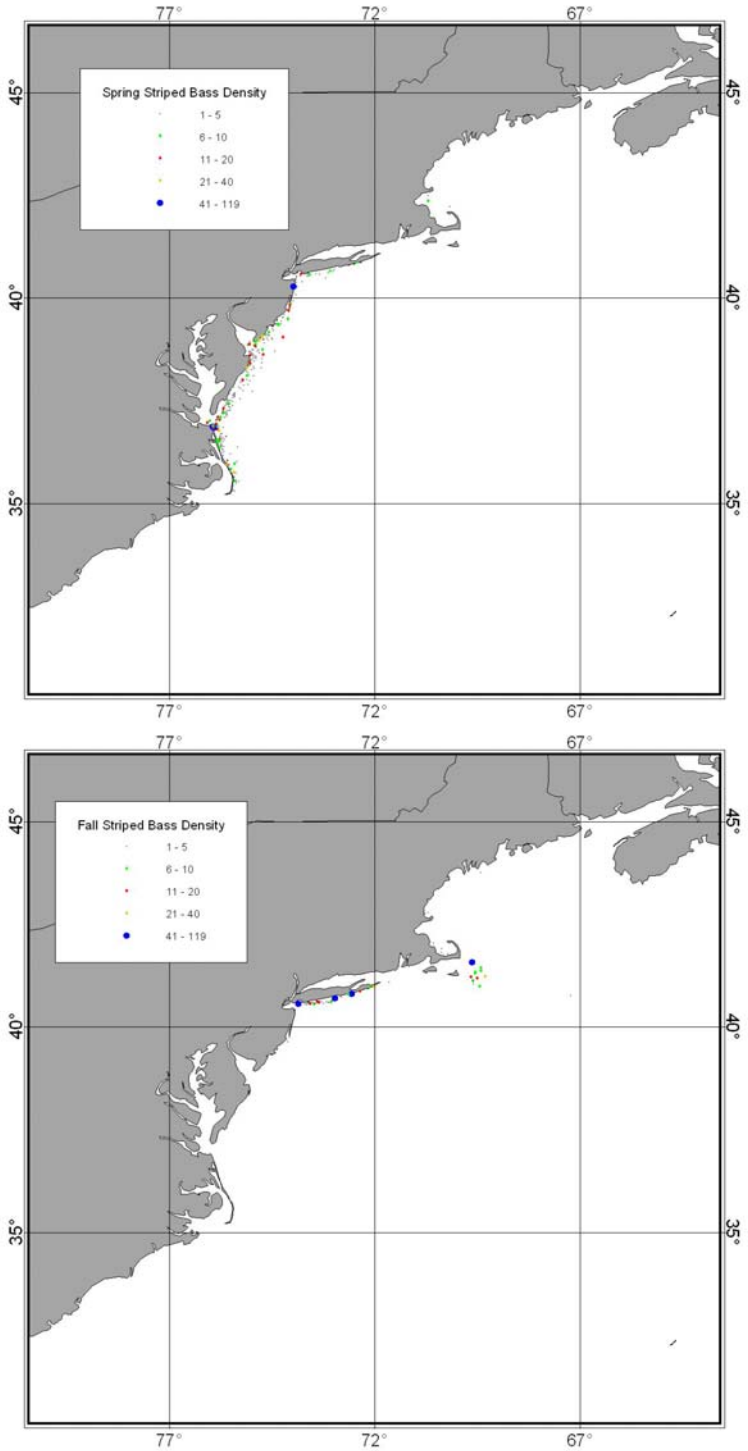

Figure 6.16.- Seasonal spatial density distribution of striped bass from the NMFS NEFS trawl survey during spring (upper panel -- March through April) and fall (lower panel -- September through November) sampling.

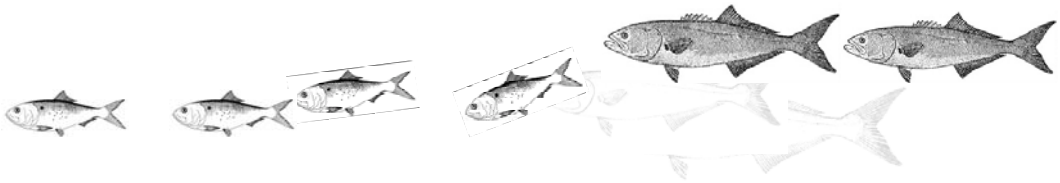

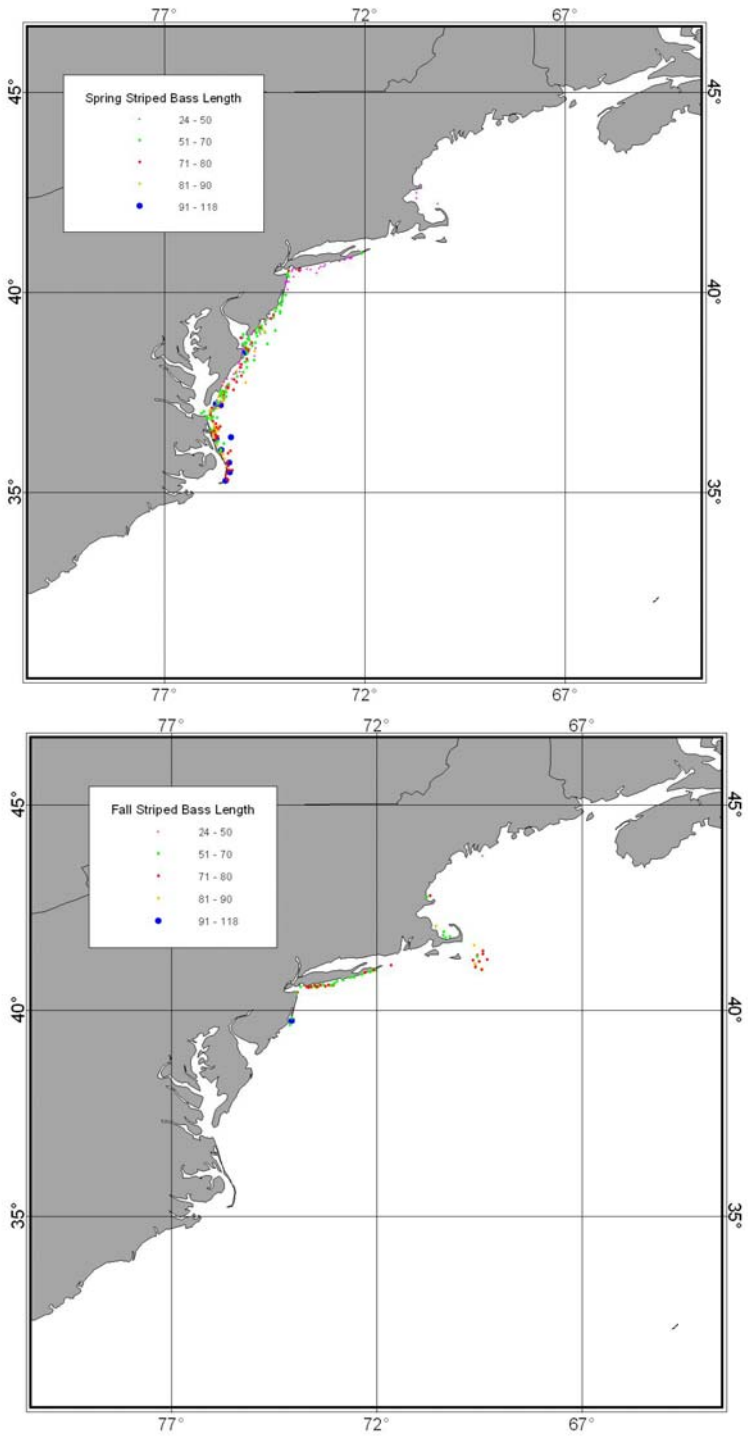

Figure 6.17.- Seasonal spatial size distribution of striped bass from the NMFS NEFS trawl survey during spring (upper panel -- March through April) and fall (lower panel -- September through November) sampling.

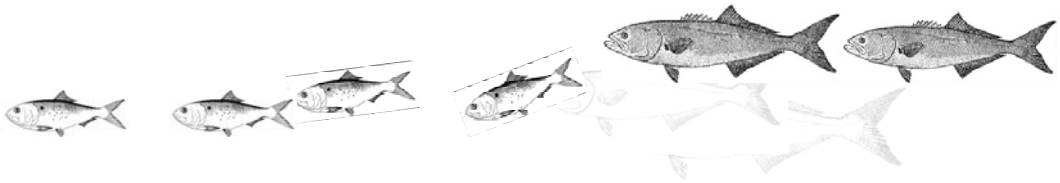

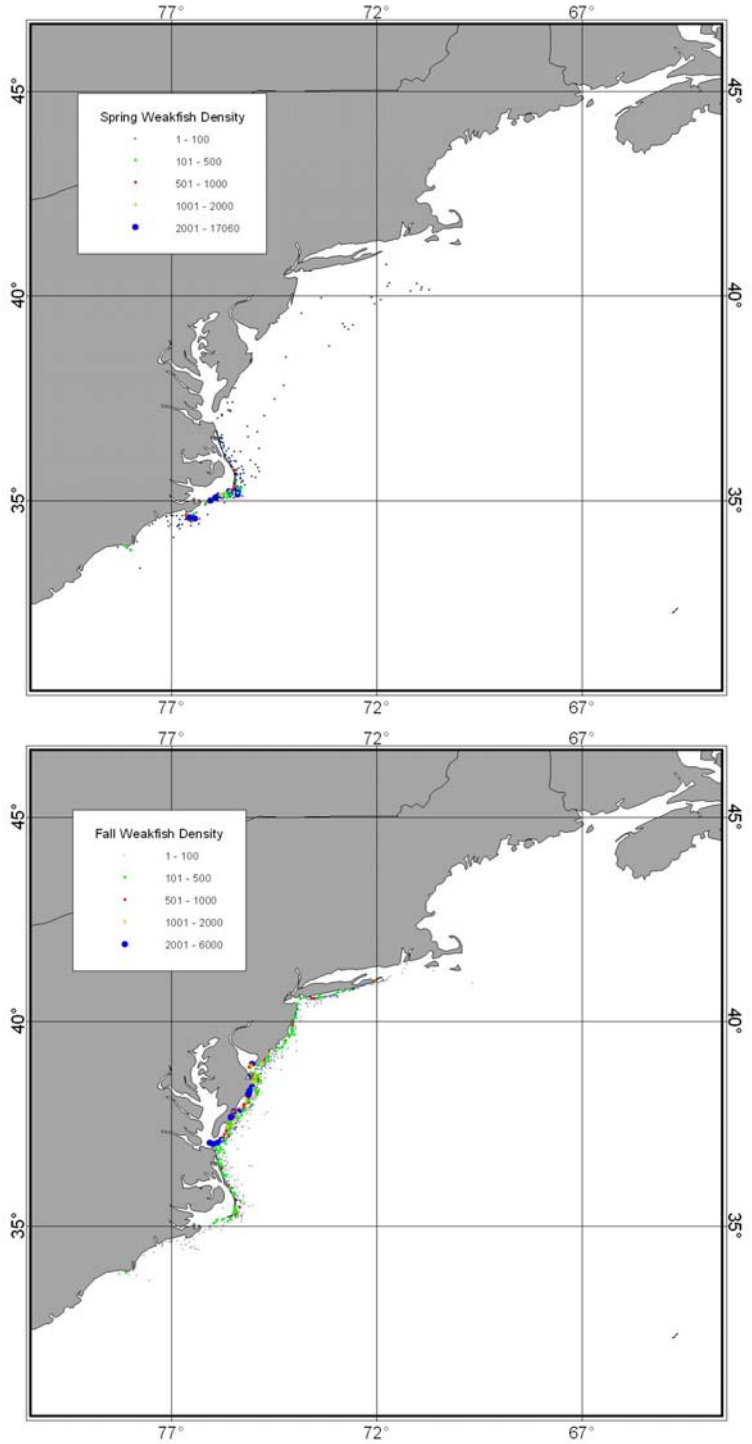

Figure 6.18.- Seasonal spatial density distribution of weakfish from the NMFS NEFS trawl survey during spring (upper panel -- March through April) and fall (lower panel -- September through November) sampling.

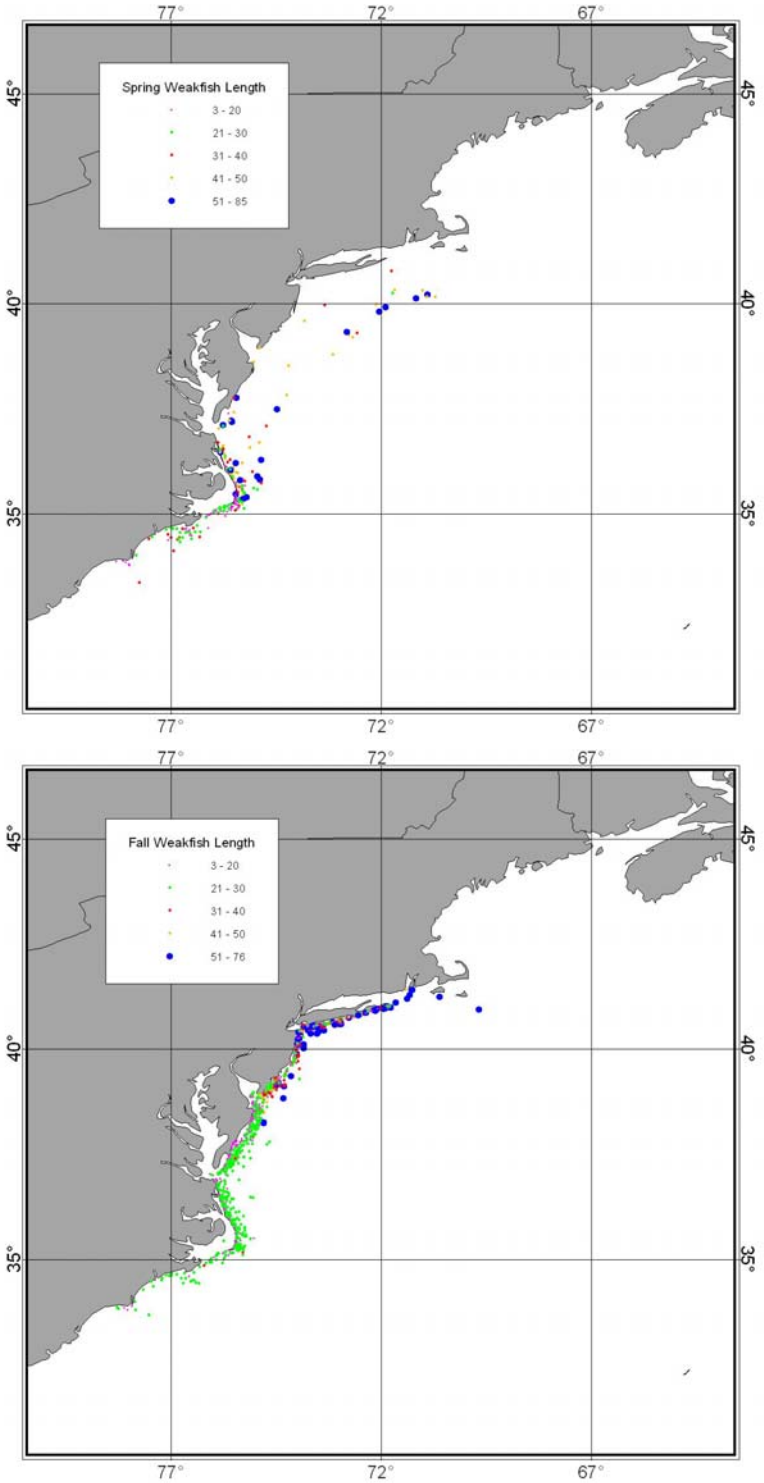

Figure 6.19.- Seasonal spatial size distribution of weakfish from the NMFS NEFS trawl survey during spring (upper panel -- March through April) and fall (lower panel -- September through November) sampling.

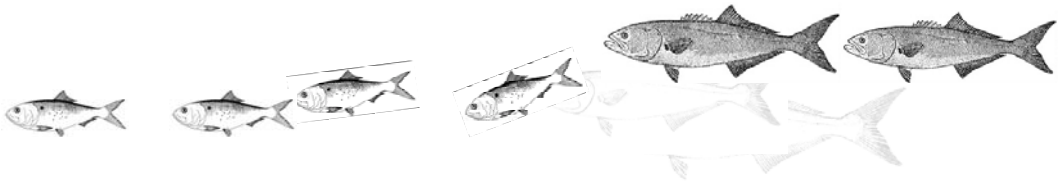

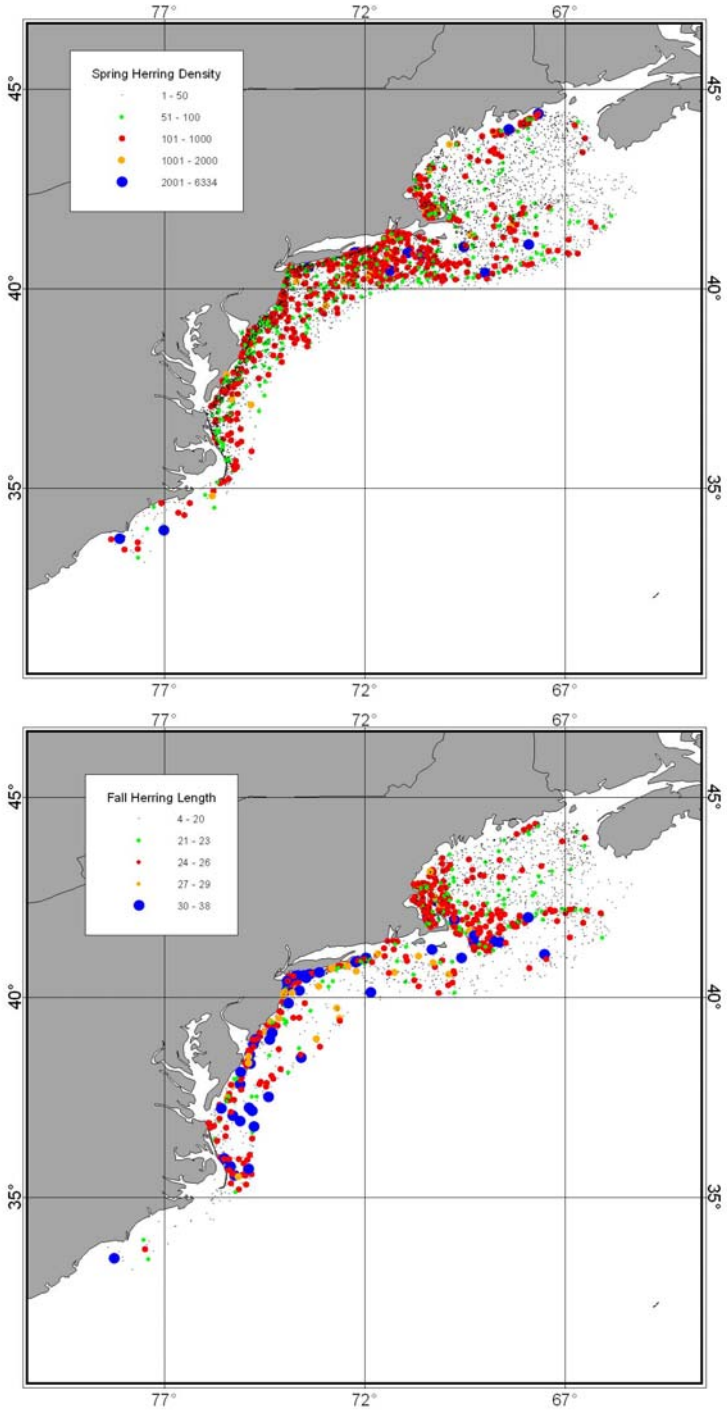

Figure 6.20.- Seasonal spatial density distribution of the herring complex (i.e., round herring, Atlantic herring, blueback herring and alewife) from the NMFS NEFS trawl survey during spring (upper panel -- March through April) and fall (lower panel -- September through November) sampling.

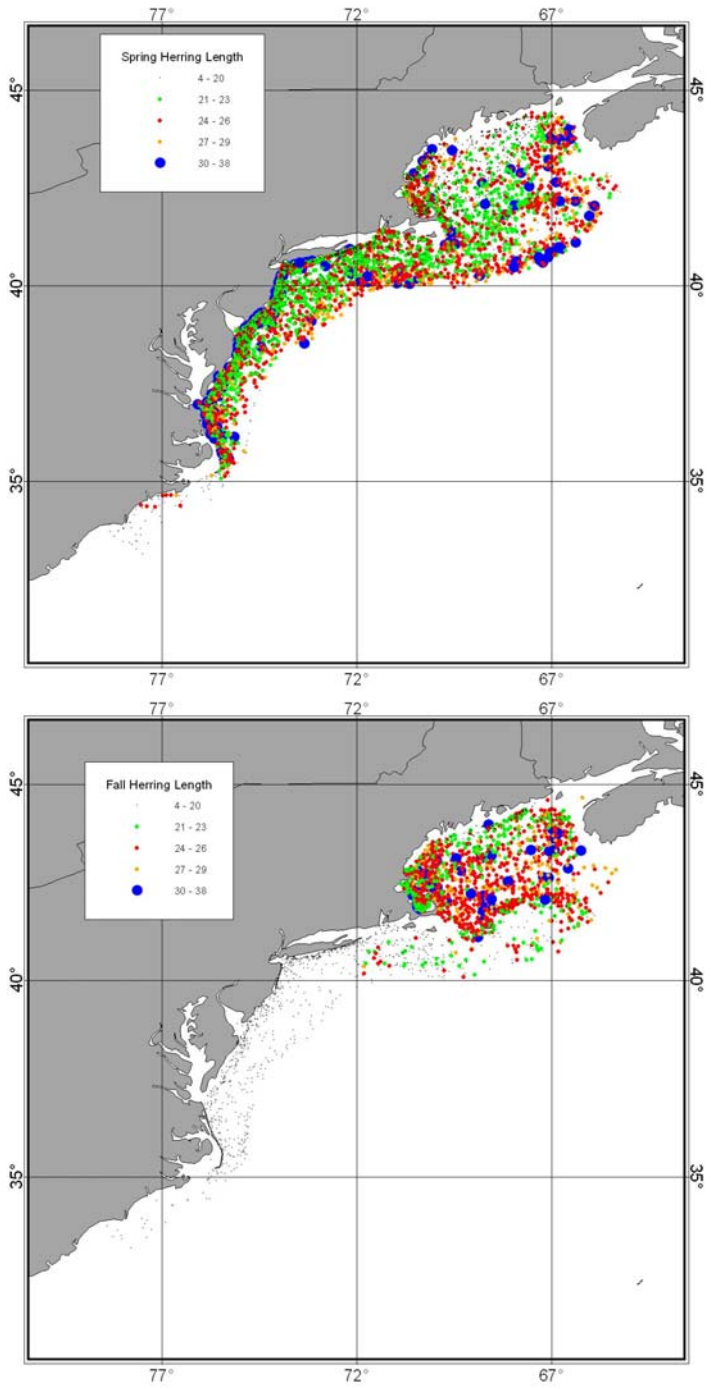

Figure 6.21.- Seasonal spatial size distribution of the herring complex (i.e., round herring, Atlantic herring, blueback herring and alewife) from the NMFS NEFS trawl survey during spring (upper panel -- March through April) and fall (lower panel -- September through November) sampling.

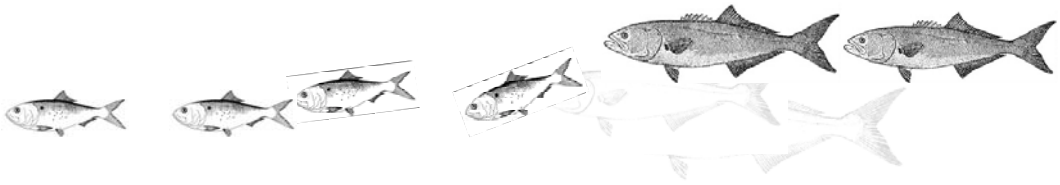

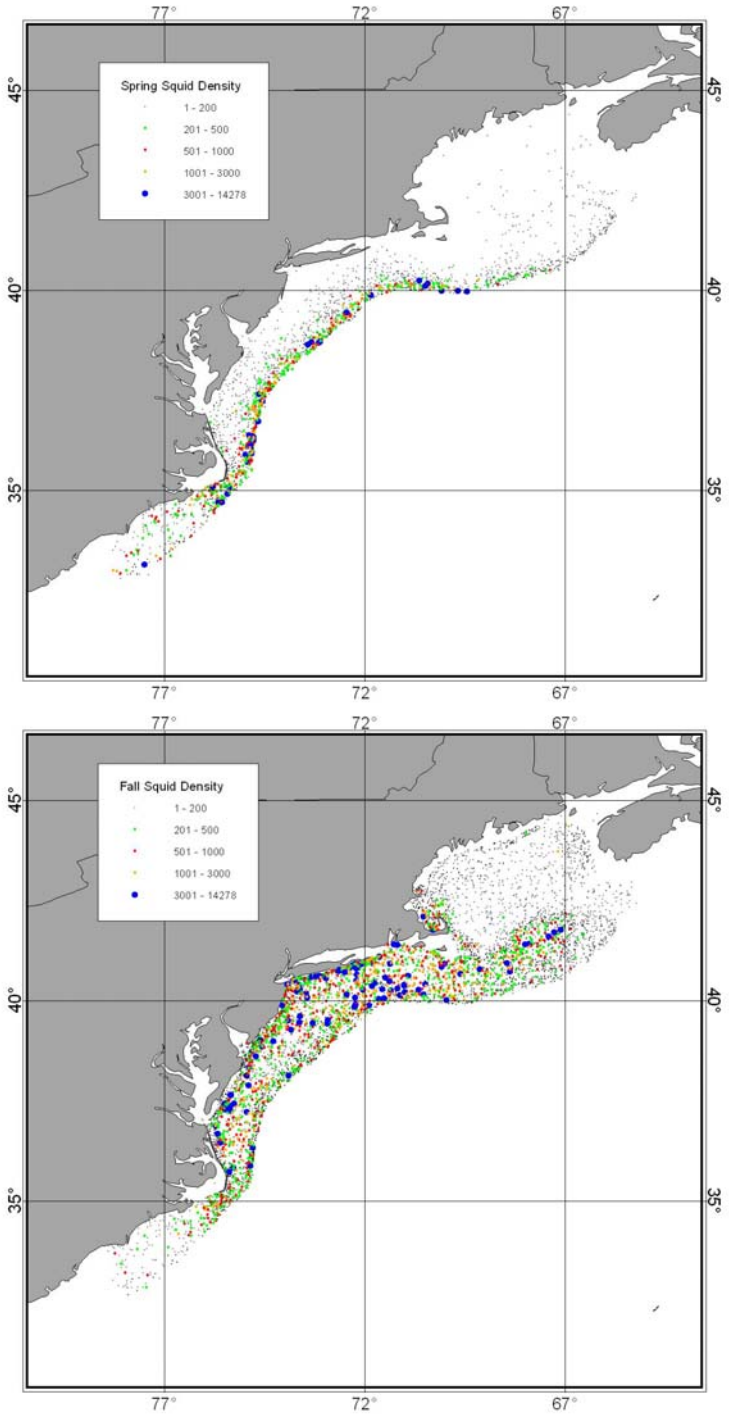

Figure 6.22.- Seasonal spatial density distribution of squids from the NMFS NEFS trawl survey during spring (upper panel -- March through April) and fall (lower panel -- September through November) sampling.

6.3 Diet Data Available for Spatial Model from MSVPA Model.-

Garrison (2004) provided his compiled diet database from his multispecies VPA model development. The regionally summarized diet composition data are listed below:

6.3.1 Striped Bass Diet Composition.- Striped Bass diet information has been compiled from two primary data sources from the literature. Hartman & Brandt (1995) provided relatively detailed information on age and season specific diet composition from collections of striped bass in the Chesapeake Bay mainstem and several tributaries. The proportion of menhaden in striped bass diets in these data is shown below. Dashes indicate no data.

Months	Age 0	Age 1	Age 2	Age 3+
Jan-Feb	-	0	0.8	0.65
Mar-Apr	-	0	0.6	0.85
May-Jun	0	0	0	0.08
Jul-Aug	0	0.2	0.25	0.50
Sep-Oct	0	0.55	0.35	0.96
Nov-Dec	0	0.55	0.98	1.0

Walters *et al*. (in press) undertook a large summary of striped bass diets from disparate sources. Summaries of data provided information by regions and in three size classes. For the mainstem and tributaries of Chesapeake and Delaware Bay the proportion of menhaden in the diets was:

Season	150-450 mm (Age 1-3)	450-600 mm (Age 4-6)	600-800 mm (Age 6-8)	800+ mm (Age 8+)
Spring	0.30	0.20	0.50	0.67
Summer	0.16	0.25	0.47	-
Fall	0.43	0.54	0.57	0.69
Winter	0.10	0	0.27	-

In North Carolina Bays and tidal estuaries:

Season	150-450 mm (Age 1-3)	450-600 mm (Age 4-6)	600-800 mm (Age 6-8)	800+ mm (Age 8+)
Spring	0.19	0.14	0.60	0.84
Summer	-	-	-	-
Fall	0.47	0.42	0.24	-
Winter	0.06	-	-	-

There is relatively little data for diets in the coastal waters of the mid-Atlantic shelf. An analysis of approximately 200 stomachs in the NEFSC food habits database showed that approximately 67% of the diet of large striped bass during spring was menhaden. In summary, these data show that the amount of menhaden consumed by age 1-6 striped bass peaks during fall, coinciding with the recruitment of menhaden to the fishery at approximately age 0.5. Menhaden comprise a

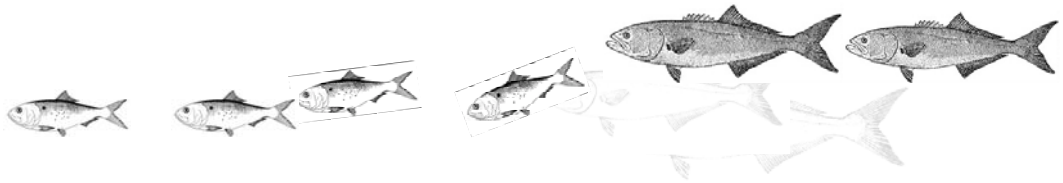

significant portion of larger striped bass diets year round, and there is evidence of menhaden consumption by large striped bass in coastal waters. The diet composition has been summarized as follows:

Season	**Age 0**	**Age 1-3**	**Age 4-8**	**Age 9+**
Spring	0	0, 0.3, 0.4*	0.4	0.7
Summer	0	0.2	0.5	0.7
Fall	0	0.55	0.65	0.9
Winter	0	0.1	0.3	0.5

* Ages 1, 2, and 3 respectively

References:

Hartman KJ and Brandt SB (1995) Trophic resource partitioning, diets, and growth of sympatric estuarine predators. Trans. Am. Fish. Soc. 124: 520-537.

Link JS, Almeida FP (2000) An overview of the history of the food web dynamics program of the Northeast Fisheries Science Center, Woods Hole, MA. NOAA Tech. Memo. NMFS-NE-159

NEFSC. Food Web Dynamics Program data on diets of Bluefish, Weakfish, and Striped Bass in nearshore continental shelf habitats. Unpublished data files

Walter JF (1999) Diet composition and feeding habits of large striped bass in Chesapeake Bay. MS Thesis. College of William and Mary, Williamsburg VA. 124 pp.

Walter JF, Overton AS, Ferry KH, and Mather ME (in review) Atlantic coast feeding habits of striped bass: A meta-analysis of data supporting a comprehensive coastwide understanding of the trophic biology. Fisheries Management and Ecology. Submitted

6.3.2 Bluefish Diet Composition.- There are few publications with information on the diets of Age 1+ bluefish, though there is a considerable amount of data on the feeding of young of the year in estuarine waters. Hartman & Brandt (1995) provide a summary of bluefish diets in the Chesapeake Bay mainstem and tributaries. They stated that Age 0-2 bluefish are in the bay primarily from late May to October. Age 2+ Bluefish undertake large scale north-south seasonal migrations in the nearshore continental shelf waters of the mid-Atlantic (Buckell *et al.* 1999). The Hartman & Brandt data show the seasonal proportion of menhaden in bluefish diets inside the estuaries as:

Months	Age 0	Age 1	Age 2+
May-Jun	0	-	-
Jul-Aug	0	0.1	0.05
Sep-Oct	0.3	0.68	0.90

Buckel *et al*. (1999) describe diet information based upon NEFSC trawl survey collections of bluefish on the continental shelf. No menhaden were observed in these stomachs. Naughton & Saloman (1984) sampled bluefish diets in the coastal waters of the Carolinas. Menhaden accounted for approximately 9% by volume of age 0-1 bluefish diets in coastal waters during the spring, and 15% by volume in larger fish. In summary, as with striped bass, bluefish

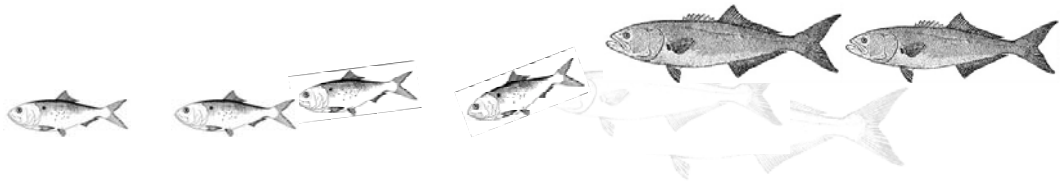

consumption of menhaden inside the estuaries peaks during fall coinciding with the presence of age 0.5 fish. The adult bluefish population overlaps with menhaden spawning aggregations in coastal waters south of Cape Hatteras during spring and winter. The proportion of menhaden in the diet by bluefish age-class was summarized as follows for this application:

Season	**Age 0**	**Age 1**	**Age 2**	**Age 3+**
Spring	0.09	0.09	0.09	0.15
Summer	0	0.1	0.1	0
Fall	0.3	0.7	0.9	0.05
Winter	0	0	0.05	0.05

References:

Buckel JA, Fogarty MJ, and Conover DO (1999) Foraging habits of bluefish, *Pomatomus saltatrix*, on the US east coast continental shelf. Fish. Bull. 97:758-775.

Hartman KJ and Brandt SB (1995) Trophic resource partitioning, diets, and growth of sympatric estuarine predators. Trans. Am. Fish. Soc. 124:520-537.

Link JS, Almeida FP (2000) An overview of the history of the food web dynamics program of the Northeast Fisheries Science Center. NOAA Tech. Memo. NMFS-NEFSC-159

NEFSC. Food Web Dynamics Program data on diets of Bluefish, Weakfish, and Striped Bass in nearshore continental shelf habitats. Unpublished data files

Naughton SP and Saloman CH (1984) Food of bluefish from the US South Atlantic and Gulf of Mexico. NOAA Tech. Memo. NMFS-SEFSC-150

6.3.3 Weakfish Diet Composition.- Hartman & Brandt (1995) provided the only detailed information in the literature from collections inside Chesapeake Bay:

Months	Age 0	Age 1	Age 2+
May-Jun	-	0.05	0.18
Jul-Aug	0	0.07	-
Sep-Oct	0	0.55	0.70
Nov-Dec	0	-	-

These data show the peak in consumption of menhaden during the fall. Merriner (1975) provides diet information from North Carolina estuaries. Overall, menhaden accounted for approximately 10% of weakfish diets by volume. The proportion of menhaden in the diet increased with age from 1 to 11 % between ages 1 and 4. The NEFSC food habits database has weakfish stomachs from coastal waters and no menhaden were observed in the diets. These data were summarized as follows:

Season	**Age 0**	**Age 1**	**Age 2**	**Age 3+**
Spring	0	0.05	0.18	0
Summer	0	0.07	0.10	0
Fall	0	0.55	0.70	0
Winter	0	0	0	0

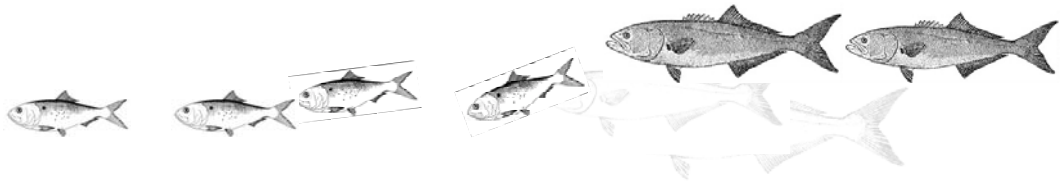

References:

Hartman KJ and Brandt SB (1995) Trophic resource partitioning, diets, and growth of sympatric estuarine predators. Trans. Am. Fish. Soc. 124: 520-537.

Link JS, Almeida FP (2000) An overview of the history of the food web dynamics program of the Northeast Fisheries Science Center, Woods Hole, MA. NOAA Tech. Memo. NMFS-NE-159

Merriner, JV (1975) Food Habits of the Weakfish in North Carolina Waters. Chesapeake Science 16: 74-76

NEFSC. Food Web Dynamics Program data on diets of Bluefish, Weakfish, and Striped Bass in nearshore continental shelf habitats. Unpublished data files

6.4 Size composition of fish prey in the diet.- Size composition data for striped bass has been summarized from Hartman (2000) and from frequency data supplied by A. Overton. Prey size frequency for both bluefish and weakfish was inferred from relationships derived by Scharf *et al.* (1998) based upon laboratory feeding experiments. This paper showed a dome shaped relationship between predator-prey length ratios and feeding success in Age-0 bluefish feeding on striped bass and silversides. Based upon this relationship, age-specific size frequency histograms were calculated based upon the length at age of bluefish and weakfish in assessment data. The derived size-frequencies result in the vast majority of menhaden consumption by these predators targets age 0 fish, consistent with the seasonal patterns described above.

Hartman, KJ (2000) The influence of size on striped bass foraging. Mar. Ecol. Prog. Ser. 194: 263-268

Scharf FS, Buckel JA, Juanes F, and Conover DO (1998) Predation by juvenile piscivorous bluefish (*Pomatomus saltatrix*): the influence of prey to predator size ratio and prey type on predator capture success and prey profitability. Can. J. Fish. Aq. Sci. 55: 1695-1703.

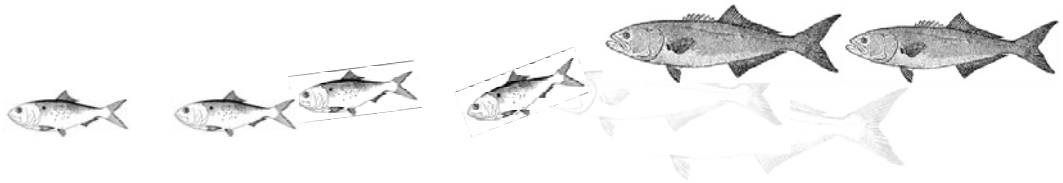

Model Parameterization and Calibration

A glossary of general target variables and terminology, including the range and types of model variables and parameters used in the Atlantic coast spatial dynamic multispecies models is given in **Table 7.1**. In the course of development of the prototype model, we have acquired a substantial population dynamics, fishery biology, ecology, bioenergetics and behavioral movements of Atlantic menhaden and bluefish (**Table 7.2**). Our primary target in year 1 was simulation of the spatial and temporal dynamics of the Atlantic menhaden stock. These efforts consisted of a thorough review of the available scientific and technical literature was conducted and assembled into a literature database (see **Appendix 1**). During year 2 we assembled the necessary life history and population dynamic parameters for bluefish that were sufficient to run the spatial predator (bluefish) – prey (menhaden) dynamic model (**Table 7.2**).

7.1 Example Sensitivity Analysis and Scenario Simulations.- The extensive syntheses outlined above were required to establish the initial parameter values made it possible to conduct some pilot runs of the model to determine the extent to which the model performs adequately and reflects observed conditions and trends in these resources. To ensure that the model was fully operational and meeting the needs of the Atlantic States Marine Fisheries Commission, we conducted an sequenced and integrated series of sensitivity analyses on model responses to variations in key biological and biophysical environmental parameters. Model simulations were run at daily time steps for at least 2 life-cycles of the longest lived species (e.g., 20 years if the oldest aged fish is 10 years) to facilitate evaluation of the changes expected from implementation of various alternative plans. A base simulation run was performed starting with current fishery condition and stock sizes to evaluate the nature and magnitude of linkages among menhaden and their key predators. In what follows, we first briefly discuss some of the issues of parameterizations, and then briefly overview some of the pilot calibration runs to evaluate model dynamics and performance.

7.2 Bioenergetics Growth Models.- Bioenergetics growth model parameters for Atlantic menhaden and bluefish to directly couple the growth, mortality and reproductive capabilities of the fish to the predator-prey and the physical environment over the unit stock range. Bioenergetic growth model estimates were obtained from published literature supplemented by a host of unpublished data from ASMFC-related projects. Bioenergetics data from Hartman's studies were obtained from Chesapeake Bay prior to 1993. To improve the basis of these models, we continue to seek more recent data (1994-2005), and perhaps other relevant data sources from other East coast areas.

7.3 Prey (Menhaden).- A menhaden bioenergetics model for the Chesapeake Bay (Luo et al. 2001) was adapted for the larger geographic region of the study. The food source (phytoplankton and detritus) will be derived from field measurement of phytoplankton and detritus biomass, and satellite remote sensing imagery (such as CZCS, SeaWiFS). It should be noted that the current Commission multispecies model does not include bottom-up processes. An example of the bioenergetic model compared to the standard von Bertalanffy lifetime growth model is shown in **Figure 7.1**.

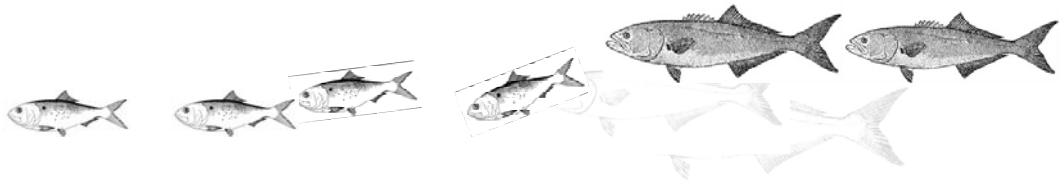

Figure 7.1.- Bioenergetics growth model (red line) for Atlantic menhaden in comparison to the von Bertalanffy lifetime growth model (black line).

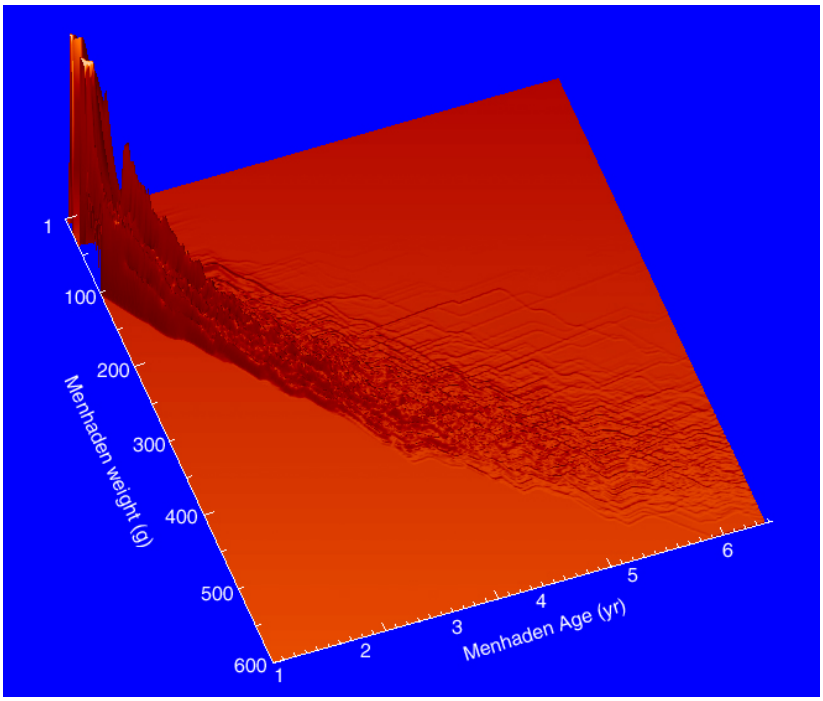

Figure 7.2.- Modeled menhaden bioenergetic growth and abundance distribution at age for a single cohort from the spatial dynamic ecosystem simulation model.

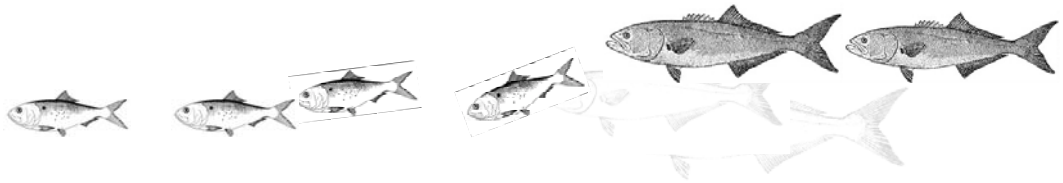

Table 7.1.- Glossary of Atlantic coast spatial dynamic multispecies model variables.

Variable	Description	Units
t	Time	Julian day
(x,y)	Spatial position coordinates	Longitude, Latitude
j(x,y)	Spatial grid cell	dimensionless
k(x,y)	Neighboring grid cell	dimensionless
B(x,y)	Substrate	dimensionless
D(x,y)	Depth	m
S(t,x,y)	Salinity	‰
T(t)	Water temperature	°C
P(a,t,x,y)	Predator abundance	Numbers of fish
N(a,t,x,y)	Prey abundance	Numbers of menhaden
L(a,t,x,y)	Animal total length	mm
W(a,t,x,y)	Animal weight	g
C(a,t,x,y)	Consumption rate	g g^{-1} d^{-1}
E	Egestion rate	g g^{-1} d^{-1}
U	Excretion rate	g g^{-1} d^{-1}
R(a,t,x,y)	Respiration rate	g O_2 g^{-1} d^{-1}
A	Assimilation efficiency	dimensionless
V_P	Predator average swimming speed	body length s^{-1}
$f_C(T)$	Temperature-dependent function for consumption	dimensionless
$f_C(N)$	Prey-dependent functional response for consumption	dimensionless
$f_R(T)$	Temperature-dependent function for respiration	dimensionless
$f_R(S)$	Salinity-dependent function for respiration	dimensionless
$f_R(V_P)$	Activity-dependent function for respiration	dimensionless
Z(a,t,x,y)	Total instantaneous mortality rate	yr^{-1}
M(a,t,x,y)	Natural mortality rate	yr^{-1}
f(P)	Predation mortality functional response	dimensionless
F(a,t)	Fishing mortality rate	yr^{-1}
s(a,t)	Size-selectivity of fishing gear	dimensionless
X(t,x,y)	Velocity along the X (Longitude) axis	cm· s^{-1}
Y(t,x,y)	Velocity along the Y (Latitude) axis	cm· s^{-1}
X_c(t,x,y)	Velocity component due to water currents	cm· s^{-1}
X_b(a,t,x,y)	Velocity component due to animal behavior	cm· s^{-1}
X_r	Velocity component due to random dispersion	cm· s^{-1}
V_N	Prey maximum average swimming speed	cm· s^{-1}
$\omega(a,t,x,y)$	Settlement probability	dimensionless
$\Omega(a,t,x,y)$	Growth rate potential	dimensionless
$\tilde{V}_{\max}(a,t)$	Maximum net displacement velocity	mm·d^{-1}
$\Psi(a,t,j)$	Stay probability	dimensionless
$\zeta(t,k)$	Transport factor	dimensionless

Table 7.2.- Population dynamics parameters in the spatial multistock production model for: (A) Atlantic menhaden; and, (B) Bluefish.

Symbol	Description	Function/Value	Units	Reference
(A) Menhaden Cohort Dynamics:				
a_f	Age-at-fertilization	0	d	
a_r	Age-at-recruitment	2	mos	
L_r	Size at recruitment	50	mm	Ahrenholz 1991
a_λ	Maximum age	10	yr	Ahrenholz et al. 1987
L_λ	Maximum size	500	mm	Ahrenholz 1991
a_m	Age-at-maturity	2.75	yr	Ahrenholz et al. 1987
L_m	Size at maturity	260	mm	Lewis et al. 1987
α	Scalar coefficient of weight-length	2.2231×10^{-6}		Luo and Ault 2005
β	Power coefficient of weight-length	3.3479		Luo and Ault 2005
F(L)	Fecundity at length	$\log F(L)=8.8645+0.0105L$	eggs	Lewis et al. 1987
T(t)	Water temperature	°C		Naval Oceanographic Office
α_C	Intercept for maximum consumption	1.294	d^{-1}	Luo et al 2001
β_C	Weight exponent for maximum consumption	-0.312		Luo et al 2001
$f_C(T)$	Function for consumption temperature dependence	$f_C(T) = f(O_{C1},O_{C2},O_{C3},O_{C4},K_{C1},K_{C2},K_{C3},K_{C4})$		Thornton and Lessem 1978
O_{C1}	Temperature for K_{C1} in $f_C(T)$	18.2*	^oC	Luo et al 2001
O_{C2}	Temperature for K_{C2} in $f_C(T)$	28.0*	^oC	Luo et al 2001
O_{C3}	Temperature for K_{C3} in $f_C(T)$	29.0*	^oC	Luo et al 2001
O_{C4}	Temperature for K_{C4} in $f_C(T)$	30.1*	^oC	Luo et al 2001
K_{C1}	Proportion of C_{max} at O_{C1}	0.525		Luo et al 2001
K_{C2},K_{C3}	Proportion of C_{max} at O_{C2} and O_{C3}	0.98		Luo et al 2001
K_{C4}	Proportion of C_{max} at O_{C4}	0.81		Luo et al 2001
ρ	Half-saturation constant	0.5		Luo et al 2001
A	Assimilation efficiency	0.7		Hewett and Johnson 1992
α_R	Intercept for maximum standard respiration	0.003301	$g\ O_2\ g^{-1}\ d^{-1}$	Luo et al 2001
β_R	Weight exponent for maximum respiration	-0.2246		Luo et al 2001
RQ	Slope for temperature dependence of respiration	2.07		Luo et al 2001

Table 7.2.- (continued)

RTO	Optimum temperature for standard respiration	33.0	^{o}C	Luo et al 2001
RTM	Maximum temperature for standard respiration	36.0	^{o}C	Luo et al 2001
SDA	Specific dynamic action coefficient	0.172		Luo et al 2001
ACT	Temperature dependence of Activity parameter $ACT=1+(2.5/(1+e^{(-0.398\ T+6.378)})$			Luo et al 2001
F_a	Proportion of consumed food egested	0.14		Luo et al 2001
U_a	Proportion of assimilated food excreted	0.10		Luo et al 2001
$f_C(S)$	Respiration dependent on salinity $f_C(S) = f(O_{s1}, O_{s2}, O_{s3}, O_{s4}, K_{s1}, K_{s2}, K_{s3}, K4_s)$			Thornton and Lessem 1978
L_∞	Ultimate length from von Bertalanffy	370.37	mm	Luo and Ault 2005
K	Brody growth coefficient	0.3595	yr^{-1}	Luo and Ault 2005
t_0	age at which length equals 0	-0.6176	yr	Luo and Ault 2005
V_P	Average swimming speed	1.0	body length s^{-1}	Wohlschlag and Wakeman 1978
M(0)	Base natural mortality rate age 0 fish	4.31	yr^{-1}	Table 7.1, ASMFC Stock Assessment 2003
M(1)	Base natural mortality rate age 1 fish	0.98	yr^{-1}	Table 7.1, ASMFC Stock Assessment 2003
M(2)	Base natural mortality rate age 2 fish	0.56	yr^{-1}	Table 7.1, ASMFC Stock Assessment 2003
M(3+)	Base natural mortality rate age 3 fish	0.55	yr^{-1}	Table 7.1, ASMFC Stock Assessment 2003
γ	Natural mortality weighting factor	1.0		

Symbol	Description	Function/Value	Units	Reference

(B) Bluefish Cohort Dynamics:

a_f	Age-at-fertilization	0	d	
a_r	Age-at-recruitment	2	mos	
L_r	Size at recruitment	50	mm	Ahrenholz 1991
a_λ	Maximum age	10	yr	Ahrenholz et al. 1987
L_λ	Maximum size	872	mm	Ahrenholz 1991
a_m	Age-at-maturity	3	yr	Ahrenholz et al. 1987
L_m	Size at maturity	180	mm	Lewis et al. 1987
α	Scalar coefficient of weight-length	3.2652×10^{-5}		Luo and Ault 2005
β	Power coefficient of weight-length	2.8509		Luo and Ault 2005

Table 7.2.- (continued)

F(L)	Fecundity at length	log F(L)=8.8645+0.0105L	eggs	Lewis et al. 1987
T(t)	Water temperature		°C	Naval Oceanographic Office
α_C	Intercept for maximum consumption	0.53	g g^{-1} d^{-1}	Hartman 1993
β_C	Weight exponent for maximum consumption	-0.288		Hartman 1993
$f_C(T)$	Function for consumption temperature dependence	$f_C(T) = f(O_{C1},O_{C2},O_{C3},O_{C4},K_{C1},K_{C2},K_{C3},K_{C4})$		Thornton and Lessem 1978
O_{C1}	Temperature for K_{C1} in $f_C(T)$	10.2*	^oC	Hartman 1993
O_{C2}	Temperature for K_{C2} in $f_C(T)$	23.0*	^oC	Hartman 1993
O_{C3}	Temperature for K_{C3} in $f_C(T)$	28.0*	^oC	Hartman 1993
O_{C4}	Temperature for K_{C4} in $f_C(T)$	34.0*	^oC	Hartman 1993
K_{C1}	Proportion of C_{max} at O_{C1}	0.15		Hartman 1993
$K_{C2,}K_{C3}$	Proportion of C_{max} at O_{C2} and O_{C3}	0.98		Hartman 1993
K_{C4}	Proportion of C_{max} at O_{C4}	0.85		Hartman 1993
ρ	Half-saturation constant	0.5		
A	Assimilation efficiency	0.7		Hewett and Johnson 1992
R	$=\alpha_R$ W^ β_R *exp(Rt*T)			
α_R	Intercept for maximum standard respiration	0.0055	g O_2 g^{-1} d^{-1}	Hartman 1993
β_R	Weight exponent for maximum standard respiration	-0.264		Hartman 1993
Rt	Exponent coefficient of temperature dependence	0.05525		Hartman 1993
L_∞	Ultimate length from von Bertalanffy	87.20	cm	Salerno 2001
K	Brody growth coefficient	0.260	yr^{-1}	Salerno 2001
t_0	age at which length equals 0	-0.93	yr	Salerno 2001
V_P	Average swimming speed	1.0	body length s^{-1}	Wohlschlag and Wakeman 1978
M(0)	Base natural mortality rate age 0 fish	0.25	yr^{-1}	Table 7.1, SEDAR 2004
M	Base natural mortality rate	0.45	yr^{-1}	Ahrenholz et al. 1987
γ	Natural mortality weighting factor	1.0		

7.4 Fish Movements: Fish behavioral movements have been modeled to queue on the spatial patterns of "growth rate potential" which are derived from both the physiology of the fish and the underlying physical and biological properties of the coastal ocean "habitats". To validate fish movements, modeled fish distributions will be compared with the seasonal distributional maps of fishes, and mark-recapture data. For example, Composite pictures of "habitat quality" for ages 0 through 3 menhaden (prey) for August and November is shown in **Figure 7.3**. Growth rate potential is a 'complex vector' of environmental and biophysical factors that influence the time-specific growth rates of animals in space. Factors involved the "habitat quality" computations shown included: animal physiology, salinity, benthic habitats, depth, prey and/or predator densities, and temperature. The modeled seasonal distributions of the entire menhaden stock is shown in **Figure 7.4**. Ontogenetic use of coastal ocean habitats by menhaden fishes as they grow and age is prevalent in the ecosystem (**Figure 7.5**), and it is a means to use "fish-habitat" associations to improve sampling survey performance and the prediction of animal distribution and abundance.

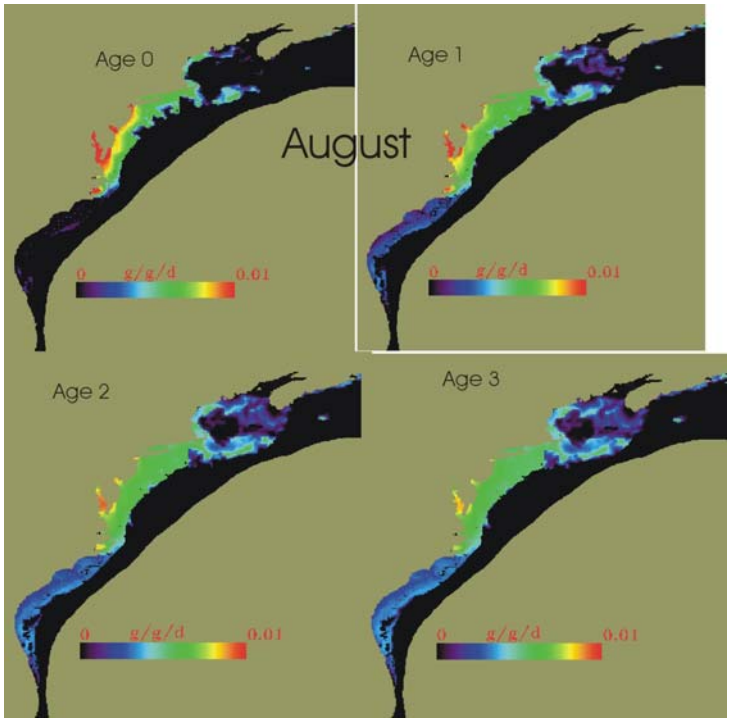

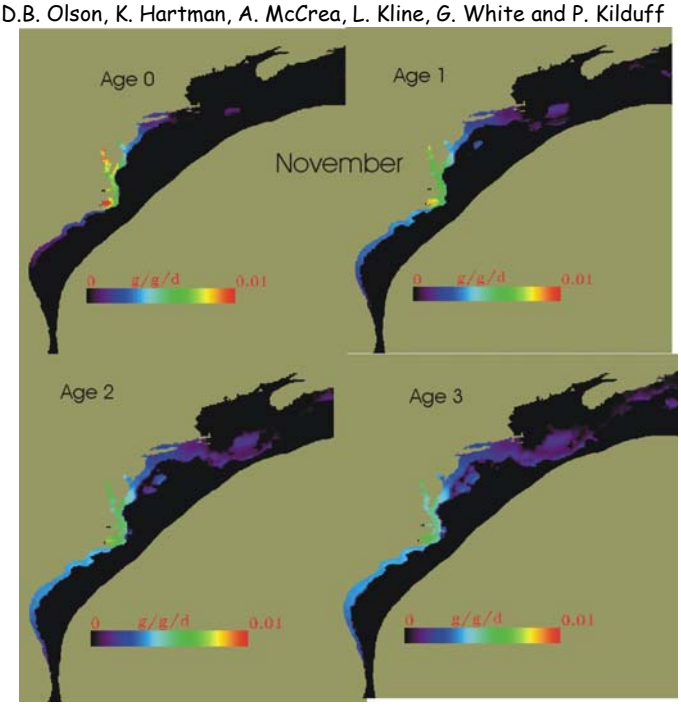

Figure 7.3.- Modeled menhaden spatial growth rate potential for ages 0-3 for August (upper 4 panels) and November (lower 4 panels).

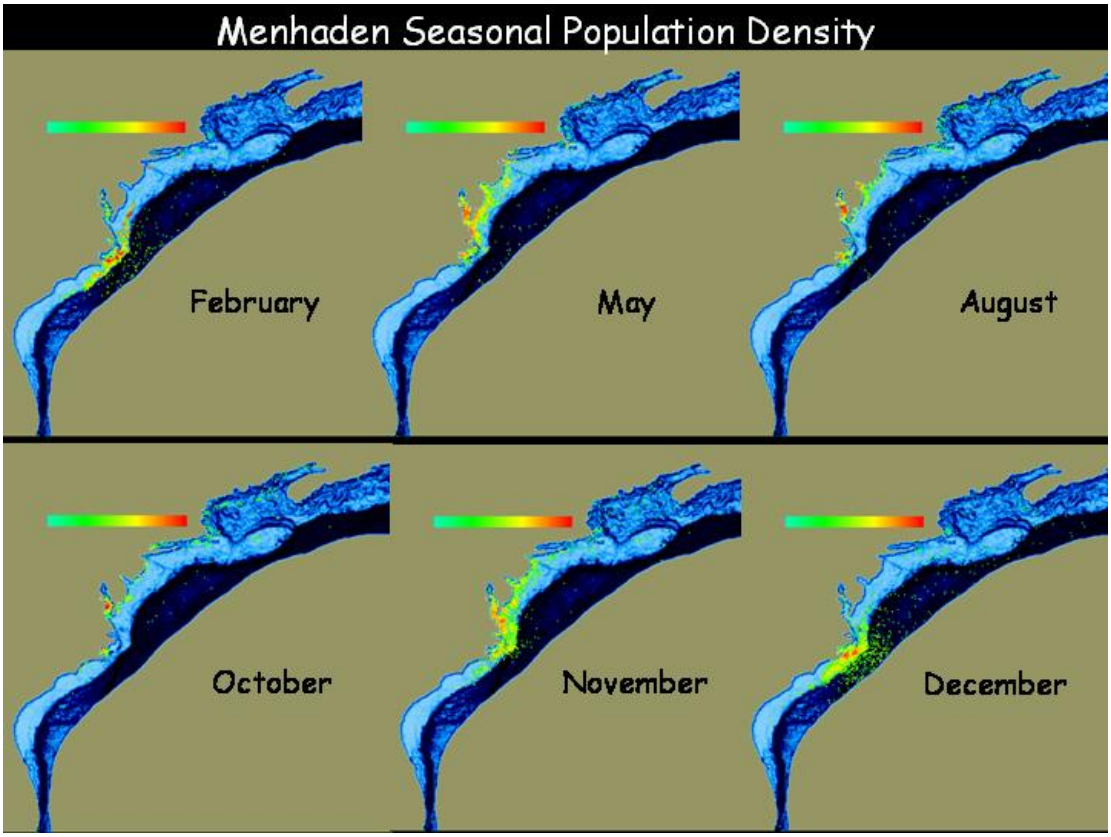

Figure 7.4.- Modeled seasonal spatial distribution of the Atlantic menhaden stock.

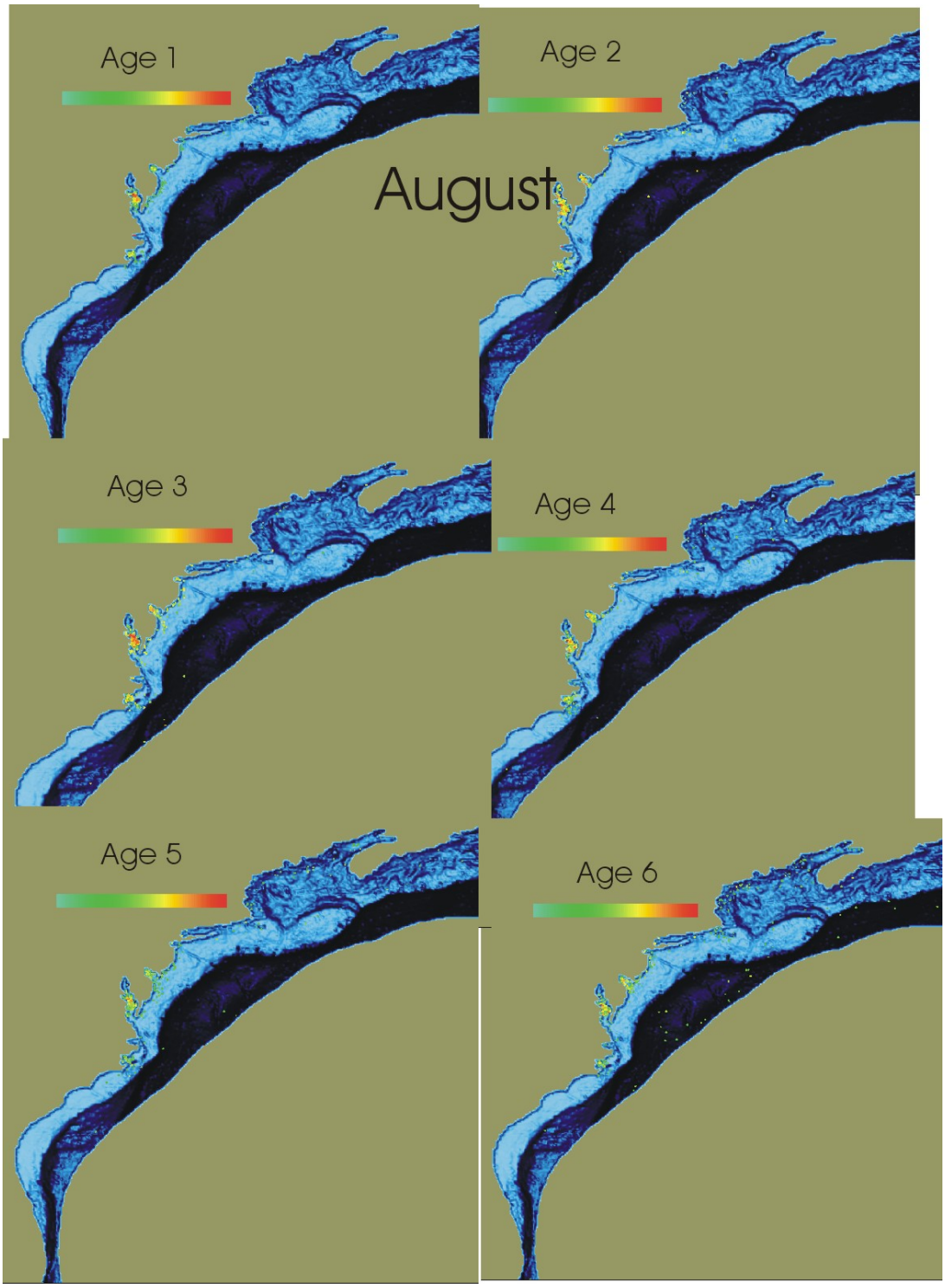

Figure 7.5.- Modeled seasonal spatial distribution of Atlantic menhaden stock age classes 1 through 6 for a typical August.

7.5 Recruitment.- Two methods are used to introduce recruitment into the model: (1) Use direct recruitment from larval transport and settlement as described above if there are hydrodynamic models available for the major nursery areas and the adjacent coastal water. This method will require significantly more time and resources than the following method. (2) Use an indirect recruitment from estimates of age-0 fish abundance distributions from formal stock assessments, or those fitted to a stock-recruitment relationship (**Figure 7.6**), if there are no hydrodynamic models available or with limited time and resources. Because of the lack of a physical oceanographic model for the Atlantic coast domain, the latter method has been used for the initial prototype demonstration model.

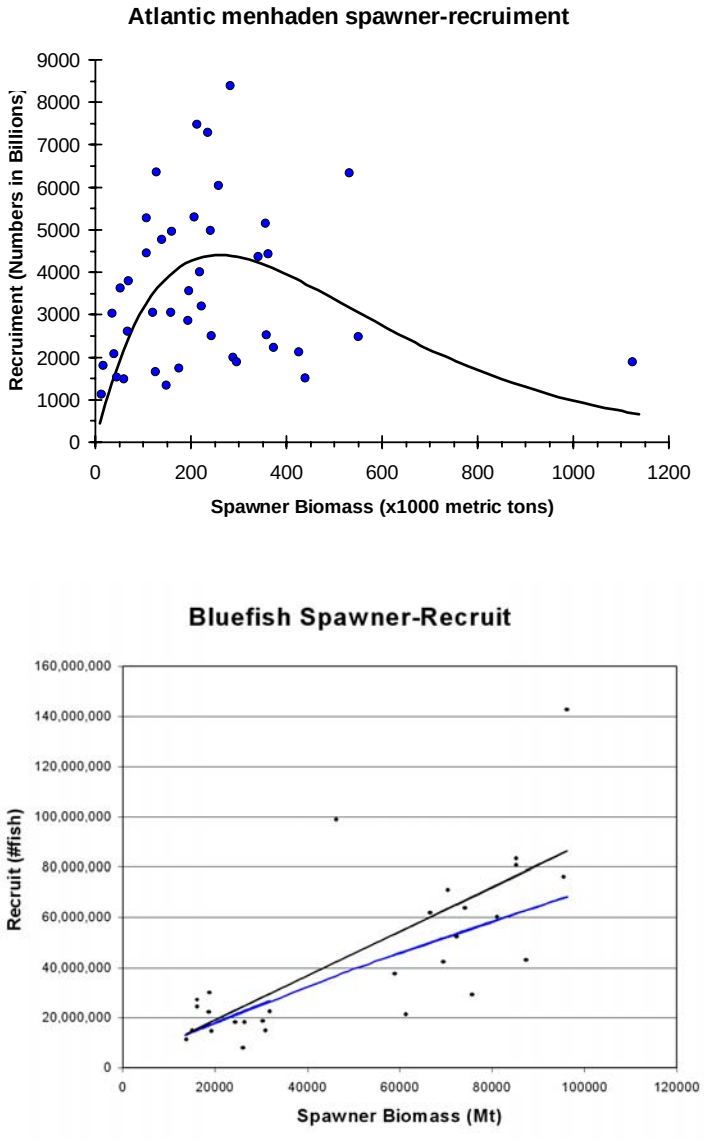

Figure 7.6.- Examples of the estimated stock and recruitment functions determined for Atlantic menhaden (upper panel) and bluefish (lower panel) used in spatial ecosystem model simulations.

Using the strategy of specifying recruitment that matched the formal VPA estimates, he spatial multispecies ecosystem simulation model was used in a comparison of modeled menhaden seasonal population distribution to those from empirical distributions observed in December by Checkley et al. (1999) are coherent and striking similar (**Figure 7.7**).

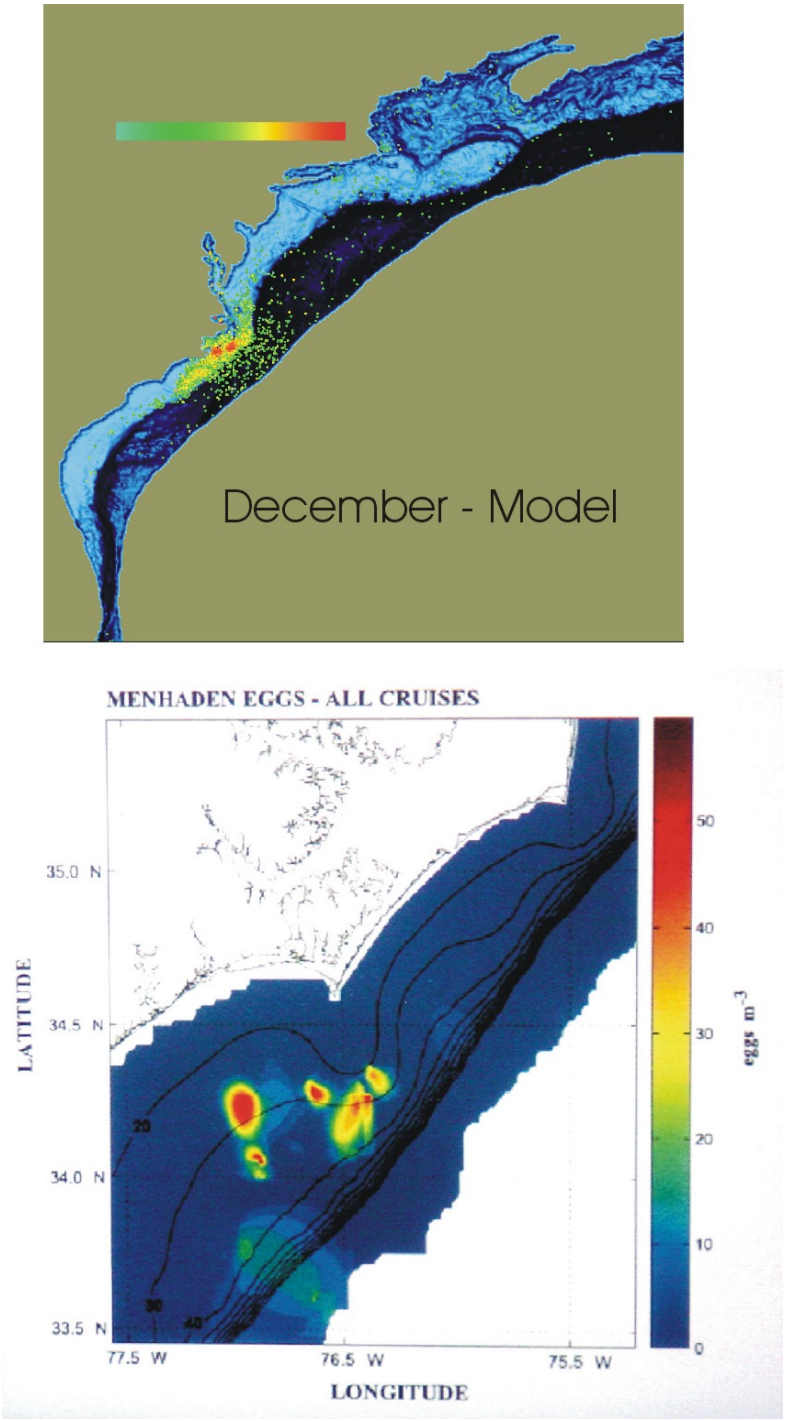

Figure 7.7.- Modeled menhaden spatial growth distribution in December compared to that observed by Checkley et al. (1999) for the same time period.

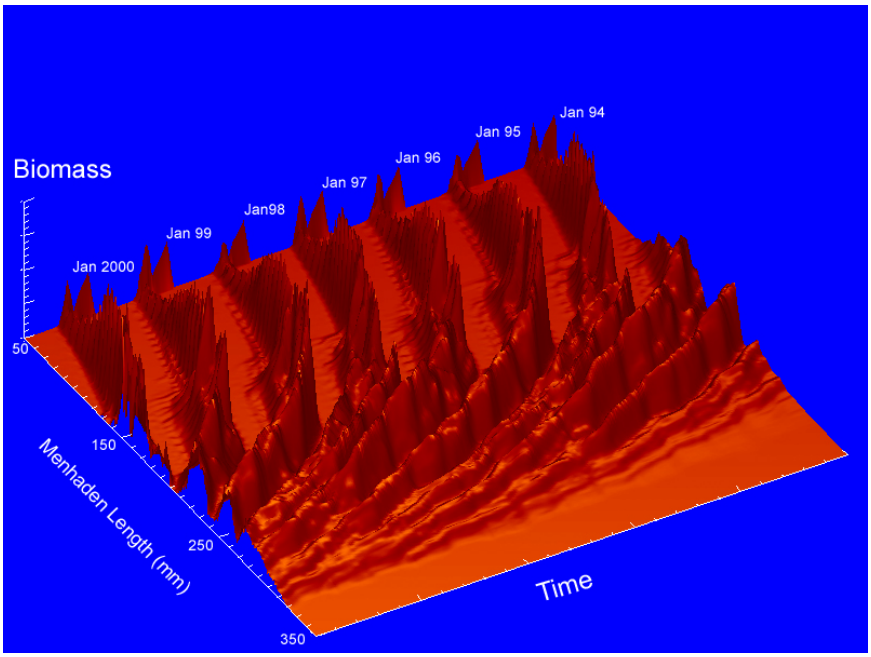

Figure 7.8.- Menhaden population biomass as a function of size and time from the multispecies spatial ecosystem model for the period November 1993 to November 2001.

7.6 Predators (Bluefish, Striped Bass, Weakfish).- Bioenergetics models for the key predator species were parameterized based on the models developed by Hartman (1993) and Hartman and Brandt (1995a,b). In the demonstration model, bluefish are the primary predator. The food source for the predators was be simplified into two categories: menhaden and other prey. Menhaden abundance is simulated by size, age and space point in the model (see **Figures 7.4** and **7.5**). The abundance of other prey will be determined seasonally and by size spectra from spatial data provided by the NEFSC trawl survey (**Figure 7.9** and **7.10**), and from a spatial ration of menhaden to other prey. This ratio will vary minimally by season and region, but if data availability allows, it will vary by month and by stratum.

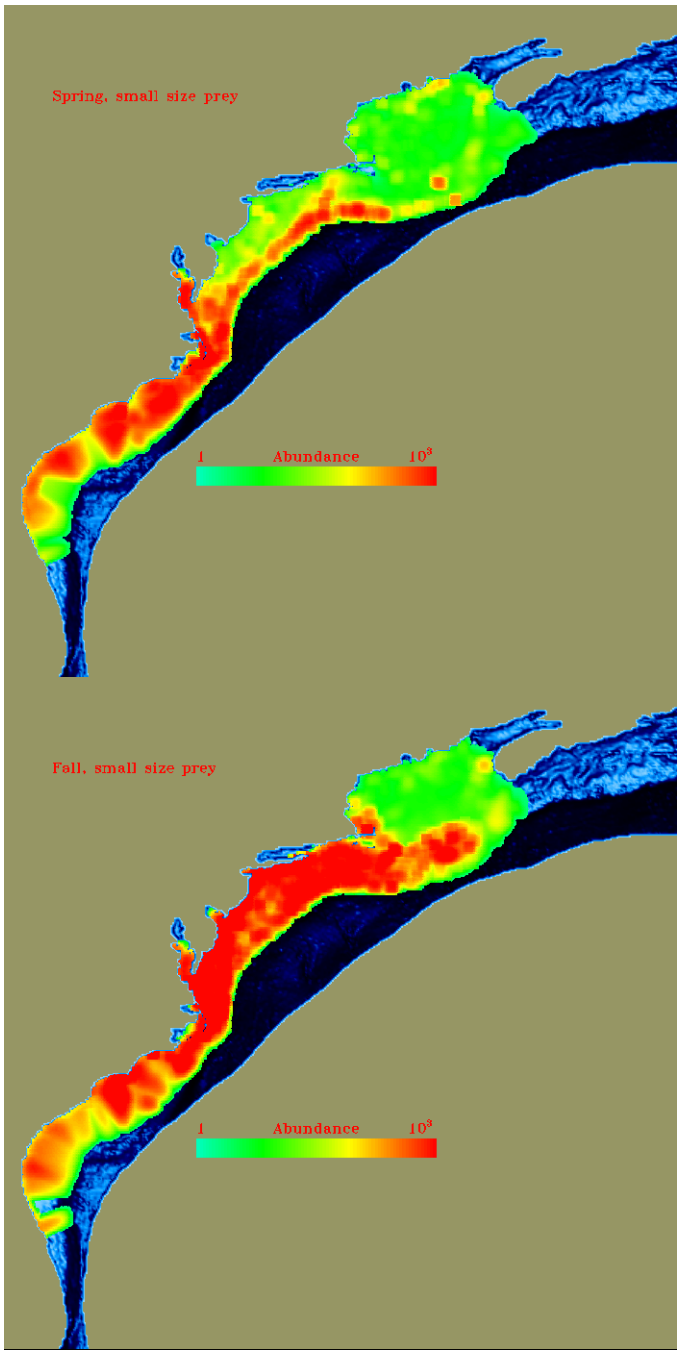

Figure 7.9.- Spatial density distribution of small prey by spring (upper panel) and fall (lower panel) season determined by synthesis of the NMFS NEFSC trawl survey 1978-2003.

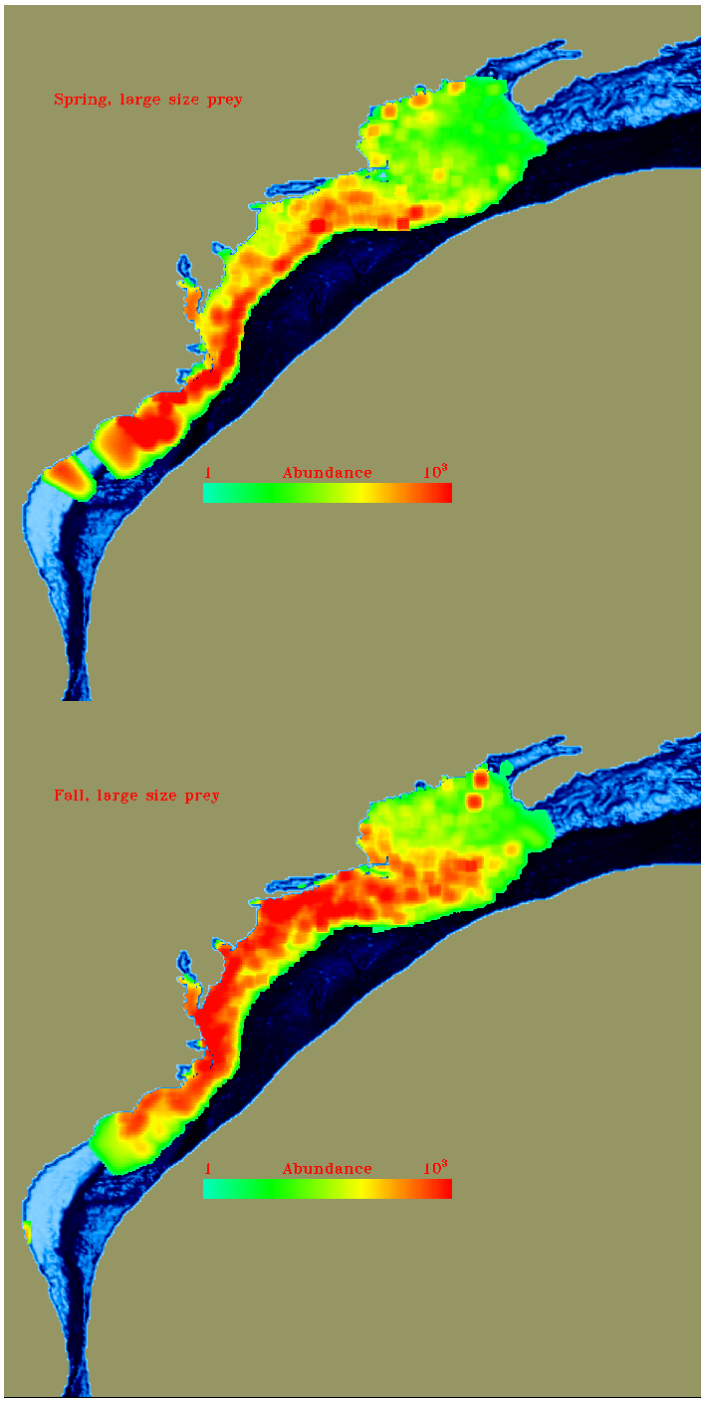

Figure 7.10.- Spatial density distribution of large prey by spring (upper panel) and fall (lower panel) season determined by synthesis of the NMFS NEFSC trawl survey 1978-2003.

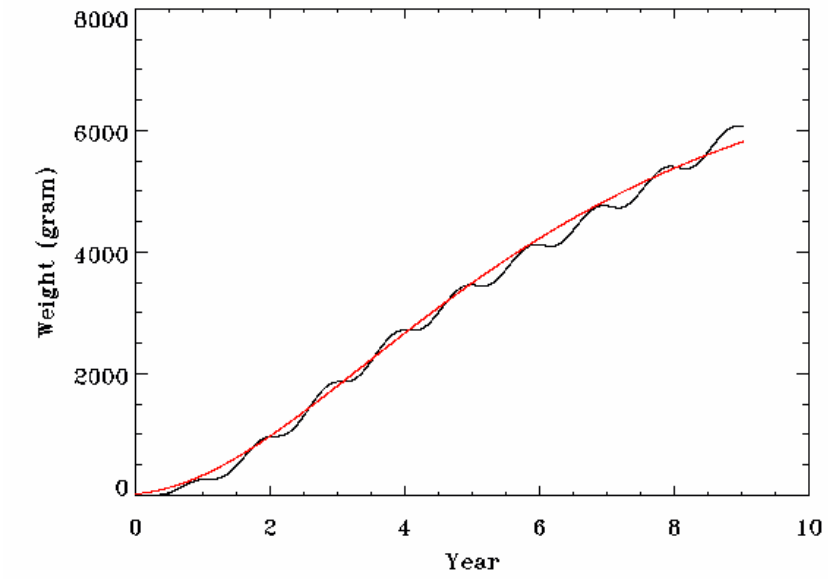

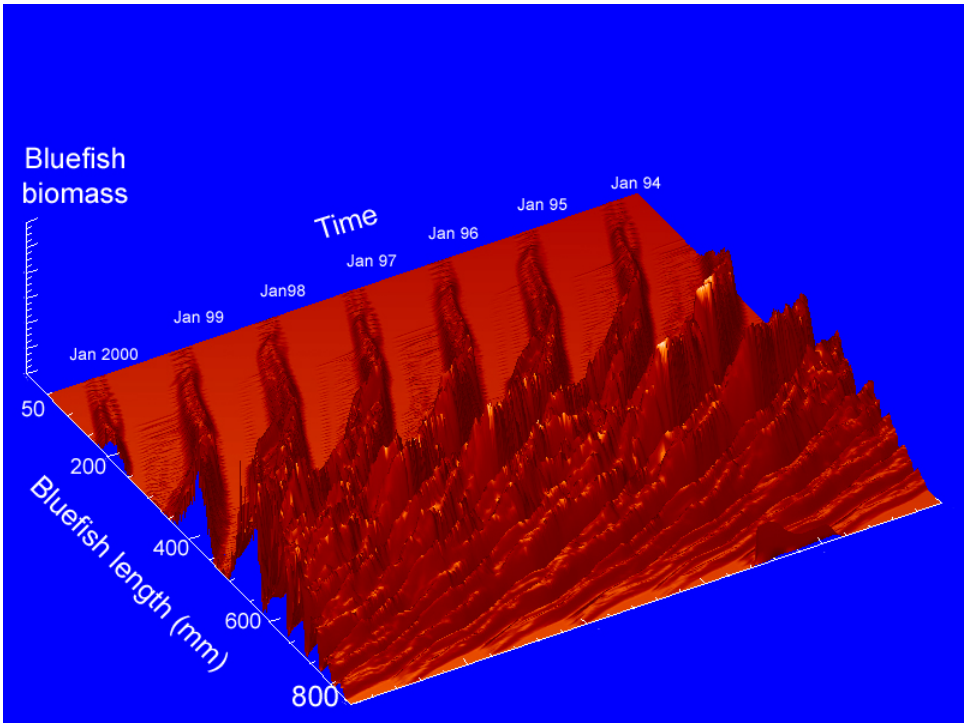

Figure 7.11.- (Upper panel) Bluefish population biomass as a function of size and time from the multispecies spatial ecosystem model for the period November 1993 to November 2001. (Lower panel) Bioenergetics growth model (red line) for Bluefish in comparison to the von Bertalanffy lifetime growth model (black line).

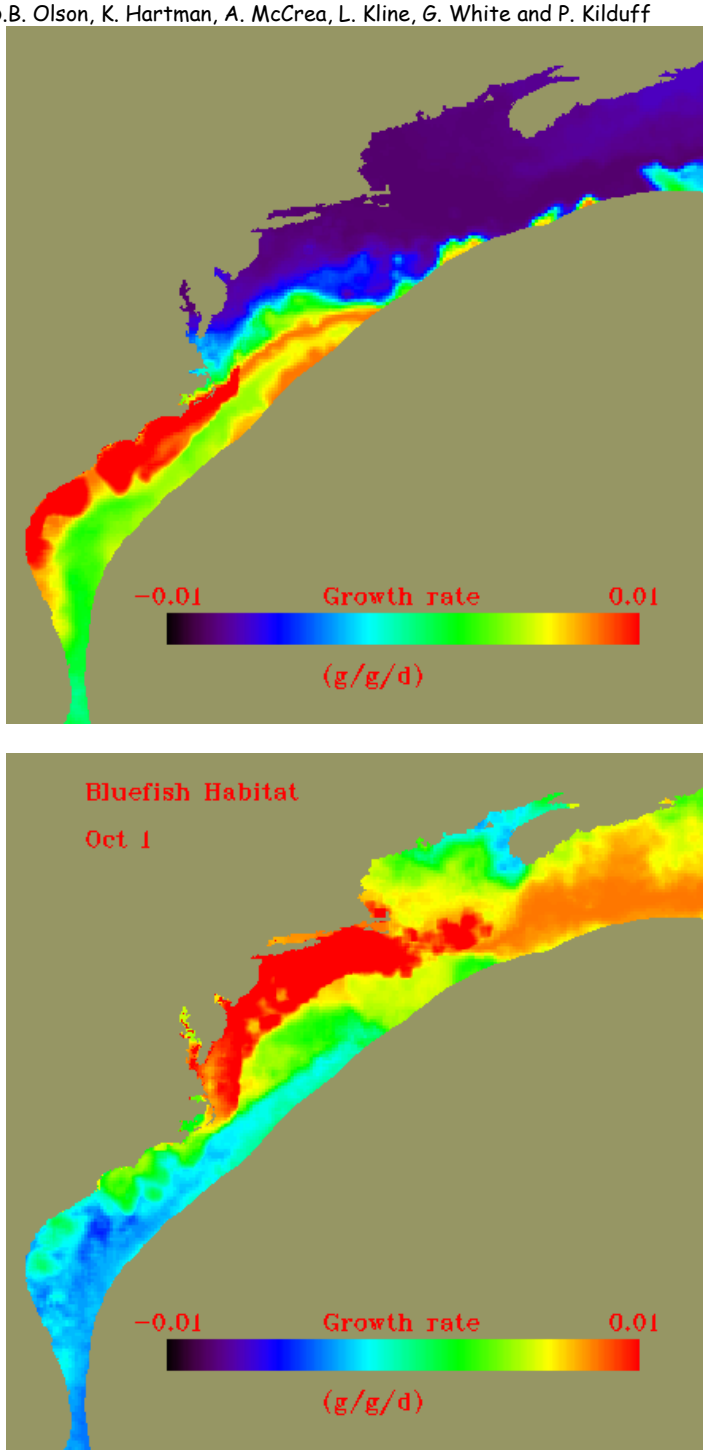

Figure 7.12.- Modeled spatial growth rate potential for age 1 Bluefish: (upper panel) for April 15th; and, (lower panel) October 1st.

7.7 Initial Population Distributions.- Seasonal spatial distribution maps of fish abundance were constructed for all age-classes of menhaden, bluefish, striped bass, and weakfish from the fishery-dependent data and fishery-independent survey data outlined earlier in this document. A method similar to stratified random sampling theory (Ault et al. 1999a) will be utilized. First, the entire spatial domain will be divided into geographic regions. Second, within each region, the habitat will be stratified according to physical properties (such as, depth, benthic type, salinity). Then, the mean and standard deviation of the abundance for each age class and each species will be estimated. Finally, the fish density will be cast onto each cell in the spatial domain according to a random Poisson distribution using the estimated means and standard deviations by stratum and region.

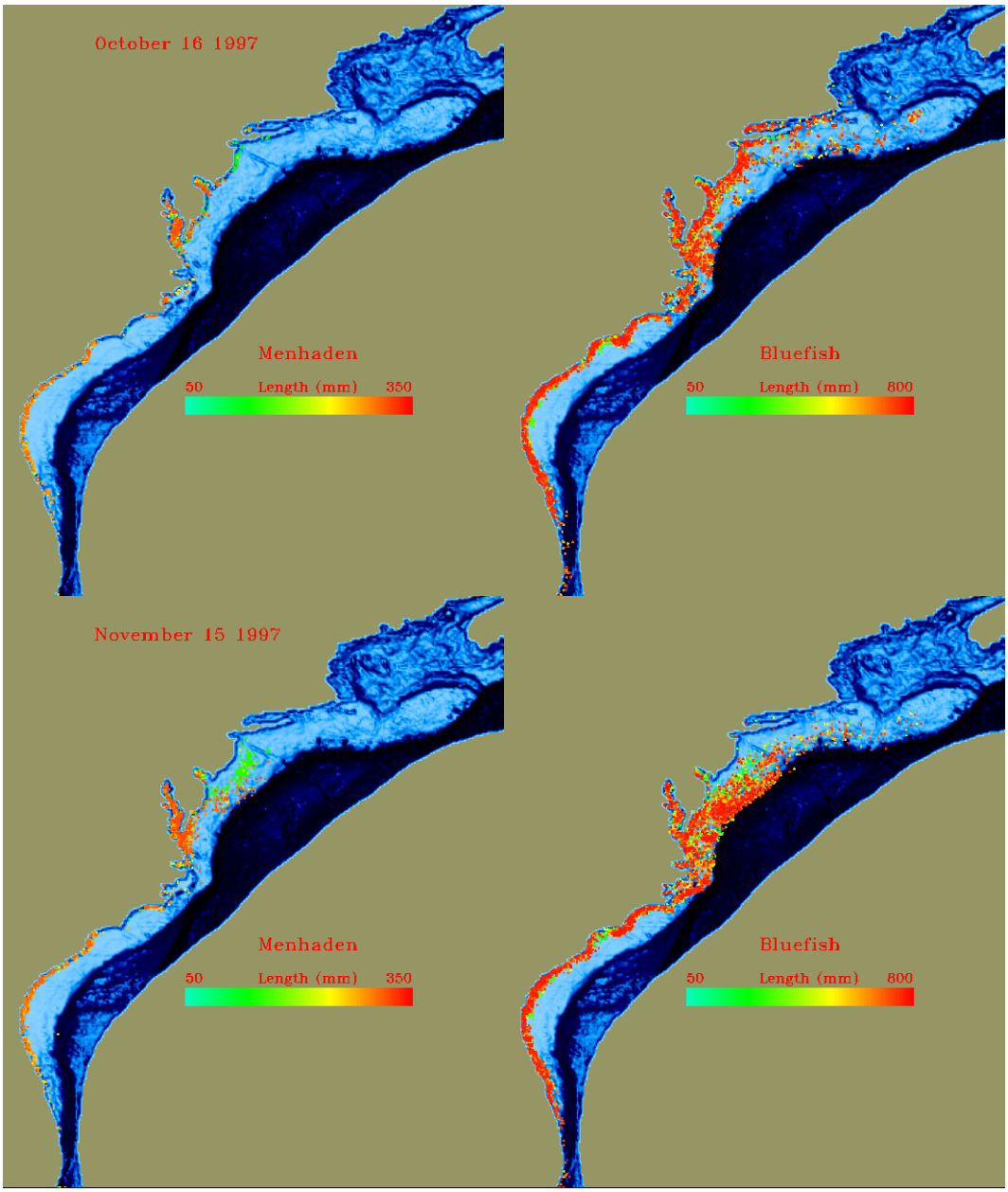

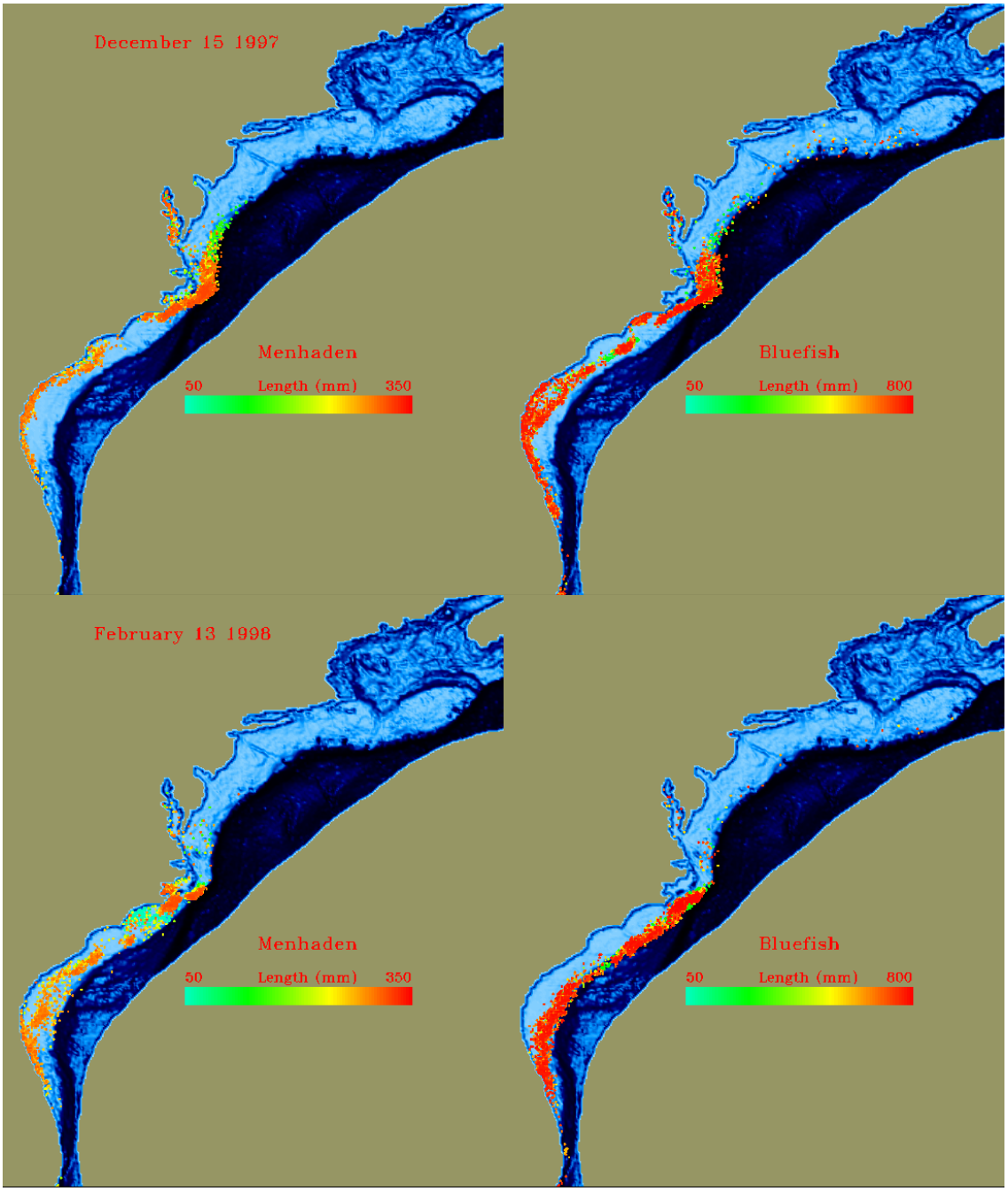

Figure 7.13.- Menhaden and bluefish seasonal spatial size distributions October 1997 to February 1998.

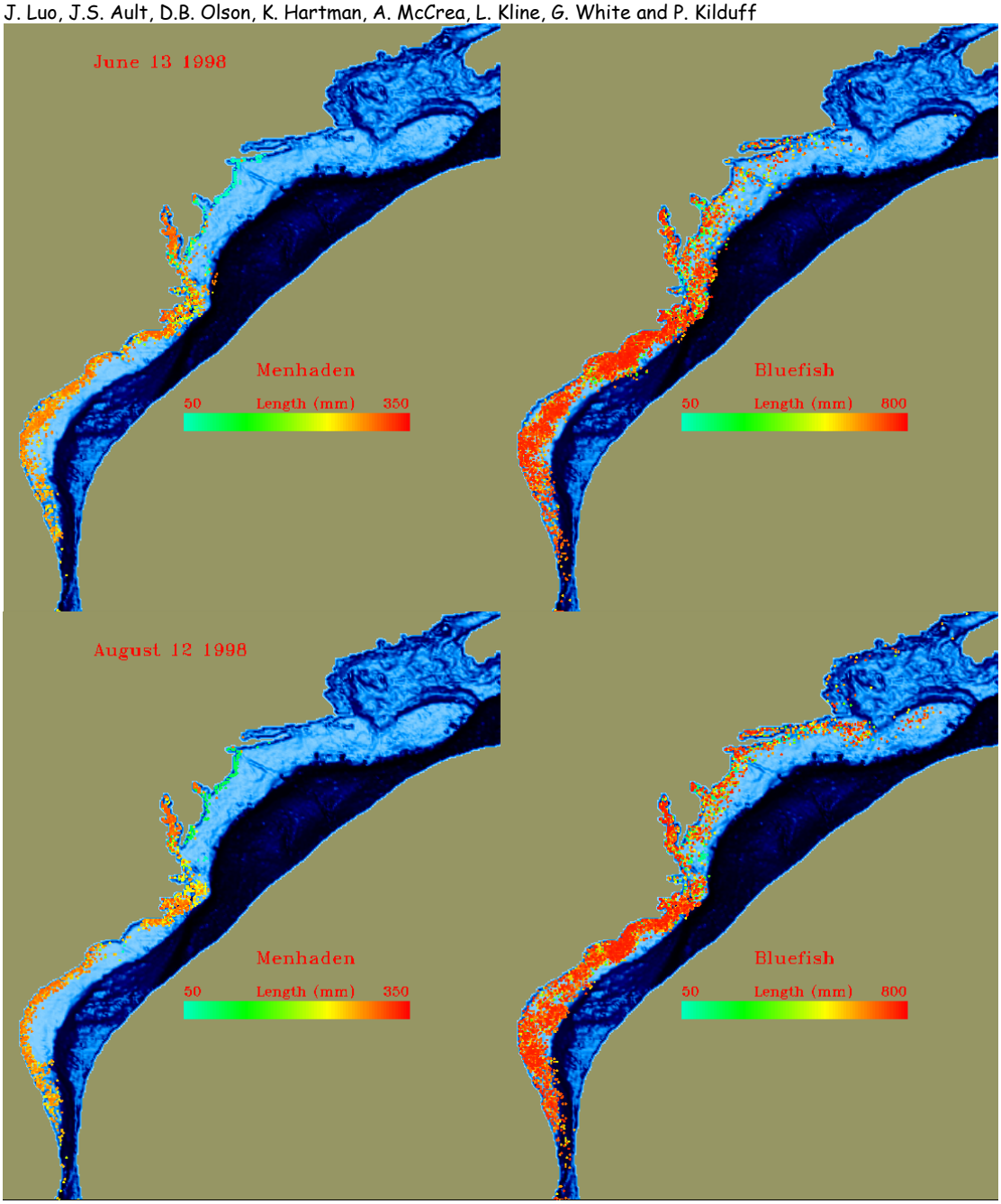

Figure 7.14.- Menhaden and bluefish seasonal spatial size distributions June 1998 and August 1998.

7.8 Effort distributions, Fishing and Environmental Impacts.- The spatial distribution of fishing effort was estimated in a similar fashion as the fish abundance distribution with modifications based upon data availability and spatial resolution. Since the spatial multispecies ecosystem model is fully structured in age and size for both predators and prey, the model tracks the size-abundance and biomass distributions of individuals over both space over time. As a result, familiar VPA-like results are available at every time daily step, and when appropriately aggregated in both space and time that can, at a minimum, describe quarterly, semi-annual, or annual catch-at-age and population-at-age statistics for stock biomass, yields, spawning biomass, and recruitment.

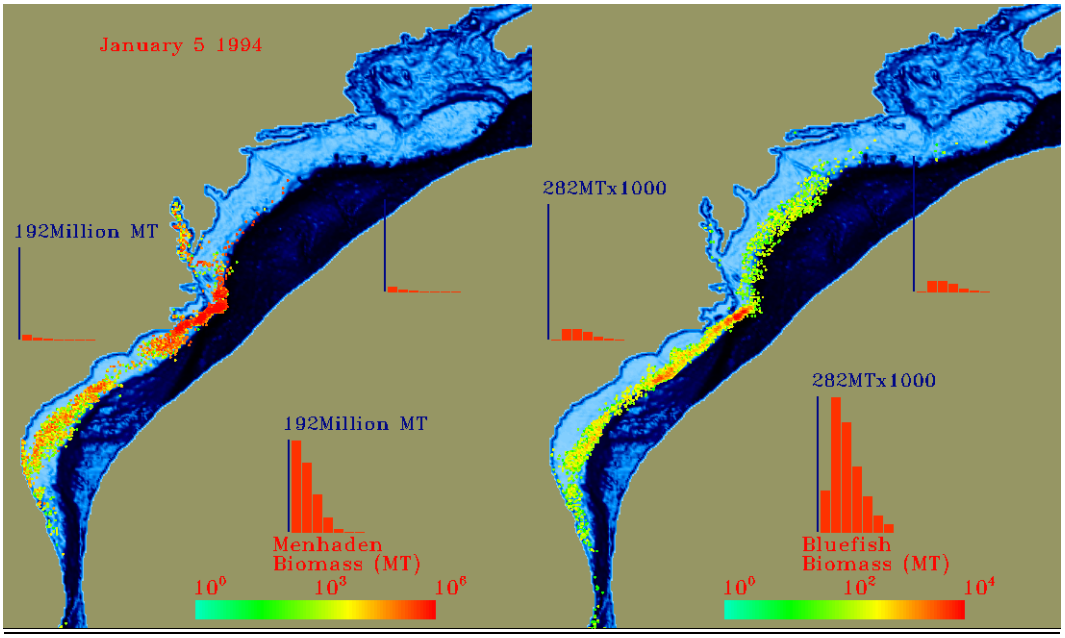

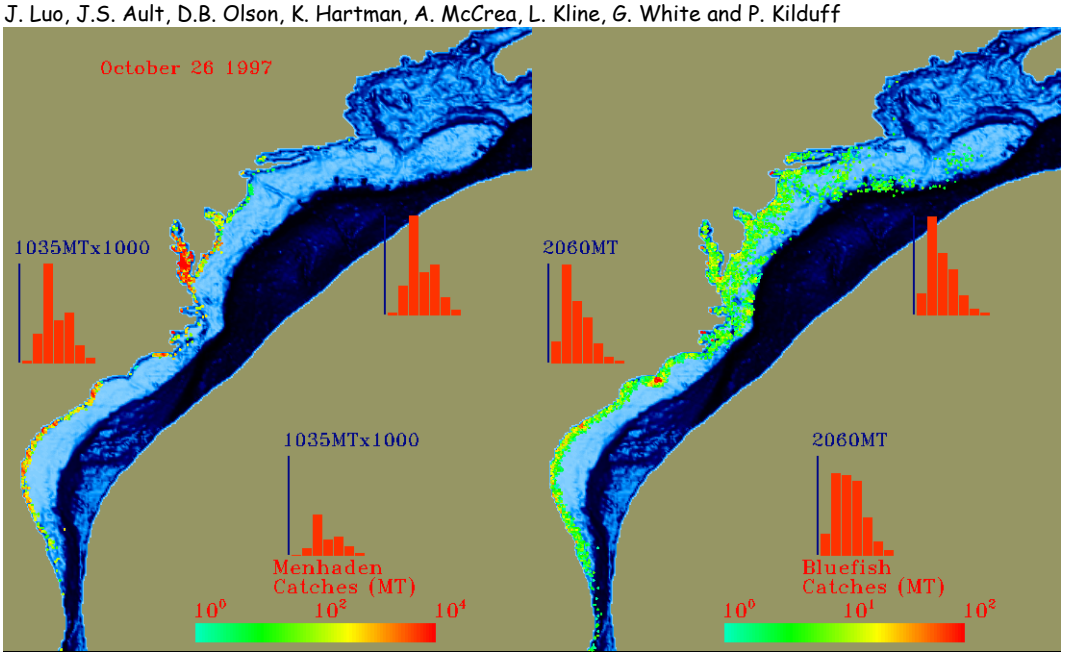
October 26 1997
1035MTx1000
1035MTx1000
Menhaden
Catches (MT)
10^0 10^2 10^4
2060MT
2060MT
Bluefish
Catches (MT)
10^0 10^1 10^2

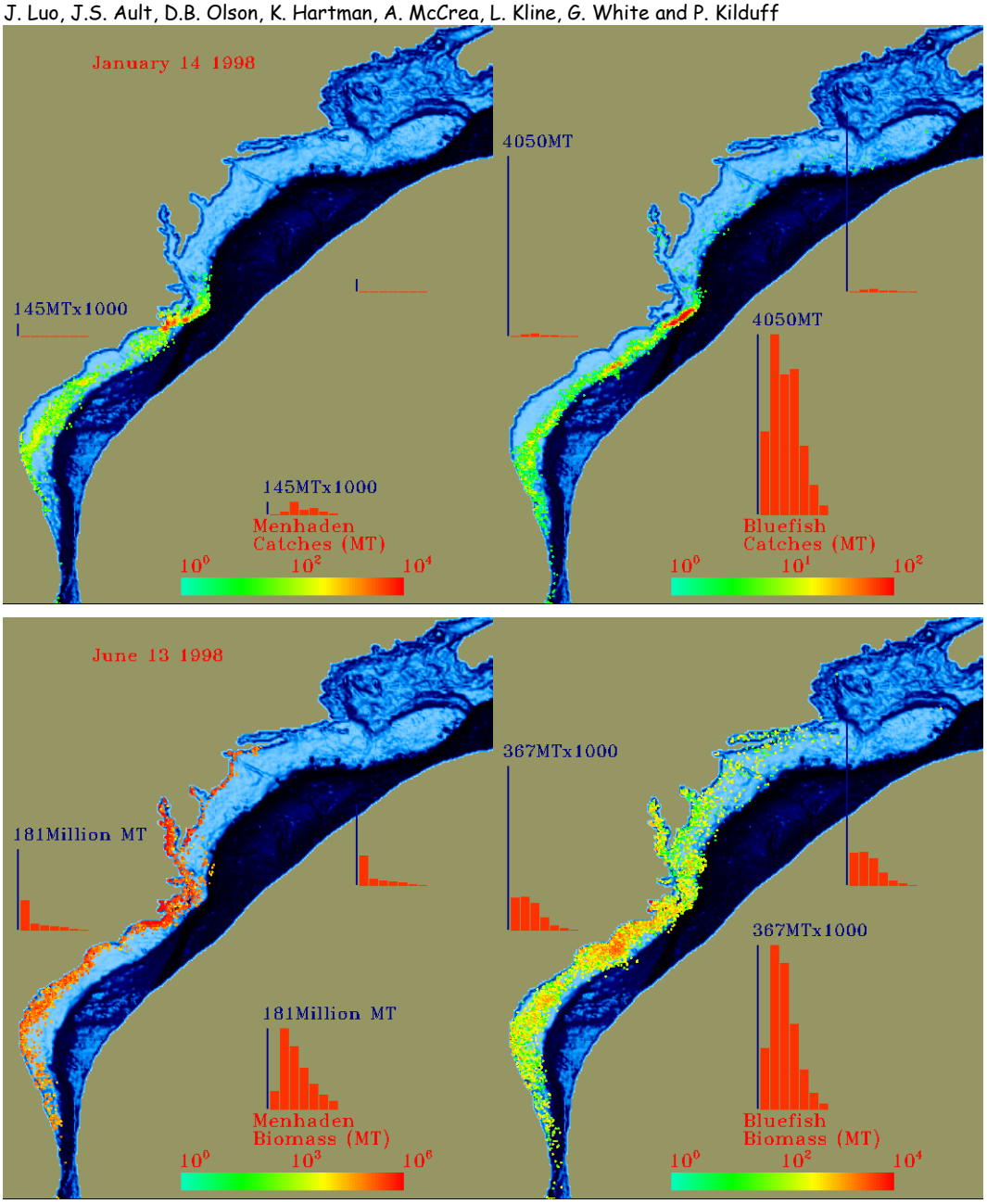

Figure 7.15.- Examples of menhaden and bluefish seasonal spatial catch distributions.

In addition, the model is also capable of producing a number of unique insights into the fishery ecosystem. For example, a dynamic "cohort table" –like graphic results from the running the spatial simulation model and aggregating the data over space to show a time-dynamic size and abundance distribution of the menhaden catch from the population (**Figure 7.16**).

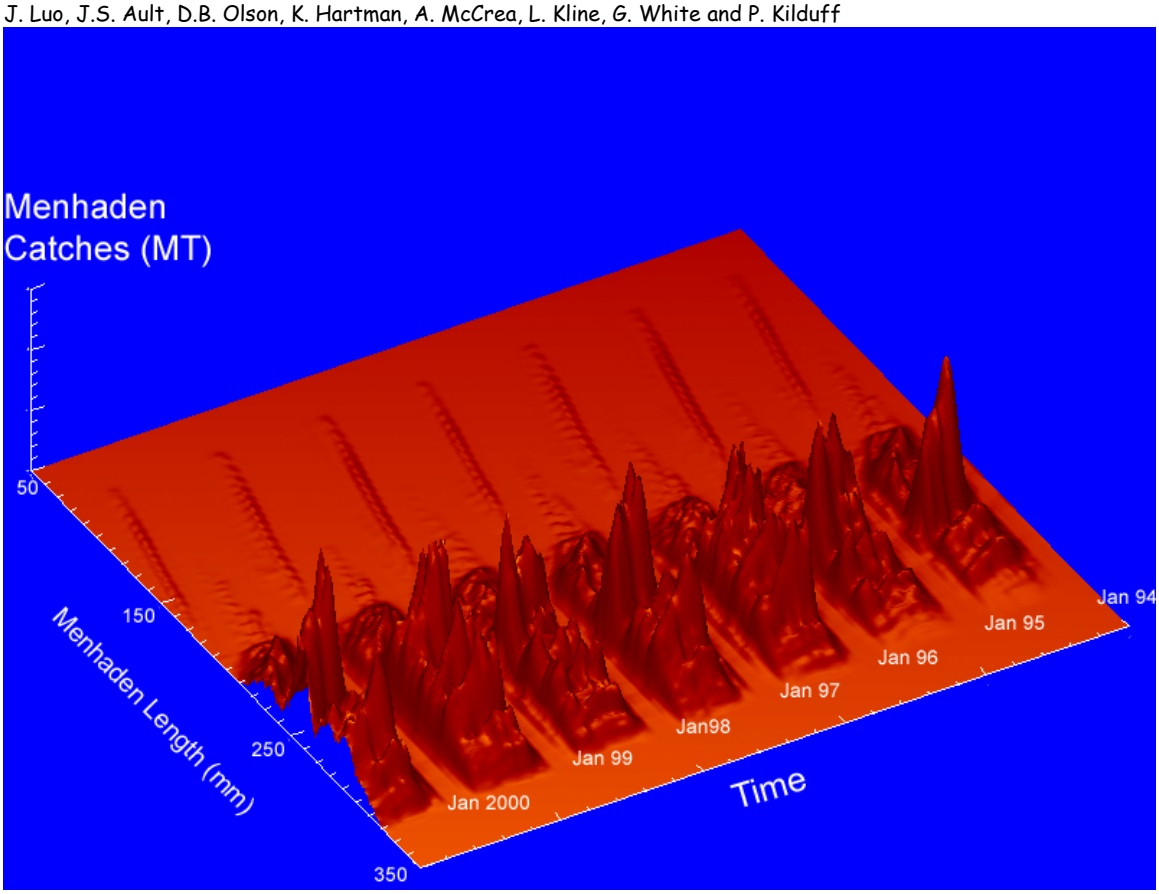

Figure 7.16.- Examples of menhaden catch distributions by size of fish from November 1994 to November 2000.

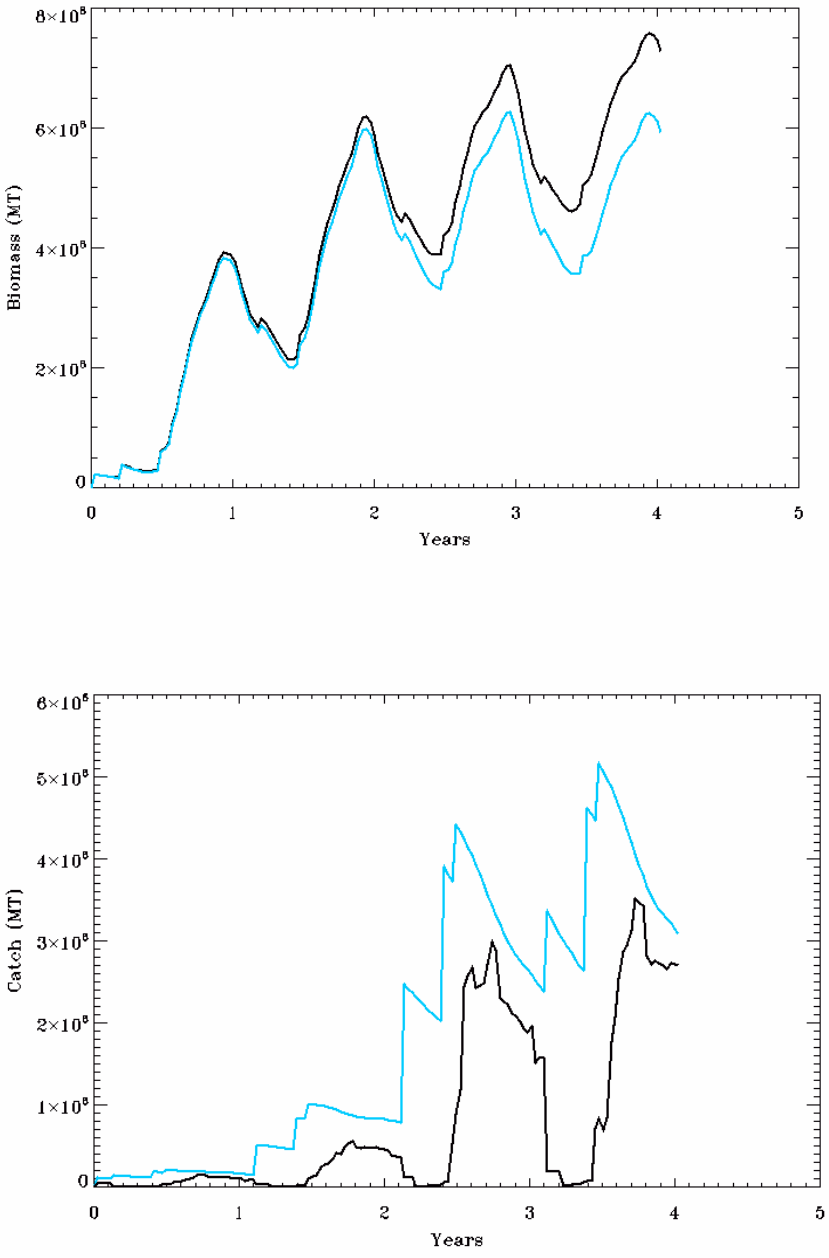

Figure 7.16.- Comparisons of menhaden stock biomass and fishery catches resulting from different spatial fishing strategies. Black line results from a fishing strategy that varied by month and area. Blue lines are for a fishing strategy that was spatially and temporally uniform.

Summary

Example results from the prototype spatial multispecies ecosystem model that we have presented here are not at this point meant to be final, nor necessarily predictive. They are simply shown to provide the reader a better sense of the types of inputs required by the model, and the types and range of quantitative outputs that can be expected from the fully coupled and integrated biophysical spatial fishery ecosystem model. In the course of our work we have identified many data gaps, such as lack of spatial indexing of data, no physical oceanographic model that covers the biophysical model domain, etc.; and, a general paucity of data on fish behavioral and physiological functions, movement rates, and intra-and inter-species interactions rates. To fill these gaps has required that we have preliminarily addressed them with a suite of simplifying assumptions. Thus, for the time being, outputs from our prototype demonstration spatial multispecies ecosystem model at any particular time point may not completely represent absolute values, but instead represent relative trends and relationships of the state variables over time. As such, the model provides invaluable insights into the dynamics of menhaden and bluefish would be expected to exhibit given the underlying dynamics and forcing in the Atlantic States fishery coastal ocean ecosystem. We recommend that future reality and consistency checks should focus the demonstration model on an evaluation of the feasibility of its application along the Atlantic coast fishery resources with limited time and fiscal resources. Subsequent model development efforts will require focused user and constituency inputs that will allow us to direct modify the ecosystem model where necessary to ultimately allow resource scientists, fishery managers and decision makers to examine the full suite of fishery assessment and management decision-making benchmarks, and perhaps a suite of new ecosystem indicator measures, to manage in a sustainable way the core fisheries of the Atlantic coast multispecies complex using an ecosystem-based approach to management.

Literature Cited

Adams, S.M. and, J.E. Breck. 1990. Bioenergetics. Pages 389-415 in C.B. Schreck and P.B. Moyle (eds.), Methods for Fish Biology, American Fisheries Society, Bethesda, Maryland.

ASMFC. 2003a. Linking Multispecies Assessments to Single Species Management. Special Report No. 79 of the Atlantic States Marine Fisheries Commission. 54 p.

ASMFC. 2003b. Atlantic Menhaden 2003 Stock Assessment Report. Atlantic States Marine Fisheries Commission. 159 p.

Ault, J.S. 1996. A fishery management system approach for Gulf of Mexico living resources. In 'GIS Applications for Fisheries and Coastal Resources Management', Rubec, P.J. and O'Hop, J. (eds.). Gulf States Marine Fisheries Commission 43:106-111.

Ault, J.S., Bohnsack, J.A., Smith, S.G., and J. Luo. 2005a. Towards sustainable multispecies fisheries in the Florida USA coral reef ecosystem. Bulletin of Marine Science 76(2):595-622.

Ault, J.S., Smith, S.G., and J.A. Bohnsack. 2005b. Evaluation of average length as an indicator of exploitation status for the Florida coral reef fish community. ICES Journal of Marine Science **62**:417-423.

Ault, J.S., Luo, J., Smith, S.G., Serafy, J.E., Wang, J.D., Diaz, G.A., and R. Humston. 1999a. A spatial dynamic multistock production model. Canadian J. of Fisheries and Aquatic Sciences 56 (S1):4-25.

Ault, J.S., Diaz, G.A., Smith, S.G., Luo, J. and J.E. Serafy. 1999b. An efficient sampling survey design to estimate pink shrimp population abundance in Biscayne Bay, Florida. North American Journal of Fisheries Management 19(3):696-712.

Ault, J.S., Luo, J., and J.D. Wang. 2003. A spatial ecosystem model to assess spotted seatrout population risks from exploitation and environmental changes. Pages 267-296 in S. Bortone (ed.). Biology of the Spotted Seatrout. CRC Press.

Ault, J.S., and D.B. Olson. 1996. A multicohort stock production model. Transactions of the American Fisheries Society 125(3):343-363.

Ault, J.S., Bohnsack, J.A., and G.A. Meester. 1998. A retrospective (1979-1996) multispecies assessment of coral reef fish stocks in the Florida Keys. Fishery Bulletin 96(3):395-414.

Berg, H.C. 1993. Random walks in biology. Princeton University Press, New Jersey, xxx p.

Bleck, R., and Boudra, D.B. 1986. Wind-driven spin up in eddy-resolving ocean models formulated in isopycnic and isobaric coordinates. Journal Geophysical Research 91:7611-7621.

Bohnsack, J.A., and Ault, J.S. 1996. Management strategies to conserve marine biodiversity. Oceanography 9(1):73-82.

Brandt, S.B., Mason, D.M., and Patrick, E.V. 1992. Spatially-explicit models of fish growth rate. Fisheries 17:23-33.

Cosner, G.C., DeAngelis, D.L., Ault, J.S., and D.B. Olson. 1999. Effects of spatial grouping on the functional response of predators. Theoretical Population Biology 56(1):56-65.

DeAngelis, D.L., and Gross, L.J. 1992. Individual-based models and approaches in ecology. Chapman & Hall, New York, 525 p.

Diaz, G.A., Smith, S.G., Serafy, J.E. and J.S. Ault. 2001. Allometry of the growth of pink shrimp *Farfantepenaeus duorarum* in a subtropical bay. Transactions of the American Fisheries Society 130(2):328-335.

Ehrhardt, N.M., and J.S. Ault. 1992. Analysis of two length-based mortality models applied to bounded catch length frequencies. Transactions of the American Fisheries Society 121(1):115-122.

Fox, W.W., Jr. 1970. An exponential surplus yield model for optimizing exploited fish populations. Transactions of the American Fisheries Society 90:80-88.

Fox, W.W., Jr. 1975. Fitting the generalized stock production model by least-squares and equilibrium approximation. U.S. National Marine Fisheries Service Fishery Bulletin 73:23-37.

Gray, W., and D. Lynch. 197x. Time-Stepping Schemes for Finite Element Tidal Model Computations. Advances in Water Resources, 1(2):83-95.

Gulland, J.A. 1983. Fish stock assessment: a manual of basic methods. John Wiley, 223 p.

Gutierrez, A.P. 1996. Applied population ecology: a supply-demand approach. John Wiley, 300 p.

Hartman, K. 1993. Striped bass, bluefish, and weakfish in the Chesapeake Bay: energetics, trophic linkages, and bioenergetic model applications. Ph.D. dissertation, University of Maryland, College Park, MD.

Hartman, K. J., and S. B. Brandt. 1995a. Comparative energetics and the development of bioenergetics models for sympatric estuarine piscivores. Canadian Journal of Fisheries and Aquatic Sciences 52:1647-1666.

Hartman, K. J., and S. B. Brandt. 1995b. Predatory demand and impact of striped bass, bluefish, and weakfish in the Chesapeake Bay: applications of bioenergetics models. Canadian Journal of Fisheries and Aquatic Sciences 52:1667-1687.

Humston, R., Ault, J.S., Lutcavage, M. and D.B. Olson. 2000. Schooling and migration of large pelagic fishes relative to environmental cues. Fisheries Oceanography 9(2):136-146.

Humston, R., Olson, D.B., and J.S. Ault. 2004. Behavioral assumptions in models of fish movement and their influence on population dynamics. Transactions of the American Fisheries Society 133:1304-1328.

Jobling, M. 1994. Fish bioenergetics. Fish and Fisheries Series 13, Chapman & Hall, 309 p.

Kitchell, J.F., Stewart, D.J.,, and D. Weininger. 1977. Applications of a bioenergetics model to yellow perch (Perca flavescens) and walleye (Stizostedion vitreum). J. Fish. Res. Board Can. 34:1922-1935.

Lindeman, K.C., Pugliese, R., Waugh, G.T. and J.S. Ault. 2000. Developmental pathways within a multispecies reef fishery: management applications for essential habitats and marine reserves. Bulletin of Marine Science 66(3):929-956.

Luo, J., Hartman, K.J., Brandt, S.B., Cerco, F.C., Rippetoe, T.H. 2001. A spatially-explicit approach for estimating carrying capacity: an application for the Atlantic menhaden (Brevoortia tyrannus) in Chesapeake Bay. Estuaries 24(4):545-556.

Pella, J.J., and Tomlinson, P.K. 1969. A generalized stock production model. Inter-American Tropical Tuna Commission Bulletin 13:419-496.

Quinn, T.J., and Deriso, R.B. 1999. Quantitative Fish Dynamics. Oxford University Press.

Rothschild, B.J. 1986. Dynamics of Marine Fish Populations. Harvard University Press, Cambridge, MA.

Rothschild, B.J. 2000. "Fish stocks and recruitment": the past thirty years. ICES J. Marine Science 57:191-201.

Rothschild, B.J., and Ault, J.S. 1992. Linkages in ecosystem models. South African Journal of Marine Science 12:1101-1108.

Rothschild, B.J., and J.S. Ault. 1996. Population-dynamic instability as a cause of patch structure. Ecological Modelling 93(1-3):237-249.

Rothschild, B.J., Ault, J.S., Goulletquer, P., and Heŕal, M. 1994. Decline of the Chesapeake Bay oyster population: a century of habitat destruction and overfishing. Marine Ecology Progress Series 111(2&3):29-39.

Rothschild, B.J., Ault, J.S., and S.G. Smith. 1996. A systems science approach to fisheries stock assessment and management. Pages 473-492 in Stock Assessment: Quantitative Methods and Applications for Small Scale Fisheries, Gallucci, V.F., Saila, S., Gustafson, D., and B.J. Rothschild (eds.). Lewis Publishers (Division of CRC Press). Chelsea, Michigan, 527 p.

Rubec, P.J., Bexley, J.C.W., Coyne, M.S., Monaco, M., Smith, S.G., and J.S. Ault. 1999. Suitability modeling to delineate habitat essential to sustainable fisheries. American Fisheries Society Symposium 22:108-133.

Rubec, P.J., Smith, S.G., Coyne, M.S., White, M., Wilder, D., Sullivan, A., Ruiz-Cruz, R., MacDonald, T., McMichael, R.H., Henderson, G.E., Monaco, M.E., and J.S. Ault. 2000. Spatial modeling of fish habitat in Florida. In Spatial Processes and Management of Fish Populations. Alaska Sea Grant College.

Schaefer, M.B. 1954. Some aspects of the dynamics of populations important to the management of the commercial marine fisheries. Inter-American Tropical Tuna Commission Bulletin 1(2):27-56.

Serafy, J.E., Lindeman, K.C., Hopkins, T.E., and J.S. Ault. 1997. Effects of freshwater canal discharge on fish assemblages in a subtropical bay: field and laboratory observations. Marine Ecology Progress Series 160:161-171

Thorton, K.W., and A.S. Lessem. 1978. A temperature algorithm for modifying biological rates. Trans. Amer. Fish. Soc. 107:284-287.

von Bertalanffy, L. 1949. Problems of organic growth. Nature (London) 163:156-158.

Walters, C.J., and S.J.D. Martell. 2004. Fisheries Ecology and Management. Princeton University Press. 399 p.

Wang, J.D., Luo, J., and J.S. Ault. 2003. Flows, salinity, and some implications for larval transport in south Biscayne Bay, Florida. Bulletin of Marine Science 72(3):695-723.

Appendix 1.- Menhaden References

Ahrenholz, D.W. (1991) Population biology and life history of the North American menhadens, *Brevoortia spp. Mar. Fish. Rev.* 53:3-19.

Ahrenholz, D.W., Dudley, D.L., and Levi, E.J. (1991) Overview of mark-recovery studies on adult and juvenile Atlantic menhaden, *Brevoortia tyrannus*, and Gulf menhaden, *B. patronus. Mar. Fish. Rev.* 53:20-27.

Ahrenholz, D.W., Nelson, W.R., and Epperly, S.P. (1987) Populaltion and fishery characteristics of Atlantic menhaden, *Brevoortia tyrannus*. *Fish. Bull.* 85:569-600.

Atlantic Menhaden Advisory Committee (AMAC). Atlantic menhaden management review, 2000. Report to the Atlantic Menhaden Management Board of the Atlantic States Marine Fisheries Commission, Washington, D.C., 18 pp.

Cadrin, S.X. and Vaughan, D.S. (1997) Retrospective analysis of virtual population estimates for Atlantic menhaden stock assessment. *Fish. Bull.* 95:445-455.

Checkley, D.M., Jr., Ortner, P.B., Werner, F.E., Settle, L.R., and Cummings, S.R. (1999). Spawning habit of the Atlantic menhaden in Onslow Bay, North Carolina. *Fish. Oceanogr.* 8(suppl. 2):22-36.

Colton, J.B., Smith, W.G., Kendall, A.W., Jr., Berrien, P.L., and Fahay, M.P. (1979). Principal spawning areas and times of marine fishes, Cape Sable to Cape Hatteras. *Fish. Bull.* 76:911-915.

Dietrich, C.S., Jr. (1979) Fecundity of the Atlantic menhaden *Brevoortia tyrannus*. *Fish. Bull.* 77:308-311.

Dryfoos, R.L., Cheek, R.P., and Kroger, R.L. (1973) Preliminary analyses of Atlantic menhaden, *Brevoortia tyrannus*, migrations, population structure, survival and exploitation rates, and availability as indicated from tag returns. *Fish. Bull.* 71:719-734.

Durbin, A.G., and Durbin, E.G. (1975) Grazing rates of the Atlantic menhaden *Brevoortia tyrannus* as a function of particle size and concentration. *Mar. Biol.* 33:265-277.

Durbin, A.G., and Durbin, E.G. (1998) Effects of menhaden predation on plankton populations in Narragansett Bay, Rhode Island. *Estuaries* 21:449-465.

Durbin, A.G., Durbin, E.G., Smayda, T.J., and Verity, P.G. (1982) Age, size, growth, and chemical composition of Atlantic menhaden, *Brevoortia tyrannus*, from Narragansett Bay, Rhode Island. *Fish. Bull.* 81:133-141.

Friedland, K.D., Ahrenholz, D.W., and Guthrie, J.F. (1989) Influence of plankton on distribution patterns of the filter-feeder *Brevoortia tyrannus* (Pices: Clupeidae). *Mar. Ecol. Prog. Ser.* 54:1-11.

Gottlieb, S.J. (1998) Nutrient removal by age-0 Atlantic menhaden (*Brevoortia tyrannus*) in Chesapeake Bay and implications for seasonal management of the fishery. *Ecol. Model.* 112: 111-130.

Jeffries, H.P. (1975) Diets of juvenile Atlantic menhaden (*Brevoortia tyrannus*) in three estuarine habitats as determined from fatty acid composition of gut contents. *J. Fish. Res. Board Can.* 32:587-592.

Judy, M.H. and Lewis, R.M. (1983) Distribution of eggs and larvae of Atlantic menhaden, *Brevoortia tyrannus*, along the Atlantic coast of the United States.
NOAA Tech. Rep. NMFS SSRF-774. pp 1-23.

June, F.C. (1972) Variations in size and length composition of Atlantic menhaden groupings. *Fish. Bull.* 70:699-713.

June, F.C., and Carlson, F.T. (1971) Food of young Atlantic menhaden, *Brevoortia tyrannus*, in relation to metamorphosis. *Fish. Bull.* 68:493-512.

Kroger, R.L. and Guthrie, J.F. (1973) Migrations of tagged juvenile Atlantic menhaden. *Trans. Amer. Fish. Soc.* 2:417-422.

Lewis, R.M., Ahrenholz, D.W., and Epperly, S.P. (1987) Fecundity of Atlantic menhaden *Brevoortia tyrannus*. *Estuaries*, 10:347-350.

Lewis, V.P. and Peters, D.S. (1994) Diet of juvenile and adult Atlantic menhaden in estuarine and coastal habitats. *Trans. Am. Fish. Soc.* 123:803-810.

Maillet, G.L., and Checkley, D.M. (1991) Storm-related variation in the growth of otoliths of larval Atlantic menhaden *Brevoortia tyrannus*: a time series analysis of biological and physical variables and implications for larva growth and mortality. *Mar. Ecol. Prog. Ser.* 79:1-16.

Nicholson, W.R. (1971) Coastal movements of Atlantic menhaden as inferred from changes in age and length distributions. *Trans. Amer. Fish. Soc.* 4:708-716.

Nicholson, W.R. (1972) Population structure and movements of Atlantic menhaden, *Brevoortia tyrannus*, as inferred from back-calculated length frequencies. *Chesapeake Sci.* 13:161-174.

Nicholson, W.R. (1978). Movements and population structure of Atlantic menhaden indicated by tag returns. *Estuaries*. 1:141-150.

Peppar, J.L. (1974) Northern extension of known range of Atlantic menhaden (*Brevoortia tyrannus). J. Fish. Res. Board Can.* 31:471-472.

Peters, D.S., and Schaaf, W.E. (1981) Food requirements and sources for juvenile Atlantic menhaden. *Trans. Am. Fish. Soc.* 110:317-324.

Powell, A.B. (1994) Life history traits of two allopatric clupeids, Atlantic menhaden and Gulf menhaden, and the effects if harvesting on these traits. *N. Am. J. Fish. Manage.* 14:53-64.

Powell, A.B., and Phonlor, G. (1986) Early life history of Atlantic menhaden, *Brevoortia tyrannus*, and Gulf menhaden, *B. patronus. Fish. Bull.* 84:991-995.

Quinlan, J.A., and Crowder, L.B. (1999) Searching for sensitivity in the life history of Atlantic menhaden: inferences from a matrix model. *Fish. Oceanogr.* 8:124-133.

Quinlan, J.A., Blanton, B.O., Miller, T.J., and Werner, F.E. (1999). From spawning grounds to the estuary: using linked individual-based and hydrodynamic models to interpret patterns and processes in the oceanic phase of the Atlantic menhaden, *Brevoortia tyrannus* life history. *Fish. Oceanogr.* 8(suppl. 2):224-246.

Reish, R.L., Deriso, R.B., Ruppert, D., and Carroll, R.J. (1985) An investigation of the population dynamics of Atlantic menhaden (*Brevoortia tyrannus*). *Can. J. Fish. Aquat. Sci.* 42:147-157.

Ruppert, D., Reish, R.L., Deriso, R.B., and Carroll, R.J. (1985) A stochastic population model for managing the Atlantic menhaden (*Brevoortia tyrannus*) fishery and assessing managerial risks. *Can. J. Fish. Aquat. Sci.* 42:1371-1379.

Stokesbury, M.J.W., and Stokesbury, K.D.E. (1993) Occurrence of juvenile Atlantic menhaden, *Brevoortia tyrannus*, in the Annapolis River, Nova Scotia. *Estuaries* 16:827-829.

Vaughan, D.S. and Merriner, V. (1991) Assessment and management of the Atlantic and Gulf menhaden stocks. *Mar. Fish. Rev.* 53:49-57.

Vaughan, D.S., Prager, M.H., and Smith, J.W. (2002) Consideration of uncertainty in stock assessments of Atlantic menhaden. American Fisheries Society Symposium 27:83-112, *In* J.M. Berkson, L.L. Kline, and D.J. Orth (eds.), Incorportating Uncertainty into Fishery Models.

Vaughan, D.S. and Smith, J.S. (1988) Stock assessment of the Atlantic menhaden, *Brevoortia tyrannus*, fishery. *NOAA Tech. Rep. NMFS 63*, 18 pp.

Vaughan, D.S. and Smith, J.S. (1991) Biological analysis of two management options for the Atlantic menhaden fishery. *Mar. Fish. Rev.* 53:58-66.

Vaughan, D.S., Smith, J.S., and Williams, E.H. (2002) Analysis on the status of the Atlantic menhaden stock. Report to the ASMFC Menhaden Technical Committee, NOAA Center for Coastal Fisheries and Habitat Research, Beaufort, North Carolina, 59 pp.

Warlen, S.M. (1992) Age, growth, and size distribution of larval Atlantic menhaden off North Carolina. *Trans. Am. Fish. Soc.* 121:588-598.